

PURIFICATION, CHARACTERIZATION, CRYSTALLIZATION AND  
PRELIMINARY X-RAY STRUCTURE DETERMINATION OF  
*Scytalidium thermophilum* BIFUNCTIONAL CATALASE AND  
IDENTIFICATION OF ITS CATECHOL OXIDASE ACTIVITY

A THESIS SUBMITTED TO  
THE GRADUATE SCHOOL OF NATURAL AND APPLIED SCIENCES  
OF  
MIDDLE EAST TECHNICAL UNIVERSITY

BY

DİDEM SUTAY

IN PARTIAL FULFILLMENT OF THE REQUIREMENTS  
FOR  
THE DEGREE OF DOCTOR OF PHILOSOPHY  
IN  
CHEMICAL ENGINEERING

JUNE 2007

Approval of the Graduate School of Natural and Applied Sciences

\_\_\_\_\_  
Prof.Dr. Canan Özgen  
Director

I certify that this thesis satisfies all the requirements as a thesis for the degree of Doctor of Philosophy.

\_\_\_\_\_  
Prof.Dr. Nurcan Baç  
Head of Department

This is to certify that we have read this thesis and that in our opinion it is fully adequate, in scope and quality, as a thesis for the degree of Doctor of Philosophy.

\_\_\_\_\_  
Prof.Dr. Zümrüt B. Ögel  
Co-Supervisor

\_\_\_\_\_  
Prof.Dr. Ufuk Bakır  
Supervisor

**Examining Committee Members**

Prof. Dr. Meral Yücel (METU, BIOL) \_\_\_\_\_

Prof. Dr. Ufuk Bakır (METU, CHE) \_\_\_\_\_

Prof. Dr. Gülşen Doğu (Gazi Univ., CHE) \_\_\_\_\_

Prof. Dr. Pınar Çalık (METU, CHE) \_\_\_\_\_

Prof. Dr. Mehmet Mutlu (Hacettepe Univ., FDE) \_\_\_\_\_

**I hereby declare that all information in this document has been obtained and presented in accordance with academic rules and ethical conduct. I also declare that, as required by these rules and conduct, I have fully cited and referenced all material and results that are not original to this work.**

Name, Last name : Didem Sutay

Signature :

## ABSTRACT

PURIFICATION, CHARACTERIZATION, CRYSTALLIZATION AND  
PRELIMINARY X-RAY STRUCTURE DETERMINATION OF  
*Scytalidium thermophilum* BIFUNCTIONAL CATALASE AND  
IDENTIFICATION OF ITS CATECHOL OXIDASE ACTIVITY

Sutay, Didem

Ph.D., Department of Chemical Engineering

Supervisor: Prof. Dr. Ufuk Bakır

Co-Supervisor: Prof. Dr. Zümrüt B. Ögel

June 2007, 166 pages

In this study, the aim was identification and classification of the enzyme having phenol oxidase activity produced by a thermophilic fungus, *Scytalidium thermophilum*. For this purpose, enzyme production, purification, biochemical characterization and structural analysis by X-ray crystallography studies have been performed.

At the beginning of the research, this enzyme was considered as a phenol oxidase and analyzed accordingly. However, during purification, amino acid sequencing and structural studies, the enzyme was shown to be a "catalase", with an additional catechol oxidase activity. This novel bifunctional "catalase-catechol oxidase" (CCO) was purified 10 fold with

45 % yield by anion exchange and gel filtration chromatographies. CCO was determined as a tetrameric protein having total and subunit molecular weights of 320 and 80 kDa, respectively. Isoelectric point of CCO was verified as 5.0.

CCO catalase and catechol oxidase activities were characterized in terms of their kinetic behavior at different pH and temperatures. Depending on the substrate specificity and inhibitor studies of CCO, the phenol oxidase activity was determined as catechol oxidase but not tyrosinase or laccase.

The best crystallization condition for CCO was determined and X-ray diffraction data was collected at the Daresbury Synchrotron Radiation Source (United Kingdom) at 2.7 Å resolution. The preliminary structure was solved by molecular replacement method using *Penicillium vitale* catalase structure. CCO was verified to have a tetrameric structure with two homodimers and a metal center in each polypeptide chain.

Keywords: Catalase, catechol oxidase, *Scytalidium thermophilum*, purification, characterization, crystallization, X-ray, structure determination.

## ÖZ

*Scytalidium thermophilum* ÇİFT FONKSİYONLU KATALAZININ  
SAFLAŞTIRILMASI, KARAKTERİZASYONU, KRİSTALİZASYONU,  
İLK AŞAMA X-IŞINI YAPISININ BELİRLENMESİ VE  
KATEKOL OKSİDAZ AKTİVİTESİNİN TANIMLANMASI

Sutay, Didem

Doktora, Kimya Mühendisliği Bölümü

Tez Yöneticisi: Prof. Dr. Ufuk Bakır

Tez Eş-Yöneticisi: Prof. Dr. Zümrüt B. Ögel

Haziran 2007, 166 sayfa

Bu çalışmada amaç, termofilik bir küf olan *Scytalidium thermophilum*'un fenol oksidaz aktivitesi olan enziminin tanımlanması ve sınıflandırılmasıydı. Bu amaçla, enzim üretimi, saflaştırılması, biyokimyasal karakterizasyonu ve yapısının X-ışını analizi ile belirlenmesi çalışmaları gerçekleştirilmiştir.

Çalışmanın başlangıcında, enzim fenol oksidaz olarak düşünülmüş ve buna göre incelenmiştir. Ancak, saflaştırma, amino asit sekanslama ve yapı analizi deneyleri aşamasında, enzimin aslında katalaz olduğu, ancak bunun yanında fenol oksidaz (katekol oksidaz) aktivitesi de gösterdiği tespit edilmiştir. Bu yeni katalaz-katekol oksidaz (CCO), anyon değişim ve jel filtrasyon kromatografisi yöntemleriyle % 45 verimle 10 kat saflaştırılmıştır. Enzimin moleküler ağırlığı 320 kDa olarak bulunmuş ve

80 kDa olan alt zincirlerden oluşan dördül bir yapıya sahip olduğu tespit edilmiştir. Enzimin izoelektrik noktası 5.0 olarak bulunmuştur.

Enzimin katalaz ve katekol oksidaz aktiviteleri, farklı pH ve sıcaklıklarda gösterdikleri kinetik özellikleri açısından incelenmiştir. Substrat seçiciliği ve inhibitör çalışmalarında, CCO fenol oksidaz aktivitesinin katekol oksidaz olduğu, lakkaz veya tirozinaz olmadığı tespit edilmiştir.

*S. thermophilum* CCO enzimi için en iyi kristalizasyon koşulu tespit edilmiş ve X-ışını verileri Daresbury Senkrotron Işınım Kaynağı (İngiltere) tesisinde 2.7 Å çözünürlükte elde edilmiştir. Enzimin ilk aşama yapısı moleküler yerdeğiştirme yöntemiyle, en çok homoloji gösteren *Penicillium vitale* katalaz yapısı kullanılarak çözülmüştür. CCO enziminin özdeş ikili yapıdan oluşan, toplamda dördül bir yapıya sahip olduğu ve her bir polipeptit zincirinde bir adet metal yer aldığı tespit edilmiştir.

Anahtar kelimeler: Katalaz, katekol oksidaz, *Scytalidium thermophilum*, saflaştırma, karakterizasyon, kristalizasyon, X-ışını, yapı belirleme.

To people,  
who succeed to keep  
the innocence and goodness in their heart.

## ACKNOWLEDGMENTS

I wish to express my sincere appreciation to Prof. Dr. Ufuk Bakır for her valuable guidance, supervision and endless understanding throughout the research. She made this study possible by helping and encouraging me in all stages of my Ph.D. work.

I would like to thank to Prof. Dr. Zümrüt B. Ögel for her help, valuable criticism and maintaining the collaboration with The University of Leeds.

I want to thank to Prof. Dr. Simon E.V. Phillips and Prof. Dr. Michael J. McPherson for sharing the experience and laboratory facilities during crystallography and sequencing studies in The University of Leeds.

I wish to extend my thanks to Prof. Dr. Meral Yücel and Prof. Dr. Pınar Çalık for their guidance as committee members.

My special thanks are due to all of my friends in METU and The University of Leeds, especially to Aytaç Kocabaş, Ayşe Bayrakçeken, Alev Deniz Öztürk, Arda Büyüksungur, Beril Korkmaz Erdural, Burcu Selin Aytar, Özlem Ak, Eda Çelik, Arwen Pearson, Chi H. Trinh, Mark A. Smith and Pascale Pirrat.

I want to express my deepest gratitude and love to all my family, especially to my parents Neriman-Erkan Sutay and my sister F. Duygu Sutay for their encouragement and support all through the study.

This study was supported by TÜBİTAK, Middle East Technical University and The University of Leeds. I also like to thank to the METU Molecular Biology-Biotechnology R&D Center for isoelectric focusing experiment.

## TABLE OF CONTENTS

ABSTRACT .....	iv
ÖZ.....	vi
DEDICATION .....	iiix
ACKNOWLEDGMENTS .....	ix
TABLE OFCONTENTS .....	x
LIST OF TABLES .....	xiv
LIST OF FIGURES .....	xv
LIST OF ABBREVIATIONS .....	xviii

### CHAPTER

1	INTRODUCTION.....	1
2	LITERATURE SURVEY .....	4
2.1	Proteins .....	4
2.2	Enzymes.....	7
2.2.1	Enzyme Classification .....	7
2.2.2	Enzyme Kinetics .....	8
2.2.3	Catalases .....	13
2.2.4	Phenol Oxidases .....	15
2.2.5	Bifunctionality of Catalases and Phenol Oxidases .....	18
2.2.6	Antioxidant Mechanism and Responsible Enzymes .....	21
2.3	Microorganisms .....	23
2.3.1	Fungi.....	25
2.3.1.1	<i>Scytalidium thermophilum</i> .....	26
2.4	Protein Production .....	26
2.4.1	Fungal Catalase and Phenol Oxidase Production .....	28
2.5	Protein Purification and Characterization .....	30
2.5.1	Purification and Characterization of Catalases	

	and Phenol Oxidases .....	31
2.6	Protein Three-Dimensional Structure Determination .....	34
2.6.1	Protein Structure .....	34
2.6.2	Sample Preparation for Crystallization .....	35
2.6.3	Protein Crystallization.....	37
2.6.3.1	Crystal Systems .....	42
2.6.3.2	Differences in Crystal Systems of Proteins and Conventional Molecules .....	47
2.6.3.3	Protein Crystallization Techniques.....	47
2.6.3.4	Storing Protein Crystal Under Cryo-Conditions.....	50
2.6.4	Protein Crystal Structure Analyzing Techniques.....	51
2.6.4.1	Electron Microscopy .....	51
2.6.4.2	Nuclear Magnetic Resonance Spectroscopy .....	52
2.6.4.3	X-Ray Diffraction .....	52
2.7	Scope of the Study.....	61
3	MATERIALS AND METHODS.....	62
3.1	Materials .....	62
3.2	Microbial Strain, Maintenance and Cultivation.....	62
3.3	Total Protein Determination .....	63
3.4	Enzyme Assays .....	63
3.5	Determination of Optimum Culture Conditions of CCO Production .....	64
3.5.1	Effect of Glucose Concentration on CCO Production and Biomass Generation.....	64
3.5.2	Effect of Nitrogen Source Concentration on CCO Production.....	65
3.5.3	Effect of Inducers on CCO Production .....	65
3.6	CCO Purification .....	65
3.7	Comparison of CCO with Catalases from Different Sources ...	67
3.8	Analytical Gel Electrophoresis and Isoelectric Focusing of CCO .....	67
3.9	Activity Staining of CCO.....	68
3.10	Glycosylation of CCO.....	69

3.11	Aminoacid Sequencing of CCO.....	69
3.12	UV-Vis Spectroscopy of CCO .....	70
3.13	Characterization of CCO Catalase and Catechol Oxidase Activities .....	70
3.13.1	Effect of pH on CCO Activity and Stability .....	70
3.13.2	Effect of Temperature on CCO Activity and Stability .....	71
3.14	Crystallization of CCO.....	71
3.14.1.	Screening for Crystallization Conditions .....	72
3.14.2.	Setting Crystallization Experiments .....	73
3.14.3.	Seeding.....	74
3.14.4.	Storing Protein Crystal at Cryo-Conditions .....	74
3.14.5.	X-Ray Data Collection and Solving Protein Structure .....	76
4	RESULTS AND DISCUSSIONS .....	77
4.1	Medium Optimization Results.....	77
4.1.1	Effect of Glucose Concentration on CCO Production and Biomass Generation.....	78
4.1.2	Effect of Nitrogen Source Concentration on CCO Production.....	78
4.1.3	Effect of Inducers on CCO Production .....	80
4.2	Purification of CCO .....	82
4.3	Comparison of <i>S. thermophilum</i> CCO with Catalases from Different Sources .....	91
4.4	Molecular Weight and Isoelectric Point of CCO.....	93
4.5	Glycosylation of CCO.....	97
4.6	Amino Acid Sequencing of CCO .....	99
4.7	UV-Vis Spectra of CCO.....	107
4.8	Characterization of CCO Activities .....	108
4.8.1	Effect of pH on CCO Activity and Stability .....	108
4.8.2	Effect of Temperature on CCO Activity and Stability .....	112
4.8.3	Substrate Specificity and Effect of Inhibitors on CCO Catechol Oxidase Activity .....	116
4.9	CCO Kinetics .....	118

4.10	Determination of Crystal Structure of <i>S. thermophilum</i> CCO.....	121
4.10.1	Crystallization of CCO .....	121
4.11	Solving Crystal Structure of CCO .....	127
5	CONCLUSIONS .....	131
6	RECOMMENDATIONS .....	133
	REFERENCES.....	134
APPENDICES		
A.	Medium Compositions.....	151
B.	Protein Measurement by Bradford Method.....	152
C.	Anion Exchange Chromatography .....	153
D.	Gel Filtration Chromatography .....	154
E.	SDS-PAGE Protocol .....	155
F.	Coomassie Based Gel Staining Protocol .....	157
G.	Glycoprotein Detection Protocol .....	158
H.	Protein Blotting Procedure .....	161
I.	Crystallization Score Sheet.....	163
J.	<i>S. thermophilum</i> CCO Amino Acid Sequence.....	164
	CURRICULUM VITAE.....	165

## LIST OF TABLES

### TABLE

2.1	Practical differences of protein and conventional low molecular weight compound crystals .....	47
2.2	Software packages used for protein X-ray crystallography .....	59
2.3	The distribution of all catalase structures and their sources given in PDB .....	60
4.1	Two-step purification results of <i>S. thermophilum</i> CCO based on catalase activity .....	89
4.2	Two-step purification results of <i>S. thermophilum</i> CCO based on catechol oxidase activity .....	90
4.3	Comparison of <i>S. thermophilum</i> CCO with other catalases .....	92
4.4	Sequence alignment statistics of <i>S. thermophilum</i> CCO .....	105
4.5	Phenolic substrate specificity of CCO .....	116
4.6	Effect of inhibitors on CCO catechol oxidase activity .....	117
4.7	Screening kit parameters.....	123
C.1	Anion exchange column data.....	153
D.1	Gel filtration column data .....	154
F.1	SimplyBlue SafeStain Microwave Protocol .....	157
G.1	Recommended gel or membrane staining conditions.....	160

## LIST OF FIGURES

### FIGURE

2.1 Amino acid structure in a polypeptide .....	5
2.2 Structures of 20 common amino acids.....	6
2.3 The catalytic power of an enzyme .....	8
2.4 Enzyme-substrate interaction .....	9
2.5 Michaelis-Menten curve.....	10
2.6 Lineweaver-Burk plot.....	11
2.7 Oxidation of phenolics by tyrosinase and catechol oxidase .....	16
2.8 The reactions of catalase.....	20
2.9 Mechanisms of ROS production and enzymatic disposal of superoxide and hydrogen peroxide.....	23
2.10 Taxonomic groups .....	25
2.11 <i>Scytalidium thermophilum</i> .....	27
2.12 Protein structure .....	36
2.13 Two-dimensional solubility diagram illustrated by the change of protein concentration with precipitating agent concentration.....	39
2.14 Examples of crystallization experiment results.....	39
2.15 Examples of well-shaped crystals.....	40
2.16 Examples of not well-shaped crystals .....	41
2.17 Crystal nucleation conditions .....	43
2.18 Crystal lattice .....	44
2.19 Types of crystal systems .....	45
2.20 The unit cell.....	45
2.21 Bravais lattices .....	46
2.22 Vapor diffusion techniques .....	50
2.23 Synchrotron radiation ring.....	53

2.24	Bragg's law.....	54
2.25	X-ray data collection .....	55
2.26	An example of X-ray diffraction pattern.....	55
2.27	Electron density map at different resolutions .....	56
2.28	Flow diagram showing the processes necessary for progressing from gene to X-ray crystal structure.....	57
3.1	Hanging drop vapor diffusion plate setting technique.....	73
3.2	Streak seeding technique .....	75
4.1	Effect of glucose concentration on <i>S. thermophilum</i> CCO production and biomass generation.....	79
4.2	Effect of nitrogen source concentration on <i>S. thermophilum</i> CCO production.....	80
4.3	Effect of inducers on <i>S. thermophilum</i> CCO production.....	81
4.4	<i>S. thermophilum</i> CCO purification by anion exchange chromatography .....	84
4.5	CCO-Catalase activity distribution in anion exchange fractions .....	85
4.6	CCO-Catechol oxidase activity distribution in anion exchange fractions.....	85
4.7	<i>S.thermophilum</i> CCO purification by gel filtration chromatography .....	87
4.8	CCO-Catalase activity distribution in gel filtration fractions .....	88
4.9	CCO-Catechol oxidase activity distribution in gel filtration fractions.....	88
4.10	SDS-PAGE of <i>S.thermophilum</i> CCO .....	93
4.11	Native PAGE and activity staining of CCO.....	95
4.12	IEF of <i>S.thermophilum</i> CCO .....	96
4.13	Glycosylation test of <i>S. thermophilum</i> CCO on 4-12 % SDS-PAGE gel.....	98
4.14	Determination of CCO digestion by trypsin on 2-12 % SDS-PAGE gel with coomassie staining.....	100
4.15	Taxonomic tree of sequence alignment of <i>S. thermophilum</i> CCO .....	103
4.16	Taxonomic tree of structural alignment of <i>S. thermophilum</i> CCO .....	104

4.17	Sequence alignment of <i>S. thermophilum</i> CCO .....	106
4.18	UV-Vis spectra of CCO.....	108
4.19	pH-dependence of CCO-catalase activity .....	110
4.20	pH-dependence of CCO-catechol oxidase activity .....	110
4.21	pH-dependence of CCO-catalase stability .....	111
4.22	pH-dependence of CCO-catechol oxidase stability .....	111
4.23	Temperature dependence of CCO-catalase activity.....	113
4.24	Temperature dependence of CCO-catechol oxidase activity .....	113
4.25	Temperature dependence of CCO-catalase stability.....	114
4.26	Temperature dependence of CCO-catechol oxidase stability .....	114
4.27	Activation energy of CCO catalase activity .....	115
4.28	Activation energy of CCO catechol oxidase activity .....	115
4.29	Michaelis Menten curve of CCO catalase activity .....	119
4.30	Lineweaver Burk plot of CCO catalase activity .....	119
4.31	Michaelis Menten curve of CCO catechol oxidase activity .....	120
4.32	Lineweaver Burk plot of CCO catechol oxidase activity .....	120
4.33	Initial large scale CCO crystal in 28 % PEG-1500 at pH 6.0 and 18 °C .....	122
4.34	CCO crystal in 24 % PEG-3500 at pH 6.0 and 18 °C.....	122
4.35	CCO crystal in 24 % PEG-2000 at 18 °C.....	124
4.36	CCO crystals after seeding in 24 % PEG-2000, 10 mM NaCl at pH 6.5 100 mM Bis-Tris buffer .....	125
4.37	The best CCO crystal in 24 % PEG-2000 at pH 6.5 100 mM Bis-Tris buffer with 10 mM NaCl, 10 mM CaCl <sub>2</sub> and 3 % 6-amino-caproic acid at 18 °C.....	126
4.38	X-ray diffraction patterns of <i>S. thermophilum</i> CCO .....	128
4.39	Three dimensional CCO structure .....	129
4.40	Heme center in CCO structure with electron density map.....	130
4.41	Heme center in CCO structure without electron density map.....	130
B.1	BSA standard curve for Bradford Method.....	151

## LIST OF ABBREVIATIONS

- 4-CN: 4-chloro-1-naphtol  
A: Alanine  
Å: Angstrom  
ABTS: 2,2'-azino-bis-3-ethylbenzthiazoline-6-sulphonic acid  
ADA: 4-amino-*N,N*-diethylaniline  
Ala: Alanine  
Arg: Arginine  
Asn: Asparagine  
Asp: Aspartic acid  
BLAST: Basic Local Alignment Search Tool  
BSA : Bovine serum albumin  
C: Cysteine  
CAT: Catalase  
CCO: Catalase-catechol oxidase  
COOH: Carboxylic acid group  
Cys: Cysteine  
C<sub>α</sub>: Central carbon atom  
D: Aspartic acid  
Da: Dalton  
DMPDA: *N,N*-dimethylphenylenediamine  
E: Enzyme  
E: Glutamic acid  
E<sub>a</sub>: Activation energy  
EC: Enzyme Commission  
EI: Enzyme-inhibitor  
ES: Enzyme-substrate complex  
ESI: Enzyme-substrate-inhibitor complex  
F: Phenylalanine  
G: Glycine

Gln: Glutamine  
Glu: Glutamic acid  
Gly: Glycine  
GPx: Glutathione peroxidase  
H: Histidine  
H<sub>2</sub>O<sub>2</sub>: Hydrogen peroxide  
HB: Benzidine  
HCl: Hydrochloric acid  
His: Histidine  
I: Isoleucine  
Ile: Isoleucine  
IUBMB: International Union of Biochemistry and Molecular Biology  
K: Lysine  
L: Leucine  
L-Dopa: 3,4-dihydroxy-L-phenylalanine  
Leu: Leucine  
Lys: Lysine  
M: Methionine  
Met: Methionine  
N: Asparagine  
NaCl: Sodium chloride  
NCBI: National Center for Biotechnology Information  
NH<sub>2</sub>: Amino group  
NMR: Nuclear magnetic resonance  
MPD: 2-methyl-2,4-pentanediol  
P: Proline  
PAGE: Polyacrylamide gel electrophoresis  
PDB: Protein Data Bank  
PEG: Polyethylene glycol  
Phe: Phenylalanine  
Pro: Proline  
Prx: Peroxiredoxin  
Prxox: Cys-sulfenic acid  
PVDF: Polyvinylidene difluorobenzene

ROS: Reactive oxygen species  
Q: Glutamine  
R: Arginine  
S: Serine  
SDS: Sodiumdodecyl sulphate  
Ser: Serine  
SOD: Superoxide dismutase  
SRS: Synchrotron Radiation Source  
T: Threonine  
Thr: Threonine  
Trp: Tryptophan  
Tyr: Tyrosine  
U: Enzyme activity unit  
V: Valine  
Val: Valine  
W: Tryptophan  
Y: Tyrosine

## CHAPTER 1

### INTRODUCTION

Enzymes are proteins, composed of amino acids, which are produced by all living organisms. They are specific molecules which catalyze bioreactions by lowering the activation energy, thus, increasing the reaction rate, without changing the position of the equilibrium (Berg *et al.*, 2002; Horton *et al.*, 1996). Enzymes have been safely used for thousands of years. Today, they are used in many industrial areas such as food, pharmaceutical, textile, paper and pulp industries, waste water treatment plants and also for analytical purposes.

The enzyme studied in this research was a bifunctional catalase, with an additional catechol oxidase activity. Catalases (EC 1.11.1.6), belonging to oxidoreductases, are a group of metalloenzymes with the major function for degradation of hydrogen peroxide ( $H_2O_2$ ) to dioxygen and water (Goldberg and Hochman, 1989). Fungi are reported as effective producers of these enzymes (Isobe *et al.*, 2006). Phenol oxidases (POs) are responsible for oxidation of various phenolic compounds in the presence of molecular oxygen. There are three different types of POs present in nature; laccases (E.C. 1.10.3.2), catechol oxidases (E.C. 1.10.3.1) and tyrosinases (E.C. 1.14.18.1). Another group of enzymes, peroxidases (E.C. 1.11.1.7), can also be considered as a member of PO family.

The reason of co-existence of catalase and phenol oxidase activities in the same enzyme can be explained by the fact of hydrogen peroxide formation during phenol oxidation. These reactions are related with the antioxidant mechanism and oxidative stress, which arises from the increase in the concentration of reactive oxygen species (ROS) and/or a decrease in their detoxification mechanisms (Aoshima and Ayabe, 2007; Schrader and Michael, 2006).

For protein purification, many methods are available. The first step generally used is fractionation and the next step involves chromatographic methods. Anion exchange chromatography, based on separation by charge; and gel filtration chromatography, based on separation by size, were used in this study. There are numerous analytical tools for protein detection and characterization. Gel electrophoresis (SDS-PAGE, native-PAGE and isoelectric focusing), the most commonly used method for visualization of the protein content, was used in this research (Ducruix and Giegé, 1992). Kinetic characterization at different pH and temperatures were also performed.

To determine the three dimensional crystal structure of a protein molecule, the first step covers the crystallization of the purified enzyme. There are different crystallization techniques such as batch crystallization, liquid-liquid diffusion, dialysis and vapor diffusion (Drenth, 1999). Since interactions between molecules in a crystal can be controlled by several factors such as temperature, pH, salts, hydrogen-bond competitors, hydrophobic additives and organic solvents, a wide range of crystallization conditions should be tested to achieve a well-ordered crystal (Howard and Brown, 2002). To analyse the protein crystal, techniques such as X-ray, nuclear magnetic resonance and electron microscopy can be used (Ducruix and Giegé, 1992; Whitford, 2005). X-ray analysis, which was used in this research, is the most common technique for protein structure determination studies.

The microorganism used in this research was *Scytalidium thermophilum*, was a thermophilic fungus, also known as *Humicola insolens*, *Torula thermophila* and *Humicola grisea* var. *thermoida*. The amino acid sequence of *S. thermophilum* has been published in the United States Patent (No. 5646025) (Inventor: Donna Moyer from Davis, CA, USA) but purification, characterization, crystallization and X-ray structure determination of the enzyme was first introduced in this research. In addition, catechol oxidase activity of *S. thermophilum* catalase was also studied and reported in this current research.

## CHAPTER 2

### LITERATURE SURVEY

#### 2.1. Proteins

Proteins are the most versatile macromolecules in living systems and have diverse crucial biological functions varying from DNA replication, catalyzing reactions, forming cytoskeletal structures, transporting oxygen and electrons, storage, movement and defence in living systems. They are connected with other molecules such as lipids, carbohydrates, nucleic acids, phosphate groups, flavins, heme groups and metal ions by covalent or non-covalent bonds. Complexes of proteins with lipids are called as lipoproteins, where as those with carbohydrates are called as glycoproteins. Protein components such as hemes or metal ions are generally named as prosthetic groups, where the complex of a metal ion with a protein leads to a metalloprotein (Berg *et al.*, 2002; Whitford 2005).

Proteins consist of amino acids that are assembled together into a polypeptide chain. A polypeptide chain is composed of a regularly repeating part, named as main chain or backbone, and a variable part, including individual side chains. Amino acids are joined together by peptide bonds by the reaction of amino group of one molecule with the carboxyl group of the other to form a polypeptide chain and each amino acid in the polypeptide is called a residue. Amino acids are “building blocks” of proteins and have in common a central carbon atom ( $C_{\alpha}$ ) to

which attached a hydrogen atom, an amino group ( $\text{NH}_2$ ), and a carboxylic acid group ( $\text{COOH}$ ) as shown in Figure 2.1. The side chain attached to  $\text{C}_\alpha$  distinguishes one amino acid from another. Amino acid sequences are read from amino group (N terminal) to the carboxyl group (C terminal) (Berg *et al.*, 2002, Whitford 2005).

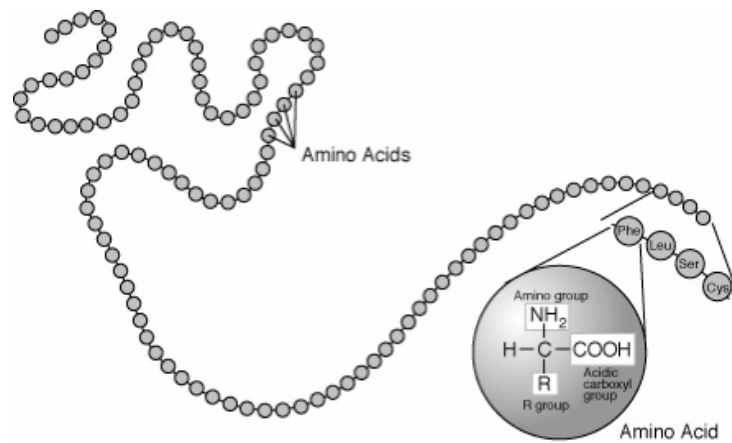


Figure 2.1. Amino acid structure in a polypeptide (Millard, 2006)

There are 20 different side chains specified by the genetic code, hence, 20 different amino acids as shown in Figure 1.2. Depending on the nature of the side chain, the amino acids are generally classified in three groups. The first class comprises Ala, Val, Leu, Ile, Phe, Pro and Met which have strictly hydrophobic side chains. The four charged residues Asp, Glu, Lys and constitute the second class. The third class involve Ser, Thr, Cys, Asn, Gln, His, Tyr and Trp, which contain polar side chains. Glycine has only a hydrogen atom as side chain and is the simplest of the 20 amino acids. Glycine has special properties and usually considered either to form a fourth class or belong to the first class (Branden and Tooze, 1991).

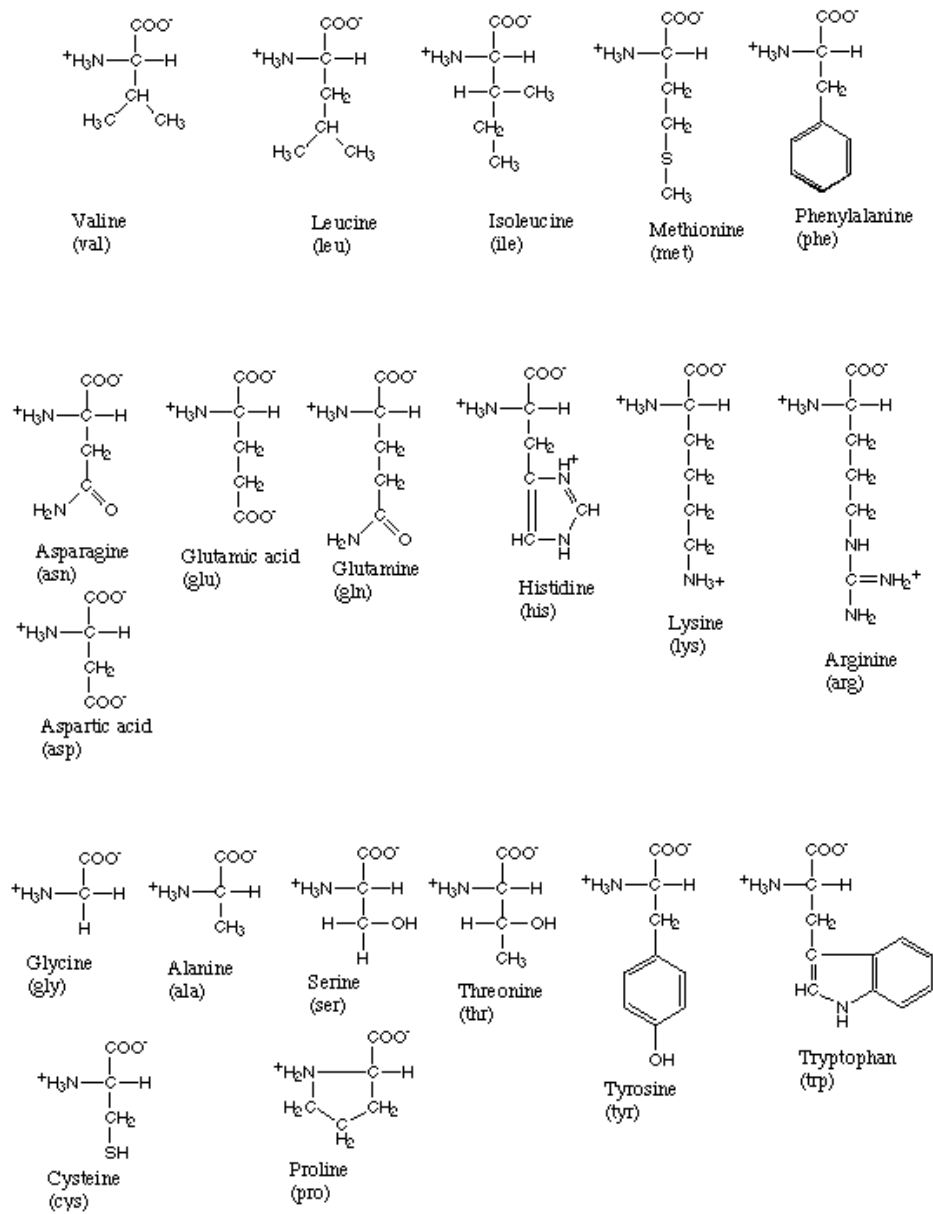


Figure 2.2. Structures of 20 common amino acids (Willmot, 2005)

## **2.2. Enzymes**

Enzymes are molecules which catalyze bioreactions and nearly all of them are proteins. They are very specific upon the reactants, called substrates, which they convert into products by lowering the activation energy, thus, increasing the reaction rate. The catalytic efficiency of enzymes is very high, they accelerate reactions  $10^3$  to  $10^7$  fold compared to uncatalyzed reactions, without changing the position of the equilibrium (Berg *et al.*, 2002; Horton *et al.*, 1996).

### **2.2.1. Enzyme Classification**

Enzymes are classified by International Union of Biochemistry and Molecular Biology (IUBMB) on the basis of the reactions that they catalyze, into six groups: oxidoreductases, transferases, hydrolases, lyases, isomerases and ligases. Oxidoreductases catalyze oxidation reduction reactions. Transferases are responsible for group-transfer reactions and many of them require the presence of coenzymes. Hydrolases catalyze hydrolysis reactions by transferring the functional groups to water. Lyases are responsible for nonhydrolytic and nonoxidative elimination of reactions and addition or removal of groups to form double bonds. Isomerases catalyze isomerization reactions meaning structural changes within a molecule. These reactions are among the simplest enzymatic reactions since they have only one substrate and one product. Ligases catalyze ligation of two substrates and require chemical potential energy such as ATP to carry out the reaction. These groups are further subdivided and a four-digit number starting with the letters EC, referring to Enzyme Commission, is defined for specific identification of all enzymes (Berg *et al.*, 2002; Horton *et al.*, 1996).

### 2.2.2. Enzyme Kinetics

Catalysis takes place on a particular three-dimensional region in the enzyme, called active site, which is capable of binding the substrate and the cofactor, if any. There are also residues participating in making and breaking of bonds on the active site. The catalytic power of an enzyme (E) comes from binding a substrate (S) to form enzyme-substrate complex (ES) (substrate binding step) and converting it to final product (P) (catalytic step) as shown in Figure 2.3 (Berg *et al.*, 2002; Horton *et al.*, 1996).



Figure 2.3. The catalytic power of an enzyme (Willmot, 2005)

Since the interactions between enzyme and substrate are maintained by weak forces requiring close-contact, a substrate should have a specific shape to fit into the active site. This phenomena was explained by Emil Fisher in 1890 by lock and key model (Figure 2.4-a). However, some flexible enzymes also exist whose active sites can be modified by the substrate. This concept was described by Daniel E. Koshland, Jr., in 1958 as induced fit model (Figure 2.4-b) (Berg *et al.*, 2002).

The study of the rates of enzyme catalyzed reactions, called enzyme kinetics, provide information of specificities, catalytic mechanisms and activities of the enzymes (Horton *et al.*, 1996). The activity of an enzyme can be measured either by determining the rate of product formation or

substrate utilization during reaction. In each case, generally, the time course initially increases linearly but tends to decrease at longer times, because of substrate depletion, reaching the equilibrium, product or time-dependent inhibition, instability, assay method artifact or changes in assay conditions. To avoid these time-dependent effects on the reaction, enzyme activities are measured in the initial linear range (Eisenthal and Danson, 1992).

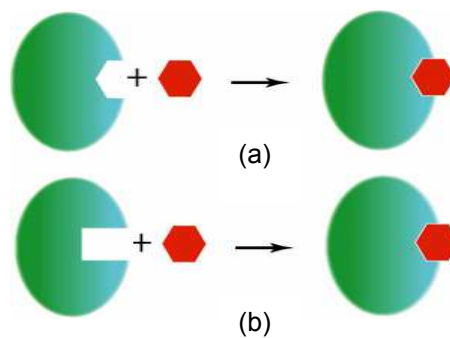


Figure 2.4. Enzyme-substrate interaction (a) Lock and key model, (b) Induced fit model (International Biopharmaceutical Association, 2004)

Like many other chemical reactions, enzyme-catalyzed reactions can be described by rate equations. The mostly used one is the Michaelis-Menten equation which relates the initial reaction rate (velocity) to substrate concentration is given in Equation (2.1) (Whitford, 2005):

$$v_0 = V_{\max} [S] / K_m + [S] \quad (2.1)$$

where  $K_m$  is defined as (Equation 2.2);

$$K_m = (k_2 + k_{-1}) / k_1 \quad (2.2)$$

In Michaelis-Menten equation, the velocity is related to substrate concentration through two parameters,  $V_{max}$  and  $K_m$ , that are characteristic for an enzyme under defined conditions (pH, temperature, ionic strength etc.).  $V_{max}$  is the maximum velocity of the reaction which is achieved at high substrate concentrations when the enzyme is saturated with the substrate.  $K_m$  is the initial concentration of the substrate at  $\frac{1}{2} V_{max}$  (Figure 2.5).  $K_m$  is a measure of the affinity of enzyme for the substrate, which means, the lower the  $K_m$ , the more tightly the substrate is bound.  $K_m$  values are also used to distinguish enzymes having the same function (Horton *et al.*, 1996).

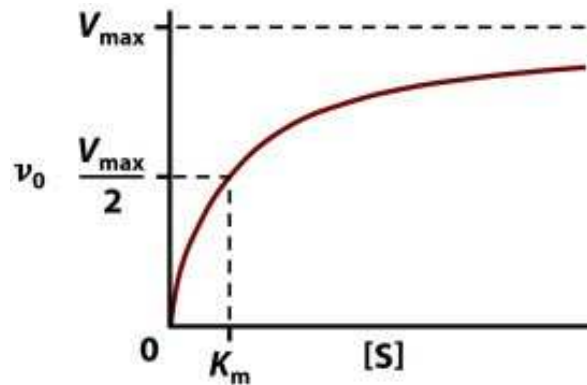


Figure 2.5. Michaelis-Menten curve (Knight, 2006)

Another catalytic constant (turnover number),  $k_{cat}$ , is a measure of the catalytic activity of an enzyme, telling how many reactions per second a molecule of enzyme can catalyze and it is defined as (Equation 2.3) (Horton *et al.*, 1996);

$$k_{cat} = V_{max} / [E]_{total} \quad (2.3)$$

Determination of  $V_{max}$  and  $K_m$  from the Michaelis-Menten graph is generally difficult because the curve approaches  $V_{max}$  asymptotically. Therefore, Michaelis-Menten equation is usually analysed by linear plots. The most commonly used linear transformation is the double-reciprocal, or Lineweaver-Burk plot of  $1/v_0$  versus  $1/[S]$  (Figure 2.6) according to the Equation (2.4) (Horton *et al.*, 1996; Whitford, 2005):

$$1/v_0 = \{K_m / (V_{max} [S])\} + (1/ V_{max}) \quad (2.4)$$

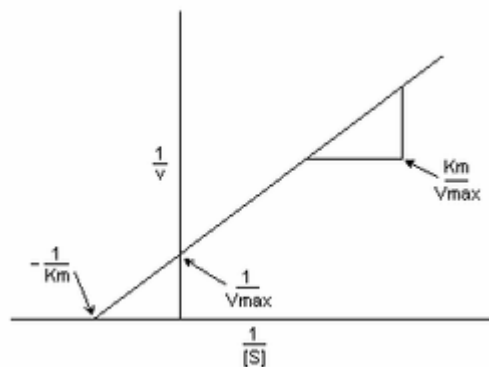


Figure 2.6. Lineweaver-Burk plot (Wikipedia, 2007)

Since the Lineweaver-Burk plot is unsatisfactory to adequately define deviations away from linearity at low and high substrate concentrations, a line-fitting or linear regression analysis method, called Eadie-Hofstee, was developed. The Equation (2.5) was derived (Whitford, 2005):

$$v_0 = -K_m v_0 / [S] + V_{max} \quad (2.5)$$

In this method, initial velocity of the reaction in a range of different substrate concentrations is measured before substantial substrate depletion or product formation. Double-reciprocal plots are also useful to determine the patterns of enzyme inhibition (Whitford, 2005).

Enzymes can be inhibited by binding of specific molecules and ions, called inhibitors (I). Natural inhibitors regulate metabolism and many drugs and toxic agents act by inhibiting enzymes. Experimentally, inhibitors are used to determine the enzyme action mechanism (Berg *et al.*, 2002).

Enzyme inhibition can be either reversible or irreversible. Irreversible inhibitors are bound tightly with covalent bonds to the enzymes to form enzyme-inhibitor complex (EI), by alkylation or acylation of the side chain of an active site amino acid residue, and can not be easily removed. Some important drugs, such as penicillin and aspirin, are irreversible inhibitors (Berg *et al.*, 2002; Horton *et al.*, 1996)

Reversible inhibitors are bound to the enzymes by non-covalent bonds and they are characterized by an easy dissociation of enzyme-inhibitor complex. There are different types of reversible inhibition: competitive, uncompetitive and noncompetitive. Competitive inhibitors are the most common inhibitors in biochemistry. They compete with substrates to prevent binding of substrate to active site of the enzyme and forming

active enzyme-substrate complex (ES). Many classical competitive inhibitors have similar shape of substrate, they bind to enzyme but do not react. Competitive inhibition can be relieved by increasing the substrate concentration. In uncompetitive inhibition, the inhibitor and the substrate bind to the enzyme at different sites and an inactive enzyme-substrate-inhibitor (ESI) complex is formed. This type of inhibition is common in multi-substrate reactions. Noncompetitive inhibitors, which are not substrate analogs, can bind to enzyme (E) or enzyme-substrate complex (ES) to form inactive enzyme-inhibitor (EI) or enzyme-substrate-inhibitor (ESI) complexes, respectively. Noncompetitive inhibition can not be overcome by increasing the substrate concentration (Berg *et al.*, 2002).

### 2.2.3. Catalases

Catalases (EC 1.11.1.6) are a group of metalloenzymes with the major function for degradation of hydrogen peroxide (H<sub>2</sub>O<sub>2</sub>) to dioxygen and water (Goldberg and Hochman, 1989) as shown in Equation 2.6.



Catalases are isolated from a broad range of prokaryotic and eukaryotic microorganisms (Fraaije *et al.*, 1996). Their main function is to control the hydrogen peroxide (H<sub>2</sub>O<sub>2</sub>) concentrations in living systems, where H<sub>2</sub>O<sub>2</sub> is a normal by-product of mitochondrial electron transport,  $\beta$ -oxidation of fatty acids and photorespiration (Montavon *et al.*, 2007). Fungi are reported to be effective producers of these enzymes (Isobe *et al.*, 2006) since they are aerobic microorganisms and suffer from the toxic effects of molecular oxygen. Fungal cells have catalases, peroxidases and superoxide dismutases to keep the reactive oxygen species (ROS)

(H<sub>2</sub>O<sub>2</sub>, superoxide and hydroxyl radicals and singlet oxygen) at non-harmful concentrations (Calera *et al.*, 2000). Catalases of different fungi; *Alternaria alternata* (Caridis *et al.*, 1991), *Aspergillus fumigatus* (Bemmann *et al.*, 1981; Paris *et al.*, 2003; Shibuya *et al.*, 2006), *Aspergillus nidulans* (Calera *et al.*, 2000), *Aspergillus niger* (Kikuchi-Torii *et al.*, 1982; Kulys *et al.*, 2003), *Aspergillus oryzae* (Hisada *et al.*, 2005), *Blakeslea trispora* (Gessler *et al.*, 2002), *Neurospora crassa* (Pereza *et al.*, 2002; Gessler *et al.*, 2002), *Penicillium marneffeii* (Pongpom *et al.*, 2005), *Penicillium simplicissimum* (Fraaije *et al.*, 1996) *Penicillium vitale* (Hudkova *et al.*, 1975; Kulys *et al.*, 2003), *Phanerochaete chrysosporium* (Kwon and Anderson, 2001), *Septoria tritici* (Levy *et al.*, 1992), *Scytalidium thermophilum* (Kulys *et al.*, 2003) and *Thermoascus aurantiacus* (Wang *et al.*, 1998) have been isolated until now and they are generally tetrameric enzymes with a subunit size in the range of 61-97 kDa. The pI values are generally acidic; 3.5 for *Aspergillus nidulans* (Calera *et al.*, 2000), 4.5 for *Thermoascus aurantiacus* (Wang *et al.*, 1998), 5.1 (calculated) and 4.0 (experimental) for *Scytalidium thermophilum* (Kulys *et al.*, 2003), except 6.5 for *Aspergillus niger* (Mosavi-Movahedi *et al.*, 1987) catalases.

Catalases can be classified in three groups: monofunctional heme (typical) catalases, catalase-peroxidases and manganese catalases. The largest subgroup are typical catalases which generally are tetramers with a total molecular weight range of 200-340 kDa with four prosthetic haem group and have a strong absorbance in the Soret band with R<sub>z</sub> (A<sub>406</sub>/A<sub>280</sub> ratio) values around 1. Catalase-peroxidases are generally homodimers having molecular weights between 120-340 kDa. The characteristic feature of catalase-peroxidases is their bifunctional catalytic ability and relatively lower R<sub>z</sub> values. Third group includes manganese catalases, which have manganese ion in their active sites instead of heme. Only a few of them are known, having unusual oligomeric structures with a molecular weight range of 170-210 kDa (Zamocky and Koller 1999). Another group of catalases, catalase-catechol oxidases are introduced in this study, which are capable of decomposing H<sub>2</sub>O<sub>2</sub> (catalase activity) and

also oxidising of catechol in the absence of H<sub>2</sub>O<sub>2</sub> (catechol oxidase activity). But there is only one study identifying the catechol oxidase activity of mammalian catalase where the enzyme was not characterized (Vetrano *et al.*, 2005).

Catalases are used in industry wherever hydrogen peroxide is used as a disinfectant. Recently, hydrogen peroxides have been tested as bleaching agents to replace chlorine-based chemicals. Catalase, with its ability of hydrogen peroxide decomposition, can be used to remove excess peroxide, i.e. removal of hydrogen peroxide used in disinfection of contact lenses and also for excess hydrogen peroxide removal before dye addition in textile industry. Catalases are also used in food industry, for example, for disposing of hydrogen peroxide used in milk pasteurization prior to cheese making (Chu *et al.*, 1975; Amorim *et al.*, 2002; Chen *et al.*, 2007).

#### **2.2.4. Phenol Oxidases**

Phenol oxidases (POs) are a group of enzymes which are responsible for oxidation of various phenolic compounds in the presence of molecular oxygen. There are different types of POs present in nature and three major groups of these enzymes are laccases (E.C. 1.10.3.2, *p*-benzenediol: oxygen oxidoreductase), catechol oxidases (E.C. 1.10.3.1, *o*-diphenol oxidoreductase) and tyrosinases (E.C. 1.14.18.1, monophenol monooxygenase). Another group of enzymes, peroxidases (E.C. 1.11.1.7), can also be considered as a member of PO family.

Laccases are widely distributed in plants and fungi, but not in animals, where the related protein is ceruloplasmin. Their functions are related to sexual differentiation, pigmentation of fruiting bodies, lignolysis, detoxification and others. These enzymes act on *p*- and *o*-diphenols, showing more affinity for the first group (Sanchez-Amat and Solano, 1997).

Catechol oxidases are the key enzymes for melanin synthesis, acting on a variety of substituted *o*-diphenols to yield the corresponding *o*-quinones (Figure 2.7). They have a pair of copper ions at the active site. These enzymes may also show cresolase activity, so that they are able to catalyze the hydroxylation of monophenols to *o*-diphenols. Thus, they catalyze the straightforward formation of *o*-quinones either from monophenols or *o*-diphenols. The molecular and structural differences between catechol oxidases (EC 1.10.3.1) and cresolases (EC 1.14.18.1) are ill defined since they are exclusively based on the substrates oxidized. There are enzymes from numerous sources that display both catalytic activities (Sanchez-Amat and Solano, 1997).

Tyrosinase catalyzes the hydroxylation of monophenols to *o*-diphenols (cresolase activity) as shown in Figure 2.7. Tyrosinases are a group of copper proteins that also catalyze the reaction of catechol oxidase (EC 1.10.3.1), if only 1,2-benzenediols (*o*-diphenols) are available as substrate (IUBMB Nomenclature).

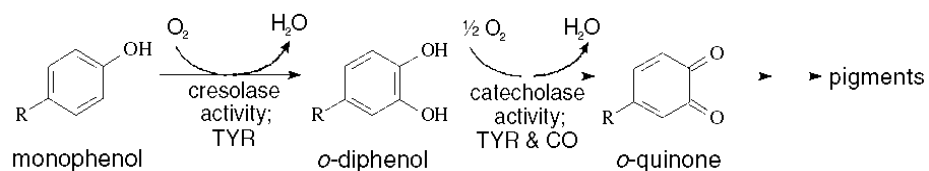


Figure 2.7. Oxidation of phenolics by tyrosinase and catechol oxidase (Marusek *et al.*, 2006)

Another group of enzymes, peroxidases (E.C. 1.11.1.7), are also regarded as phenol oxidases. They are produced mainly by a number of microorganisms and plant sources and they catalyze reactions in the presence of hydrogen peroxide (Durán and Esposito, 2000).

Bifunctional phenol oxidases; sweet potatoes (*Ipomoea batatas*) catechol oxidase (Gerdemann *et al.*, 2001) and mushroom (*Agaricus bisporus*) tyrosinase (Yamazaki *et al.*, 2004; Garcia-Molina *et al.*, 2005) have been determined to have catalase activity.

POs are very common in nature, they can be found in almost all plants, animals and microorganisms. POs have been implicated in a range of roles, one of which is in mycelial morphogenesis where the fungal mycelium undergoes changes in response to the presence of another fungus. Laccases have been implicated in lignin degradation and/or detoxification of lignin degradation products, pigmentation accumulation, sporulation detoxification of toxic compounds, plant pathogenesis and mycelial morphogenesis. Laccase isoenzymes can vary between and within species, and can also have different functions within these species and under different environmental conditions. Peroxidases in plants have been implicated in the production of highly toxic compounds that are antifungal in nature, in the production of melanin and melanin-like pigments and in the formation of different mycelial formations. Tyrosinase is involved in the biosynthesis of melanins and other polyphenolic compounds in bacteria, fungi, plants and animals. All of these enzymes may have some role to play in the offence and defence of fungi during interactions (Score *et al.*, 1997).

POs have very wide substrate range and final oxidation products of these substrates are quinones, which are highly reactive molecules and polymerize into brown, red or black water-insoluble compounds (Durán and Esposito, 2000).

Besides many physiological functions such as growth and differentiation, pigmentation, detoxification of toxic phenolics, and lignin decomposition (Dittmer *et al.*, 1997; Burke and Cairney, 2002), phenol oxidases have wide application areas in various industries including food and pharmaceutical (Opie *et al.*, 1995; Mayer and Staples, 2002; Bauer *et al.*,

1999); waste-water and soil treatment processes (Durán and Esposito, 2000); production of biomaterials (Yamada *et al.*, 2000); for analytical purposes such as biosensor preparation (Bauer *et al.*, 1999).

Phenols, substrates of POs, are compounds having hydroxyl group attached to the benzene ring and are generally named as derivatives of the simplest member of the family, phenol. However, phenolics can be very large in size, such as condensed tannins (Tomás-Barberán and Espin, 2001). Phenolics are present in wastes from several industrial processes, as coal conversion, olive oil production, petroleum refining, paper and pulp production, production of organic chemicals, etc. These compounds are harmful to the environment, animals and humans and in addition, they give an undesirable taste and odor to drinking water, even in very low concentrations. Hence, removal of phenolics from industrial aqueous wastes is an important problem (Russell and Burton, 1999).

#### **2.2.5. Bifunctionality of Catalases and Phenol Oxidases**

In addition to their primary activities, both catalases and phenol oxidases have been reported to have further enzymatic activities. And interestingly, their activities generally overlap, which means, catalases have oxidative activity and phenol oxidases have catalatic activity.

As explained previously, the major function of catalases is the degradation of hydrogen peroxide to dioxygen and water. Secondary function of catalases is reported as the oxidation of hydrogen donors such as methanol, ethanol, formic acid, phenols, with the consumption of peroxide, called peroxidic activity (Packer, 1984). The third and the novel function of catalases; oxidase activity in the absence of hydrogen peroxide, was introduced by Vetrano *et al.* (2005) for mammalian catalases. And the outcome of our research was the evidence of a new class of catalases; fungal catalase with oxidase activity.

The reaction mechanisms of three types of catalase activities, summarized by Vetrano *et al.* (2005), were shown in Figure 2.8. The hydrogen peroxide-degrading catalytic activity was shown in Figure 2.8-a. Catalase heme interacts with a molecule of hydrogen peroxide and an oxyferryl porphyrin centered radical (compound I) was formed. Binding of a second molecule of hydrogen peroxide results in breakdown of compound I and formation of molecular oxygen and water. Peroxidative activity of catalase was shown in Figure 2.8-b. Interaction of compound I with low molecular weight alcohols results in substrate oxidation via single electron transfer. In Figure 2.8-c, oxidase activity of catalase was demonstrated. Catalase heme interacts with a strong reducing substrate such as benzidine (HB) and molecular oxygen. A compound II-like intermediate was formed. In subsequent electron transfers the substrate was oxidized and the enzyme returns to its original state. The model suggested by Vetrano *et al.* (2005) is consistent with the consumption of 1 mole of oxygen for 2 mole of product formed. An incomplete reaction could potentially result in formation of radical centered intermediates and production of superoxide (dashed arrow). Similar reaction pathway was also proposed by Vlasits *et al.* (2007) for monofunctional catalases, whereas a non-scrambling mechanism was suggested for catalase-peroxidases.

In contrast to single study about catalase with oxidative activity, there are more reports of phenol oxidases with catalytic activity, described in literature. In year 1972 and 1973, Jolley and Russell *et al.* introduced oxytyrosinase concept in which they observed a reaction between mushroom tyrosinase and hydrogen peroxide yielding a spectroscopically observable product. They studied the reaction of tyrosinase with hydrogen peroxide in the presence of molecular oxygen and detected oxytyrosinase spectrum. Recently, Yamazaki *et al.* (2004) and Garcia-Molina *et al.* (2005) also reported that mushroom tyrosinase exhibits catalase activity. Additionally, catalase-like activity of isoenzymes of sweet potatoes (*Ipomea batatas*) was determined by Gerdemann *et al.* (2001).

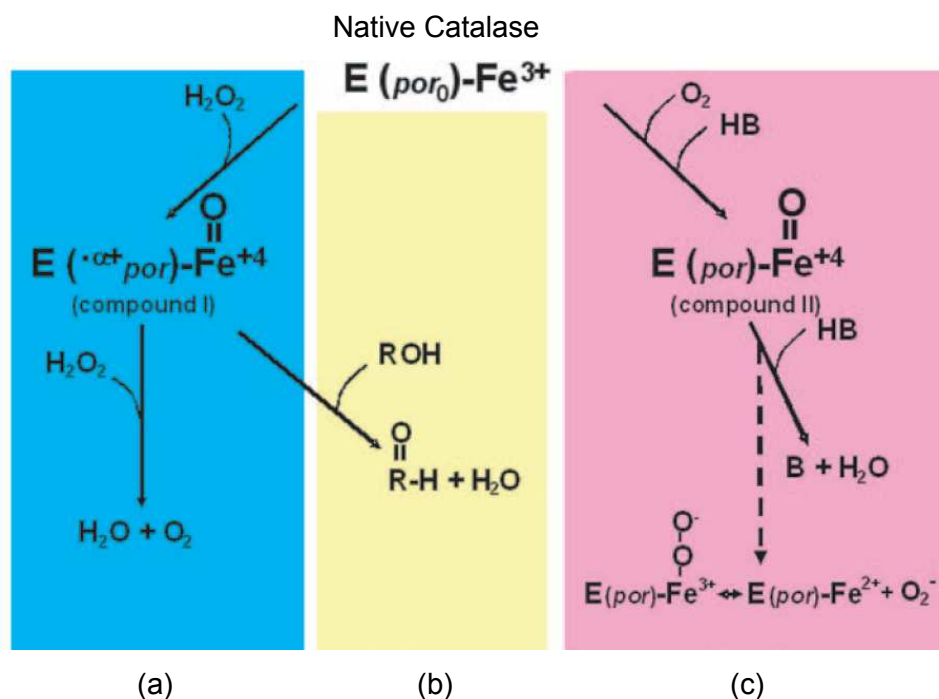


Figure 2.8. The reactions of catalase, (a) Catalytic, (b) Peroxidative, (c) Oxidative (Vetrano *et al.*, 2005)

The relationship between catalases and phenol oxidases can be explained by the fact of hydrogen peroxide formation during phenol oxidation. Hydrogen peroxide, which is the substrate of catalase, was reported by Akagawa *et al.* (2003) as a by-product of phenol autooxidation reaction. They investigated the ability of hydrogen peroxide production by polyphenols in polyphenol-rich beverages. Catechol, hydroquinone, pyrogallol, 1,2,4-benzenetriol and catechins yielded significant amount of hydrogen peroxide. Aoshima and Ayabe (2007) also reported that only a small amount of hydrogen peroxide was detected in tea and coffee immediately after opening caps of bottles, but hydrogen peroxide was gradually produced after opening the caps and maintaining the exposure to air. This result was again due to the oxidation of phenolics in tea and coffee and production of hydrogen peroxide.

These two examples of co-existence of phenols and hydrogen peroxide in the presence of oxygen was related with the oxidative stress and antioxidant mechanism.

#### **2.2.6. Antioxidant Mechanisms and Responsible Enzymes**

Oxidative stress arises from the increase in the concentration of reactive oxygen species (ROS) and/or a decrease in their detoxification mechanisms. The sources of oxidative stress are exposure to environmental oxidants, toxins like heavy metals, ionizing and UV radiation, heat shock and inflammation (Schrader and Michael, 2006). In eukaryotic and prokaryotic organisms, ROS are by-products of the metabolism, mainly aerobic respiration (Aguirre *et al.*, 2005). High levels of ROS has a toxic effect on biomolecules such as DNA, proteins and lipids and has also effect on human pathologies such as ischemia reperfusion injury, atherosclerosis, hypertension, inflammation, cystic fibrosis, cancer, type-2 diabetes, or neurodegenerative diseases such as Parkinson's or Alzheimer's disease. Furthermore, oxidative stress has also been linked to aging (Schrader and Michael, 2006). In contrast, ROS is produced in the cell to regulate different functions, including immunity, cell proliferation, cell differentiation, signal transduction and ion transport (Aguirre *et al.*, 2005).

ROS include radical species, containing free and unpaired electrons such as the superoxide anion ( $O_2^{\cdot-}$ ) and the most highly reactive and toxic form of oxygen, the hydroxyl radical ( $\cdot OH$ ). Hydrogen peroxide ( $H_2O_2$ ) is also described to ROS, although it has no unpaired electrons, and thus is not a radical (Schrader and Michael, 2006). ROS are formed by oxygen excitation, partial reduction and the formation of radicals or peroxides with other compounds (Fig 2.9-a). ROS are produced either by excitation of  $O_2$  to O, ozone ( $O_3$ ), and singlet oxygen ( $^1O_2$ ) or by reduction to superoxide anion ( $O_2^{\cdot-}$ ), hydrogen peroxide ( $H_2O_2$ ) and hydroxyl radical ( $\cdot OH$ ).

Oxygen is generated by the photosystem II (PSII) and is reduced by respiratory chain cytochrome oxidase (COX). Superoxide reacts only with itself, with nitric oxide, and other radicals. Hydrogen peroxide reacts with iron sulfur centers and cysteines of certain proteins. However, both superoxide and hydrogen peroxide can spontaneously form singlet oxygen and hydroxyl radical, which are much more reactive (Aguirre *et al.*, 2005).

Antioxidant enzymes, including superoxide dismutase, catalases and peroxidases, prevent damaging effects of ROS (Fig 2.9-b). Superoxide ( $O_2^-$ ) is dismutated by superoxide dismutases (SOD) to hydrogen peroxide. Hydrogen peroxide is decomposed by catalases (CAT), peroxidases, such as glutathione peroxidase (GPx), and by peroxiredoxins (Prx). The thiol of a sensitive cysteine in Prx is oxidized to a Cys-sulfenic acid (Prxox) and is reduced by reduced thioredoxin (Trxred). The Cys-sulfenic acid in Prxox can be further oxidized by hydrogen peroxide to Cys-sulfinic acid; it is reduced back to Cys-sulfenic acid by the reduced sulfiredoxin (Srxred) and ATP. There are also mechanisms that supply reducing power, such as pentose phosphate pathway and the thioredoxin and glutathione redox systems (Aguirre *et al.*, 2005).

Polyphenols are a group of antioxidants, found in fruits, vegetables and beverages such as wine, tea and coffee, act as ROS scavengers. Therefore, they are very important for human health, since polyphenols hunt ROS, which are significant cause of some diseases, and inhibit their harmful action. In contrast to these beneficial effects, presence of polyphenols has also detrimental effects on cell health. One of the ROS, hydrogen peroxide, was formed during autooxidation of phenols (Akagawa *et al.*, 2003; Aoshima and Ayabe, 2007). In this case, catalase takes the action by decomposing the formed hydrogen peroxide.

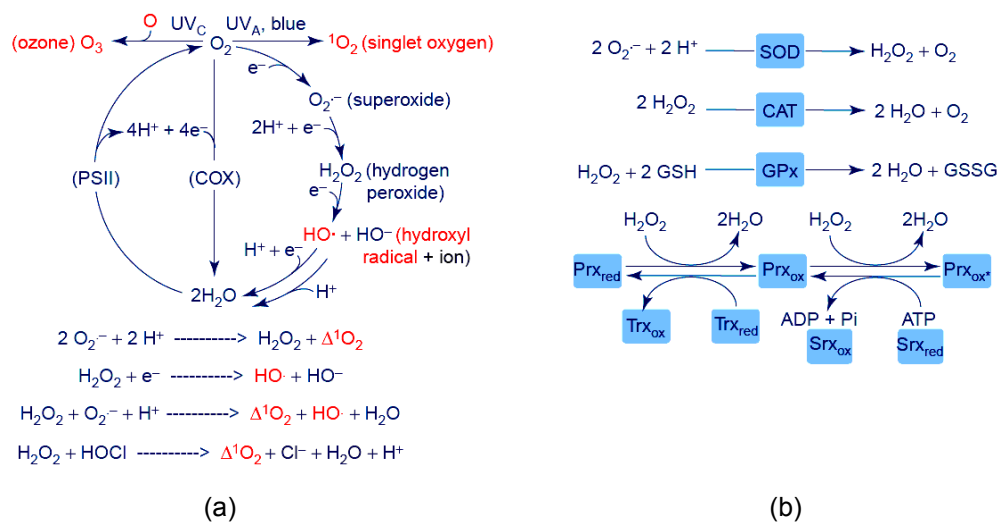


Fig 2.9. Mechanisms of ROS production and enzymatic disposal of superoxide and hydrogen peroxide (a) ROS production, (b) Disposal of superoxide and hydrogen peroxide (Aguirre *et al.*, 2005)

This mechanism can be proposed as the reason of catalase and phenol oxidase activities coexistence. In this study, *S. thermophilum* catalase was found to have an additional phenol oxidase activity, which can be explained by phenol oxidation (phenol oxidase activity), resulting with hydrogen peroxide formation, and its enzymatic decomposition (catalase activity). Similarly, Schrade and Fahimi (2006) reported that discovery of the colocalization of catalase with H<sub>2</sub>O<sub>2</sub>-generating oxidases in peroxisomes which was the first indication of their involvement in the metabolism of oxygen metabolites.

### 2.3. Microorganisms

Microorganisms (or microbial cells) are a large and diverse group of organisms which are present as a single cell or cell clusters. They can be

found almost everywhere on earth where liquid water is present such as deep in the ocean, hot springs, inside rocks etc. (Brock and Madigan, 1988).

Microorganisms are widely used in industry, and gained more attention recently because of the development of genetic engineering. Microbial technology originally began with alcoholic fermentation processes and then microbial processes were developed for the production of pharmaceuticals such as antibiotics and vitamins. Microorganisms are also used for the production of food additives (such as amino acids), enzymes, various organic chemicals, blood plasma substitutes, and steroids such as hormones. Microbial cells themselves may also be a desired product, such as yeast and mushroom. (Brock and Madigan, 1988; Wistreich and Lechtman, 1980).

A single microbial cell is generally able to carry out its growth, energy generation and reproduction independently of other cells, either of the same kind or of different kinds. Other types of cells; cells of animals and plants are different from microorganism because they can not survive alone in nature, they can exist only as parts of multicellular organisms (Brock and Madigan, 1988). Microorganisms can be found almost anywhere in the taxonomic organization, which is the study of classification to explain and identify the diversity of life (Wistreich and Lechtman, 1980). In taxonomy, living systems are classified into three groups: bacteria, archea and eucarya (Figure 2.10).

According to microorganisms-based classification, bacteria are the only prokaryotes, and there are several groups of eukaryotic microorganisms, including algae, fungi and protozoa. Viruses are out of this classification because they are not cells and they do not have a metabolism of their own (Brock and Madigan, 1988).

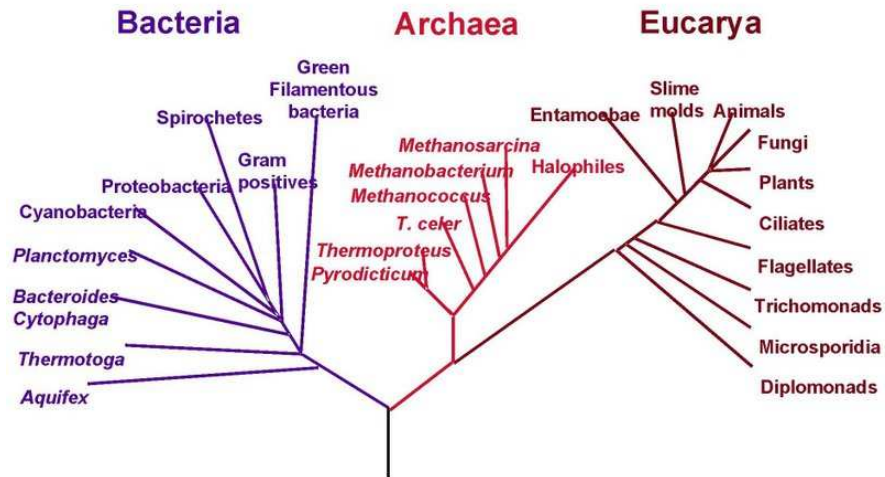


Figure 2.10. Taxonomic groups (Pan, 2005)

### 2.3.1. Fungi

The microorganism used throughout this research, *Scytalidium thermophilum*, was a member of fungi which comprise an extremely important and interesting group of microorganisms. They are widespread in nature, grow well in dark and moist conditions where organic material is available. Fungi do not contain chlorophyll and therefore they depend on other structures and enzyme systems for the energy. They are a group of organisms, being distinctive life form of great practical and ecological importance and containing more than 80,000 species (Wistreich and Lechtman, 1980).

Among 80,000 different types of species, three groups of fungi are of major practical importance: molds, yeasts and mushrooms. Molds are a type of filamentous fungi with a vegetative structure called a mycelium and they are widespread in nature, can be found on stale bread, cheese or fruit. Yeasts are unicellular fungi and do not usually form filaments and mycelium. Mushrooms are filamentous fungi forming large complicated

fruiting bodies, called “mushroom”, which is composed of a large number of individual hyphae (Brock and Madigan, 1980).

#### **2.3.1.1. *Scytalidium thermophilum***

*Scytalidium thermophilum*, also known as *Humicola insolens*, *Torula thermophila* and *Humicola grisea* var. *thermoida* (Figure 2.11), is a thermophilic fungus. *Scytalidium thermophilum* is an important fungus in the production of mushroom compost (Toumela *et al.*, 2000).

Thermophilic fungi grow massively during the last phase of the composting process, from spores that have survived the pasteurization process. They are believed to contribute significantly to the quality of the compost. The effects of these fungi on the growth of the mushroom mycelium have been described at three distinct levels. First, these fungi decrease the concentration of ammonia in the compost, which otherwise would counteract the growth of the mushroom mycelium. Second, they immobilize nutrients in a form that apparently is available to the growth of mushroom mycelium. And third, they may have a growth promoting effect on the mushroom mycelium, as has been demonstrated for *Scytalidium thermophilum* and for other thermophilic fungi (Wiegant, 1992).

### **2.4. Protein Production**

Production is the first step necessary to study the functional and structural properties of a protein. Proteins can be produced or isolated from all living systems, including plants, animals and microorganisms. Two alternative approaches are used today for protein production: they can either be isolated directly from the cell or tissue of the organism or it can be expressed in a host cell such as *Escherichia coli* which results with high level of protein production. Although functional studies require small

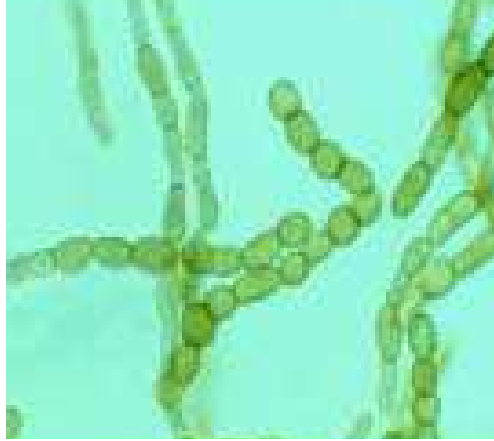


Figure 2.11. *Scytalidium thermophilum* (Cortina, 2004)

amounts of protein (generally less than 1 ng or 1 pmol), structural techniques require higher amounts of proteins (nearly 10 mg) where protein expression in a host cell may be a good alternative (Whitford, 2005).

Microorganisms are widely used sources for protein production. This technique can be carried out in containers ranging from test tubes, flasks and Petri dishes to huge steel tanks. Whatever the material of the container is, the method is called as *in vitro*, meaning “in glass”. Some microorganisms can not be grown *in vitro* and they require the medium conditions of a living animal. This procedure is called *in vivo*. Some microorganisms can be grown both *in vitro* and *in vivo* (Wistreich and Lechtman, 1980).

The production (or culture) medium of a microorganism is designed for its specific growth requirements by testing a wide variety of procedures and nutrient preparations. Different microorganisms require different culture conditions, hence each growth medium induce the production of a specific type of microorganism by inhibiting reproduction of other contaminants

(Wistreich and Lechtman, 1980). In addition to the nutritional circumstances, the environmental conditions such as temperature, pH, water and oxygen availability have also great effects on microorganism growth, differentiation and reproduction (Brock and Madigan, 1988).

The growth conditions of molds and yeasts are similar to those used for bacteria. Most fungi can grow at aerobic conditions but slower than bacteria. Since the growth conditions are similar, bacteria may grow in fungi medium. To prevent this, sugar at high concentrations, antibiotics and dyes can be added to the growth medium (Wistreich and Lechtman, 1980).

#### **2.4.1. Fungal Catalase and Phenol Oxidase Production**

Fungi are reported to be effective producers catalases (Isobe *et al.*, 2006) and various types of catalases of different fungi; *Alternaria alternata* (Caridis *et al.*, 1991), *Aspergillus fumigatus* (Bemmann *et al.*, 1981, Paris *et al.*, 2003, Shibuya *et al.*, 2006), *Aspergillus nidulans* (Calera *et al.*, 2000), *Aspergillus niger* (Kikuchi-Torii *et al.*, 1982, Kulys *et al.*, 2003), *Aspergillus oryzae* (Hisada *et al.*, 2005), *Blakeslea trispora* (Gessler *et al.*, 2002), *Neurospora crassa* (Gessler *et al.*, 2002; Perez *et al.*, 2002),

*Penicillium marneffeii* (Pongpom *et al.*, 2005), *Penicillium simplicissimum* (Fraaije *et al.*, 1996) *Penicillium vitale* (Hudkova *et al.*, 1975, Kulys *et al.*, 2003), *Phanerochaete chrysosporium* (Kwon *et al.*, 2001), *Septoria tritici* (Levy *et al.*, 1992), *Scytalidium thermophilum* (Kulys *et al.*, 2003) and *Thermoascus aurantiacus* (Wang *et al.*, 1998) have been isolated until now.

There are also studies in literature about phenol oxidases isolated from different plant materials and microorganisms. Among microorganisms, fungi were regarded as more important sources of phenol oxidases

because of their extracellular enzyme production capability. A few number of bacteria were also described as phenol oxidase producers but they are very low in compare with the fungi. One of the earliest studies about microbial phenol oxidase was the laccase production by a fungus, *Polyporus versicolor* (Mosbach, 1963). Mushroom (*Agaricus bisporus*) is the main source for tyrosinase and many other fungi were reported as producers of laccase and peroxidase. The first catechol oxidase activity of a fungus has been previously identified by our group (Ögel *et al.*, 2006). Other fungi producing phenol oxidases (generally laccases and peroxidases) are; *Coriolus versicolor* (Katayama *et al.*, 1989), *Myceliophthora thermophila* (Xu *et al.*, 1996) *Neurospora crassa* (Luke and Burton, 2001), *Panus tigrinus* (Cadimaliev *et al.*, 2005), *Phlebia radiata* (Mäkelä *et al.*, 2006), *Pleurotus ostreatus* (Amitai *et al.*, 1998; Palmieri *et al.*, 2003), *Phellinus ribis* (Min *et al.*, 2001), *Polyporus pinsitus* (Xu *et al.*, 1996), *Pycnoporus cinnabarinus* (Schliephake *et al.*, 1997), *Rhizoctonia solani* (Xu *et al.*, 1996), *Rhus vernicifera* (Durante *et al.*, 2004), *Rigidoporus lignosus* (Bonomo *et al.*, 1998), *Scytalidium thermophilum* (Xu *et al.*, 1996), *Termitomyces albuminosus* (Johjima *et al.*, 2003), *Trametes versicolor* (Pazarlıoğlu *et al.*, 2004).

## **2.5. Protein Purification and Characterization**

After production step, it is necessary to purify proteins to study their characteristics and structures. The first step for protein purification is fractionation performed by one or several precipitations induced either by addition of salts such as ammonium sulphate, organic solvents such as acetone, organic polymers such as PEG or by physical treatments such as changing the pH or the temperature (Ducruix and Giege, 1992).

The next step involves chromatographic methods which are more resolute than fractionation. Column chromatography techniques are based on separation by charge (adsorption, anion or cation exchange

chromatography and chromatofocusing), hydrophobicity (hydrophobic and reverse-phase chromatography), size (gel filtration or ultracentrifugation), peculiar structural features or activity (affinity chromatography). High pressure liquid chromatography (HPLC) can also be used which yields higher resolution compared to the standard techniques. Free-flow electrophoresis, preparative isoelectric focusing (IEF) and phase separation are newer alternative methods for protein purification (Ducruix and Giegé, 1992).

There are numerous analytical tools for protein detection and characterization. Gel electrophoresis is the most commonly used method for visualization of the protein content. It can be performed either under non-denaturing (native polyacrylamide gel electrophoresis; Native-PAGE) and denaturing (sodiumdodecyl sulphate polyacrylamide gel electrophoresis; SDS-PAGE) conditions, allowing estimation of the apparent size of the whole protein and its subunits, respectively. Other commonly used characterization technique is the isoelectric focusing (IEF), which is based on the separation according to charge, gives an estimation of the isoelectric point of the protein. To confirm the purity of the protein, electrophoretic titration in a pH gradient can be performed.

Capillary electrophoresis is an alternative technique for homogeneity analysis. Analytical ultracentrifugation and mass spectrometry can be an option for molecular weight determination. HPLC can be used for separation of small amounts of proteins for further analysis. Finally, sequence analysis is a good technique, more sensitive than analysis of amino acid composition of the proteins (Ducruix and Giegé, 1992).

Proteins can also be characterized in terms of their pH and temperature dependencies. Especially for enzymes, the effect of pH and temperature on activity and stability is a measure of its characteristic behavior at different conditions. Determination of the kinetic constants ( $K_m$ ,  $K_{cat}$  and  $V_{max}$ ), studying the inhibitor kinetics and predicting of substrate specificity are the other ways of characterization of the enzymes.

### 2.5.1. Purification and Characterization of Catalases and Phenol Oxidases

A single detailed study appears in literature about purification and characterization of a fungal wild-type thermostable catalase. Wang *et al.* (1998) performed the purification by ethanol precipitation, anion exchange and gel filtration chromatographies with a 29.9% yield and 5.1 fold purification. The molecular weights of the native enzyme and its subunits were determined by gel filtration as 330 and 75 kDa, respectively. The enzyme was verified to be a homotetrameric hemecatalase with one iron per subunit. It was 11% glycosylated with a pI of 4.5. The optimum pH was found in the range of 6-10 and the optimum temperature was 70 °C. The  $K_m$  and  $K_{cat}$  of catalase were  $4.8 \times 10^{-2}$  M and  $1.07 \times 10^5$  s<sup>-1</sup> for hydrogen peroxide, respectively. Potassium cyanide and sodium azide strongly inhibited catalase activity.

Catalase of another fungus, *Aspergillus niger*, was studied by Calera *et al.* (2000). Catalase was purified to homogeneity by anion exchange, hydrophobic and gel filtration chromatographies and found to have a molecular weight of 360 kDa with four glycosylated subunits. The pI was found as 3.5.

*Aspergillus niger* catalase was purified and characterized by Mosavi-Movahedi *et al.* (1987). Purification was performed by gel filtration and enzyme was further characterized by physical techniques including sedimentation rate, by equilibrium methods and photon correlation spectroscopy.

The inhibition kinetics of *Aspergillus niger*, *Penicillium vitale* and recombinant *Scytalidium thermophilum* catalase was studied by Kulys *et al.* (2003) in the presence of hydroxylamine. The inhibition kinetics exhibited a biphasic character where hydroxylamine was inactive in the first phase. In the second phase, a reversible inhibition was observed and *Scytalidium thermophilum* catalase inhibition was the highest.

Goldberg and Hochmann (1989) purified catalase from a bacterium *Klebsiella pneumoniae* by hydrophobic chromatography and dialysis with 50 % yield and 97.3 fold purification. The enzyme was a dimer with a total molecular weight of 80 kDa and contains heme as prosthetic group. Catalase was active in a pH range of 2.8-11.8 and stable when treated with ethanol and chloroform.

Human catalase was expressed in *Pichia pastoris* and purified by Shi *et al.* (2007). Secreted catalase was purified to a purity of 95% by ammonium sulphate fractionation, anion exchange chromatography and macro-prep ceramic hydroxiapatite with a yield of 60%.

Many studies were done and reported in the literature about microbial phenol oxidases (mainly laccases). One of the earliest studies about microbial phenol oxidase was the laccase production by a fungus, *Polyporus versicolor*, and the purification of the enzyme was performed by Mosbach (1963). Two forms of laccase (A and B) have been purified from the culture medium of *Polyporus versicolor* after induction of enzyme formation with 2,5-xylydine. The purification procedure involves ammonium sulfate precipitation, chromatography on hydroxylapatite to remove contaminating pigments, and zone electrophoresis to separate laccase A and B. The purified enzyme gives single symmetrical peaks in free electrophoresis (A) and in the ultracentrifuge (A and B). The molecular weight of laccase A has been estimated to be approximately 60 kDa. It contains 14% carbohydrate and 0.44% copper, corresponding to approximately 4 atoms per molecule.

Laccase production by a cellulolytic fungus, *Chaetmium thermophilium*, was investigated by Chefetz *et al.* (1998). Laccase was purified by ultrafiltration, anion-exchange chromatography and affinity chromatography. The purified enzyme was identified as a glycoprotein with a molecular mass of 77 kDa and an isoelectric point of 5.1.

Amitai *et al.* (1998) performed purification of laccase produced by the white rot fungus *Pleurotus ostreatus*. The concentrated extracellular medium was purified by anion exchange and gel filtration column chromatographies. A single band on PAGE detected after purification.

Cambria *et al.* (2000) studied the production, purification and characterization of extracellular laccase from *Rigidoporus lignosus*, a white basidiomycete. After production, laccase was purified by ultrafiltration, ammonium sulphate precipitation and anion exchange chromatography with a purification fold of 23.7 and a yield of 15.0%. SDS-PAGE of this enzyme showed a single band with a molecular weight of 54 kDa. The isoelectric focusing gel indicated the presence of two bands which exhibited isoelectric points of 3.2 and 3.25, respectively.

Min *et al.* (2001) investigated the white-rot fungus *Phellinus ribis* producing a single form of laccase, which was purified to apparent electrophoretic homogeneity from cultures induced with 2,5-xylydine. This protein was a dimer, consisting of two subunits of 76 kDa as determined by SDS-PAGE. The laccase appeared to be different from other known laccases by the UV-visible absorption spectrum analysis. One enzyme molecule contained one copper, one manganese and two zinc atoms.

Palmieri *et al.* (2003) also studied laccase produced in copper supplemented cultures by *Pleurotus ostreatus*. Secreted proteins were precipitated by addition of ammonium sulphate up to 80% saturation and, after extensive dialysis, loaded onto anion exchange and gel filtration chromatography columns, respectively. Finally, 8 fold purification was observed with 4.7% recovery. Atypical laccase isoenzymes from copper supplemented *Pleurotus ostreatus* cultures were determined. Both the native proteins were found to be constituted by a large subunit 67 kDa and a small subunit 18 or 16 kDa.

## **2.6. Protein Three-Dimensional Structure Determination**

Protein with a sufficiently high purity can be used in structural crystallization experiments. Protein (or any other biological macromolecule) three-dimensional structure resolution by X-ray analysis involves five steps after purification (Ducruix and Giegé, 1992):

- I. Crystallization
- II. Data measurements
- III. Phase determination
- IV. Electron density map computation
- V. Model refinement

### **2.6.1. Protein Structure**

Depending on their complexity, proteins can be described by four levels of structure. The sequence of amino acids along the polypeptide chain is called as primary structure of the protein. Despite being related to each other and having similarities in the sequence, each protein is defined by a unique sequence of amino acids. Primary structure leads to secondary structure, such as alpha ( $\alpha$ ) helix, beta ( $\beta$ ) sheet, turns and loops, which refers to regularities in local conformations in the polypeptide chain or spatial relationship of closely located amino acids in the backbone (Figure 2.12).

Tertiary structure represents the completely folded polypeptide chain. It is formed by the interaction of non-neighboring amino acids which are widely separated in the polypeptide chain. Tertiary structure describes the folding of the protein and the fold arises from linking together secondary structures forming a compact globular molecule. Elements in secondary structure interact by hydrogen bonds as in  $\beta$  sheets, disulfide bridges,

electrostatic interactions, van der Waals interactions, hydrophobic contacts and hydrogen bonds between non-backbone groups to form the tertiary structure. Some proteins contain more than one polypeptide chain, where each of these chains is called a subunit. The spatial arrangement of these subunits and the nature of their interactions describe the quaternary structure. The interactions are similar to those responsible for tertiary structure; disulfide bonds, hydrophobic interactions, charge-pair interactions and hydrogen bonds, with the exception that they take place between more than one polypeptide chains. The simplest type of quaternary structure is a dimer which consists of two subunits, where the subunits can be identical or non-identical. A dimer with identical subunits is called as homodimer. More complicated forms such as trimers, tetramers and very complex forms containing dozens of different subunits of quaternary structure are also present. (Horton *et al.*, 1996; Berg *et al.*, 2002; Whitford, 2005).

### **2.6.2. Sample preparation for crystallization**

Proteins are extracted from biological mixtures and therefore it is important to purify the protein to homogeneity before crystallization. Not only the purity, all factors that create heterogeneity such as proteolytic cleavage, denaturation, contamination and oxidation must be taken into account (Howard and Brown, 2002). The purity required should be of crystallography grade, which means, proteins should not only be pure in terms of lack of contaminants, they should also be conformationally pure (Ducruix and Giegé, 1992).

In fact, purity is not an absolute requirement for getting crystals because crystals can be grown also from mixtures and this technique is used as an alternative protein purification method. But the crystals grown from those mixtures are generally small, not well shaped and not suitable for diffraction analysis. It is believed that the poor purity is the main reason

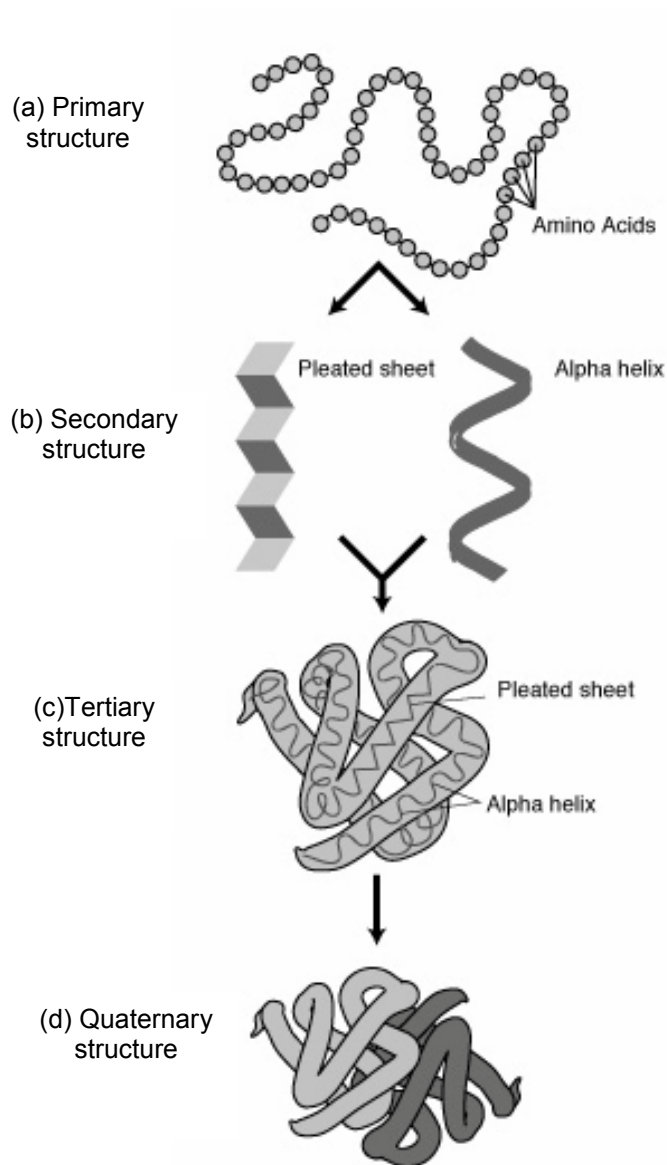


Figure 2.12. Protein structure (a) Primary structure, (b) Secondary structure, (c) Tertiary structure, (d) Quaternary structure (Millard, 2006)

for unsuccessful crystallization. The main aim of x-ray crystallography is to get high-quality monocrystals of appreciable size and this is only possible if the crystals are grown from a pure protein solution (Ducruix and Giegé, 1992).

### **2.6.3. Protein crystallization**

Protein crystallization is an old technique which has been used for many years by biochemists to isolate and purify proteins from solutions. At the beginning of 20<sup>th</sup> century, studies on protein structure determination by crystallography have been started and especially x-ray crystallography has been used as a powerful technique (Blundell and Johnsson, 1961; Howard and Brown, 2002).

Production of protein crystals rely on the controlled and ordered precipitation of proteins and this is one the difficult and slowest steps in structural studies. In some cases, it may require months for sufficiently large crystals to grow (Branden and Tooze, 1992).

To achieve the assemble of protein molecules into a periodic lattice from super-saturated solutions, the starting concentration of the pure protein should be between 0.5 and 200 mg/ml. Adding reagents (precipitants) reduce protein solubility by disturbing protein-solvent interactions so that equilibrium shifts in favor of protein-protein association. This results protein to precipitate, and under controlled conditions, precipitation occurs in crystal form (Whitford, 2005). A number of substances cause proteins to precipitate. The water-soluble polymer polyethylene glycol (PEG) is widely used because it is a powerful precipitant and a weak denaturant (Rhodes, 2000). Interactions between molecules can be controlled by several factors (Howard and Brown, 2002):

- I. Temperature (affects solubility)
- II. pH (affects both solute and solvent)
- III. Salts (salt-in or salt-out effects)
- IV. Hydrogen-bond competitors (such as urea and guanidium salts)
- V. Hydrophobic additives (nonionic detergents)
- VI. Organic solvents (modification of dielectric constant)

Depending of these parameters, solubility of protein changes and the change can be represented by a two-dimensional solubility diagram (Figure 2.13). Solubility of the protein is expressed as a function of one parameter by keeping all other parameters constant. The solubility curve divides the undersaturated and supersaturated regions. At concentrations corresponding to the solubility curve, the saturated solution is in equilibrium with the crystallized protein. Under the solubility curve, protein solution is undersaturated where the protein can not crystallize. Above the solubility curve, protein solution is supersaturated and this zone can be divided into three regions. In precipitation zone, protein is very concentrated and precipitates from the solution in an amorphous state rather in the crystalline form. In nucleation zone, protein separates under crystalline form but near the precipitation region, crystals may occur as microcrystals with the amorphous precipitate. In metastable zone, the supersaturated solution may not nucleate unless the solution is mechanically shocked or a very small crystal is introduced as a "seed". Metastable zone is ideal for growth of crystals (Ducruix and Giegé, 1992).

Examples of crystallization experiments results depending on the undersaturation, saturated and supersaturated conditions were shown in Figure 2.14. Examples of well-ordered and not well-ordered crystals were shown in Figure 2.15 and 2.16, respectively.

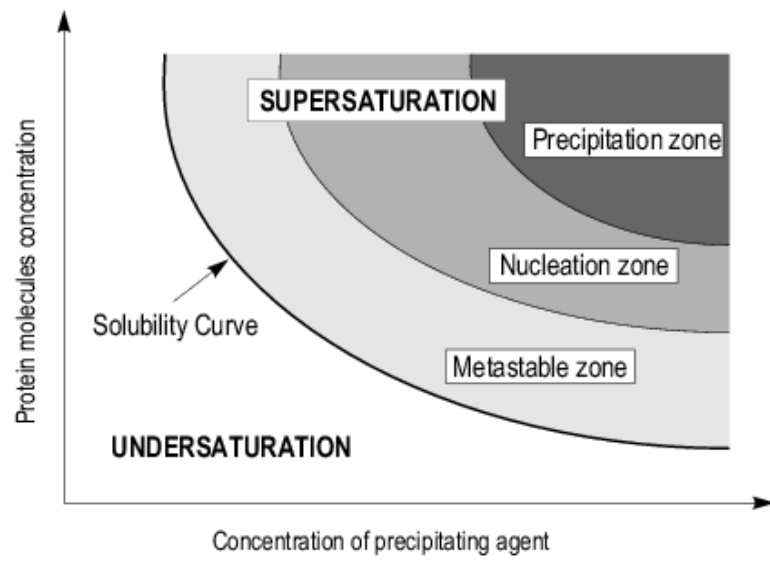


Figure 2.13. Two-dimensional solubility diagram illustrated by the change of protein concentration with precipitating agent concentration (Chirgadze, 2004)

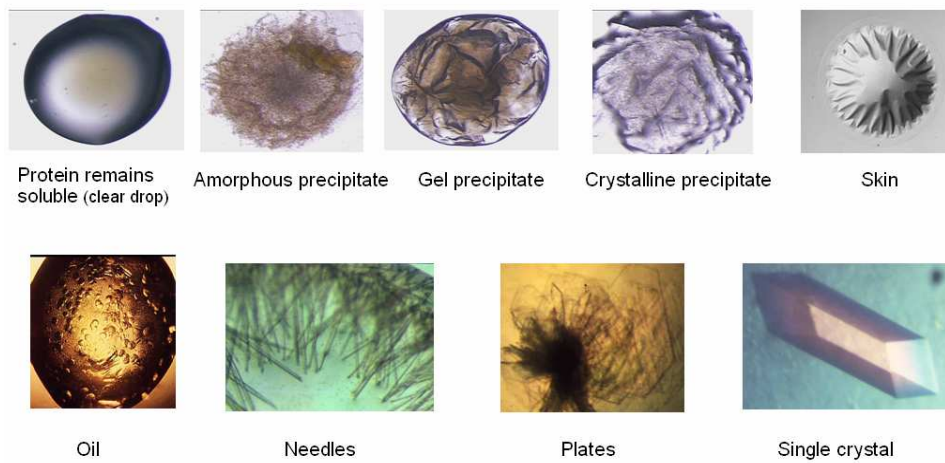
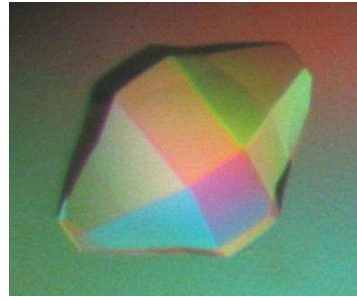


Figure 2.14. Examples of crystallization experiment results (Hampton Research, 2005)



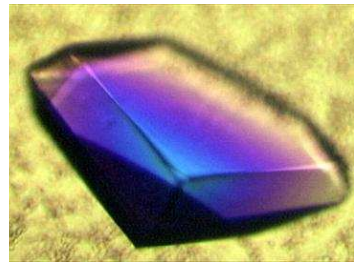
(a)



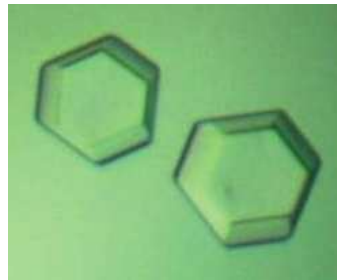
(b)



(c)



(d)



(e)

Figure 2.15. Examples of well-shaped crystals (a) Crystals of CsoR, a Cu sensing transcriptional regulator from *M. tuberculosis* by Arati Ramesh, USA, (b) Crystal of mouse Aurora A by Michael J. Romanowski, USA, (c) Crystals of a fungal iron containing dioxygenase by Tjaard, The Netherlands, (d) Crystals of Human DNA recombination factor, Dmc1 by Takashi Kinebuchi RIKEN, Japan, (e) Crystals of *Escherichia coli* tRNA Gly acceptor-stem microhelix by Volker Erdmann, Germany (Hampton Research, 2005)

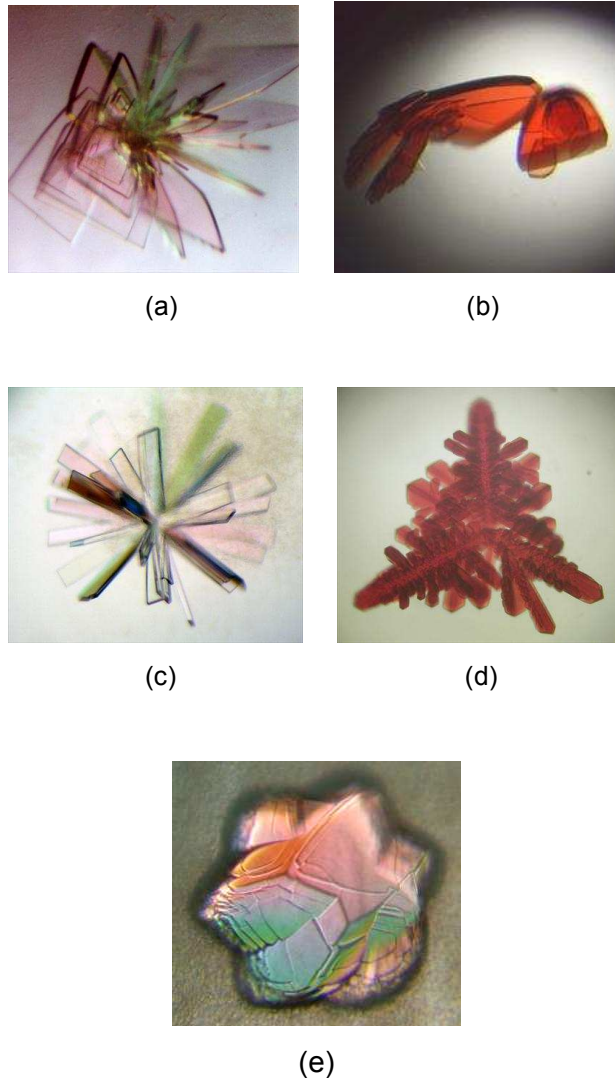


Figure 2.16. Examples of not well-shaped crystals, (a) ATPase-domain complex of HlyB by Jelena Zaitseva and Lutz Schmitt, Germany, (b) A gold fish crystal of a heme containing protein by Lianhua Xu & Shinya Fushinobu, Japan, (c) A star of *H. influenzae* carbonic anhydrase crystals by Roger S., USA, (d) Crystals of nitrite reductase from *Thioalcalivibrio nitratireducens* by Ella Slutsky A.N.Bach, Russia, (e) Picturesque crystal of multidrug efflux pump AcrB by Markus Seeger, Switzerland (Hampton Research, 2005)

It is sometimes difficult to simultaneously optimize the conditions for nucleation and growth of the crystal because the ideal conditions for nucleation and growth might differ. In this case, a new strategy involving the separate optimization of these processes should be developed. This can be accomplished by seeding, in which crystals are transferred from nucleation conditions to those that will support only growth (Figure 2.17). The size and quality of the crystals are generally altered by this method (Weber, 1997). Microseeding and macroseeding are the most commonly used techniques of homogeneous seeding. Microseeding involves the transfer of microscopic crystals from a seed source to a non-nucleated protein solution. In macroseeding, pre-grown crystals are washed and introduced individually into a pre-equilibrated protein solution (Ducruix and Giegé, 1992).

#### **2.6.3.1. Crystal Systems**

The word 'crystal' originates from the Greek word 'krystallos', meaning 'clear ice', because crystals are chemically well defined, many of them are transparent and have glittering appearance like ice. Crystals are regular three-dimensional array of atoms, ions or molecules and are beautiful geometrical solids with regular faces and sharp edges (Ducruix and Giegé, 1992).

A crystal is composed of many small identical units, called unit cells. They are the building blocks of a crystal and are repeated infinitely in three dimensions to form a crystal lattice (Figure 2.18) (Whitford, 2005).

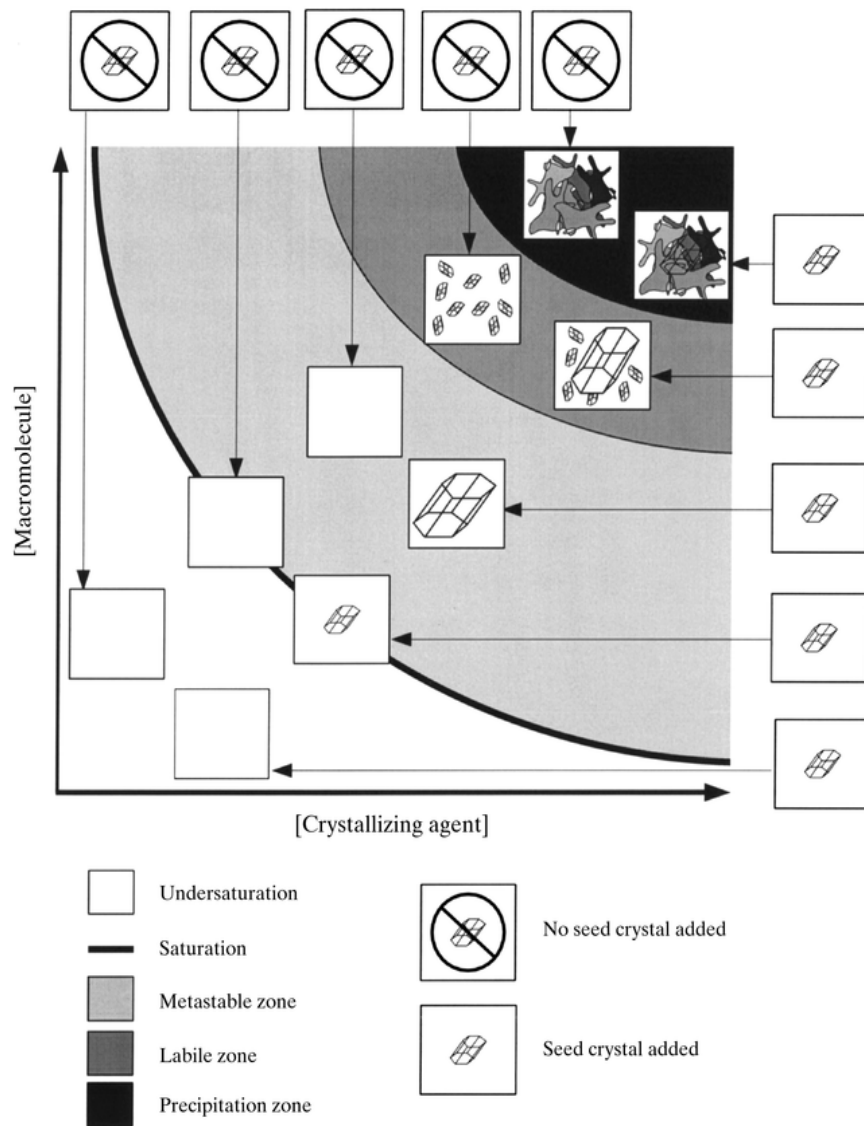


Figure 2.17. Crsytal nucleation conditions (Luft and DeTitta, 1999)

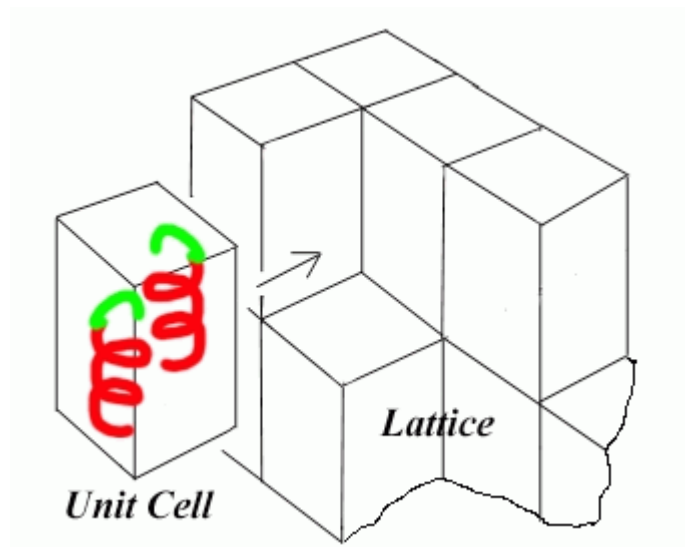


Figure 2.18. Crystal lattice (Rupp, 2006)

There are seven types of crystal systems in nature; triclinic, monoclinic, orthorhombic, tetragonal, rhombohedral, hexagonal and cubic (Figure 2.19) and each unit cell is characterized by three vectors;  $a$ ,  $b$  and  $c$ , that form the edges of parallelepiped. The unit cell is also defined by the angles between the vectors;  $\alpha$ ,  $\beta$  and  $\gamma$  (Figure 2.20) (Whitford, 2005). The unit cell may contain one or more than one molecule. For the unit cells including more than one molecule, the “asymmetric unit” is defined as the basic repeating object which is related to all the other identical objects in the unit cell by the operation of the symmetry elements and the contents of the other unit cells by the translations  $a$ ,  $b$  and  $c$  (Blundell and Johnson, 1976).

In 19th century, Auguste Bravais has recognized different arrangements within an unit cell, which are named after him, Bravais lattices. There are fourteen different Bravais lattices in three-dimensions (Figure 2.21) (Whitford, 2005).

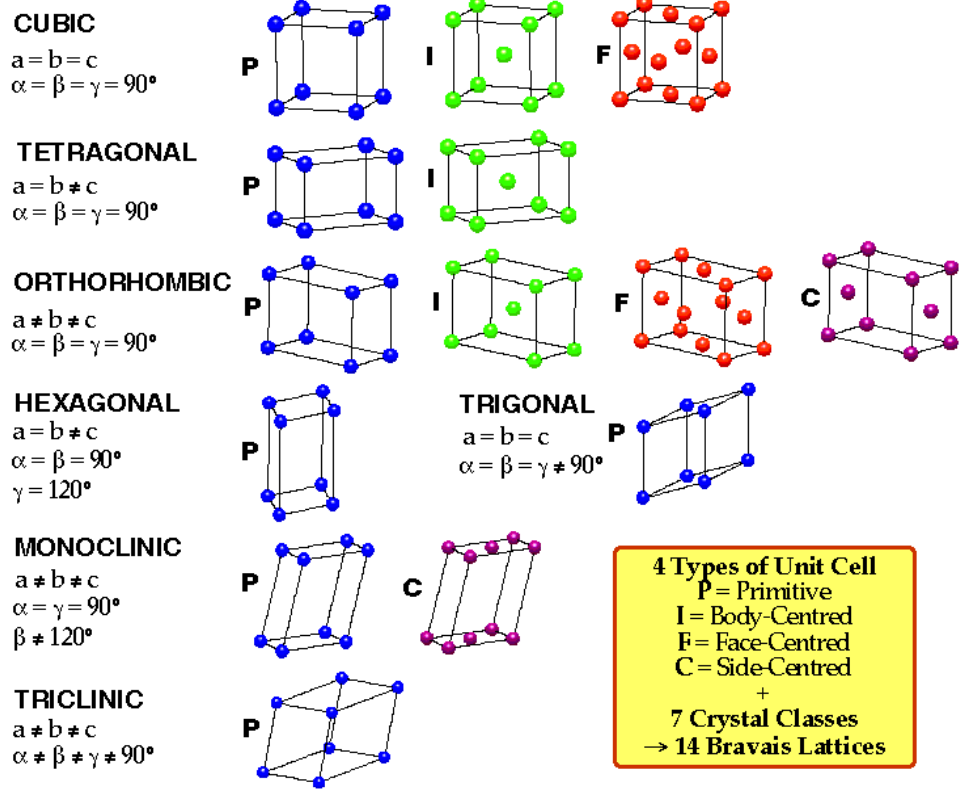


Figure 2.19. Types of crystal systems (University of Oxford, 2006)

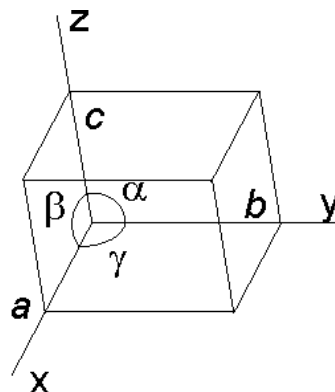


Figure 2.20. The unit cell (Powell, 2007)

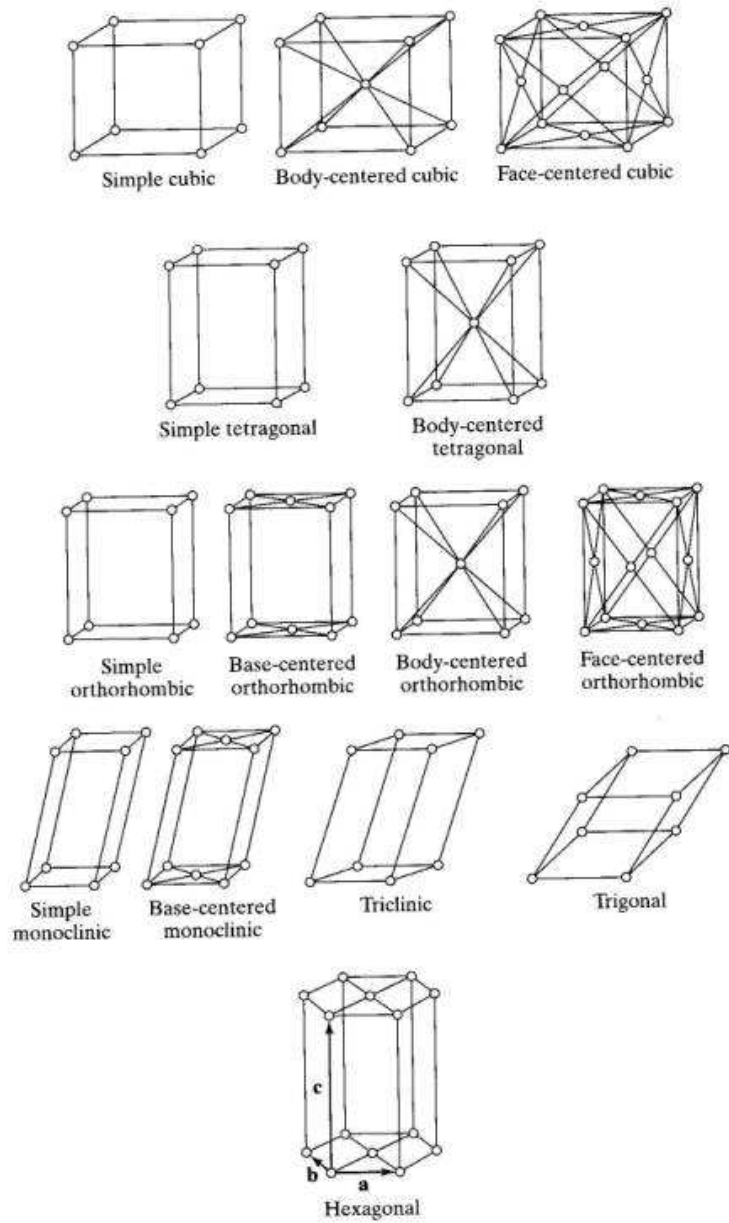


Figure 2.21. Bravais lattices (University of California, 2006)

### 2.6.3.2. Differences in Crystal Systems of Proteins and Conventional Molecules

Despite having comparable morphologies and appearance, crystals of proteins and conventional low molecular weight compounds have practical differences as summarized in Table 2.1 (McPherson, 2004). As a result of the practical drawbacks of protein crystals, it is always more difficult to grow and analyze them.

### 2.6.3.3. Protein crystallization techniques

The main aim of crystallization methods is to bring the protein solution to the supersaturation state and provide the suitable environment for crystal growth. There are different crystallization techniques such as batch

Table 2.1. Practical differences of protein and conventional low molecular weight compound crystals

Protein crystals	Conventional low molecular weight compound crystals
Weak lattice forces	Firm lattice forces
Limited in size	Highly ordered
Very soft and crush easily	Physically hard and brittle
Sensitive to temperature (cryo conditions should be used)	Easy to manipulate
Disintegrate if exposed to air	Can be exposed to air
Weak optical properties	Strong optical properties
Poor X-ray diffraction	Intense X-ray diffraction
Extensive damage under radiation	Stable under radiation
Slow kinetics for crystallization	Fast kinetics for crystallization

crystallization, liquid-liquid diffusion, dialysis and vapor diffusion (Drenth, 1999). Since the specific supersaturation requirements differ from protein to protein, a crystallization methodology involving variations should be developed (Weber, 1997).

In most of the crystallization techniques, a mother liquor is needed. Mother liquor is the solution which contains all the crystallization chemicals; buffer, salt, crystallizing agent (precipitant) etc., except protein. Crystallization occurs in the solution, in which protein and the mother liquor is mixed (Ducruix and Giegé, 1992).

In batch crystallization, the basic principle is that the precipitant is instantaneously added to the protein solution to bring the solution to a state of high supersaturation (Drenth, 1999). Crystals are expected to grow gradually from this solution after standing a few hours or perhaps a few months. This technique is used successfully for large lysozyme, ribonuclease and trypsin family enzyme crystals but there is a lack of good control of crystal growth. Therefore, this technique is useful for proteins whose nucleation and growth velocities are low or for the proteins which may give ordered crystals at even high growth rates (Blundell and Johnson, 1976).

Liquid-liquid diffusion is a crystallization technique in which the protein solution and the solution containing the precipitant (mother liquor) are layered on top of each other in a small-bore capillary. A range of supersaturation is created around the interface of the solutions and the crystals are expected to grow in this supersaturated region (Drenth, 1999).

Dialysis is a type of batch crystallization. In this method, proteins are kept in a dialysis membrane. Since the volume is constant, protein concentration does not change during operation. Precipitation and crystallization of the protein is maintained by changing the bulk solution.

This alters the protein solubility to achieve supersaturation levels required for nucleation and growth of the protein crystal. Dialysis is a suitable technique for crystallization at low ionic strength and in the presence of volatile reagents (Weber, 1997).

Vapor diffusion techniques are the most widely used crystallization methods among others in which proteins are crystallized with increasing the concentration of protein by evaporation of the solvent. The solvent gradually transferred through vapour phase from the protein solution to the mother liquor until the equilibrium is reached. Crystals tend to grow from the protein solution as it becomes more concentrated (Blundell and Johnson, 1976).

There are three different vapor diffusion methods; hanging drop, sitting drop and sandwich drop vapor diffusion. In hanging drop vapor diffusion, crystallization drops are prepared by mixing the protein solution and the mother liquor on a siliconized microscope glass cover slip. The slip is placed upside down on the crystallization well which is partially filled with the mother liquor (Figure 2.22-a). In sitting and sandwich drop vapor diffusion, as shown in Figure 2.22-b and Figure 2.22-c respectively, the crystallization drop is prepared as same as in hanging drop technique and put on a bridge in the well, not on the cover slip. These methods are preferred in a case where the protein solution has a low surface tension and tends to spread out over the cover slip (Ducruix and Giegé, 1992; Drenth, 1999).

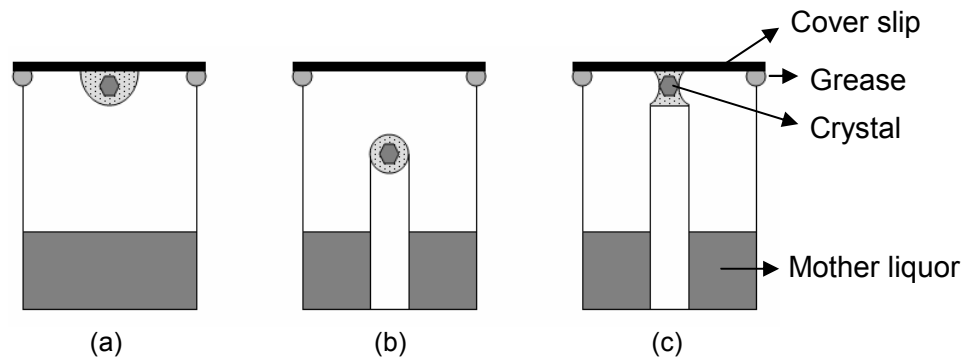


Figure 2.22. Vapor diffusion techniques; (a) Hanging drop, (b) Sitting drop, (c) Sandwich drop

#### 2.6.3.4. Storing Protein Crystal Under Cryo-Conditions

Once the crystal is produced, it should be stored until performing structural analysis. Since protein crystals are very sensitive to temperature changes and generally get damaged under radiation exposure, cryo-crystallography (cooling) was developed to protect the crystal and collect better data for structural studies. The mechanism behind that was explained by the increase of the internal order of parts of the protein at cryo-conditions which are mobile at room temperature (Ducruix and Giegé, 1992).

The most commonly used cryo-protective solvents are ethylene glycol, polyethylene glycol, MPD. In some cases, crystals are transferred into oil before freezing. Soaking of cryo-protectants and freezing process should be performed very carefully since it may lead to changes in cell dimensions and increase the mosaicity which causes low quality of structural data (Ducruix and Giegé, 1992).

#### **2.6.4. Protein Crystal Structure Analyzing Techniques**

Crystal structures are analyzed by three main techniques which are X-ray radiation, nuclear magnetic resonance (NMR) spectroscopy and electron microscopy. According to the information given in Protein Data Bank (PDB) for 15<sup>th</sup> of May 2007, 86.1% of the solved protein structures were predicted by X-ray analysis. The percentages of NMR and electron microscopy techniques are 13.5 and 0.3%, respectively.

##### **2.6.4.1. Electron Microscopy**

Electron microscopy (EM) is based on determining three-dimensional structure from a series of two-dimensional images or projections of a protein's electron density formed at an image plane. This technique is generally used for determining structures of proteins which can not be analyzed by X-ray crystallography or NMR spectroscopy (Whitford, 2005).

In early EM studies, samples were fixed using cross-linking agents followed by staining heavy metal compounds. This method was not suitable for all protein samples because they mostly lost their stabilities. To overcome this problem, EM at lower temperatures, about 100 K, has been developed and called as cryo-electron microscopy (cryo-EM). This technique relies on electron diffraction by particles immersed in a frozen lattice and widely used recently. Although cryo-EM can not produce high resolution data compared to X-ray diffraction and NMR spectroscopy, it has an advantage of requiring small amount of sample preparation and being suitable to very large protein complexes. And generally, the results of X-ray crystallography or NMR spectroscopy can be assimilated into cryo-EM data to built models based on more than one structural technique (Whitford, 2005).

#### **2.6.4.2. Nuclear Magnetic Resonance Spectroscopy**

Nuclear magnetic resonance (NMR) spectroscopy is the second widely used technique for determination of protein structure and it is a more recent method than X-ray crystallography. The chemical environment of an atomic nucleus, having a magnetic moment or spin, can be probed by NMR and the information can be used to determine the distances between atoms in the molecule. These distances can give the data required to predict the three-dimensional structural model of the molecule (Branden and Tooze, 1991).

In NMR spectroscopy, signals are obtained by placing dissolved samples into strong and homogeneous magnetic fields, which arise from the use of superconducting materials at about 4 K. Outcoming signals are detected by a probe and subjected to further processing which includes storage of raw data as well as Fourier transformation. This experimental process may take about 3-4 days. The disadvantage of this method is the long experimental process, in which proteins lose their stability. Another bottle neck of NMR is that this method is useful for proteins below 20 kDa, thus bigger proteins need to be analyzed by a different technique (Whitford, 2005).

#### **2.6.4.3. X-Ray Diffraction**

X-rays are electromagnetic radiation generated at short wavelengths with high energy. They are emitted when electrons move from a higher to a lower energy state (Branden and Tooze, 1991). X-rays are used in crystal studies because their wavelength is comparable to the planar separation (typically 0.15 nm or 1.5 Å) of atoms in a crystal lattice and the unit used is Angstrom. The data collected in X-ray analysis is the electron density of the protein since X-rays are scattered by electrons (Ducruix and Giegé, 1992; Jones *et al.*, 1996).

X-rays are generated in the laboratory by accelerating electrons into a metal plate, the anode. It emits the electrons at a specific wavelength, called monochromatic X-rays. Generally, copper is used as the anode with a characteristic radiation wavelength of 1.542 Å. Due to the high voltage, the anode heats up and therefore cooling becomes necessary. The rotating anode generator is used to achieve efficient cooling (Branden and Tooze, 1991; Ducruix and Giegé, 1992).

More powerful X-ray beams can be produced by sending by a magnet, called synchrotron radiation ring (Figure 2.23). This source can generate X-ray beams some thousand times more intense than a rotating anode generator. Polychromatic X-ray beams are produced in the synchrotron with a radiation wavelength of 0.2-2 Å. The advantage of a synchrotron facility over the rotating anode generator diffraction experiments is the strong beams allowing very short exposure times and high quality of data even with small crystals. The main drawback of synchrotron facility is that they are centralized facilities and difficult to access for preliminary work (Branden and Tooze, 1991; Ducruix and Giegé, 1992).

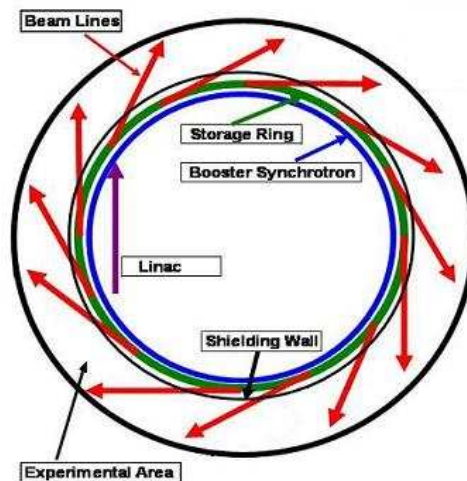


Figure 2.23. Synchrotron radiation ring (Laboratory of Synchrotron Light, 2007)

The theory of relation between X-ray diffraction pattern obtained in the experiment and the nature of the crystal was explained by Lawrence Bragg in the early days of crystallography. Crystals are composed of planes and the X-rays that are reflected from these planes travel different distances. Bragg showed that diffraction only occurs when the difference in distance is equal to the X-ray beam wavelength. This distance is dependent on the angle between the primary beam and the planes, called as reflection angle. The Bragg's law states the relationship between the reflection angle ( $\theta$ ), the distance between the planes ( $d$ ) and the wavelength ( $\lambda$ ) by the equation;  $2d \sin \theta = \lambda$ . Bragg's law can be used to determine the unit cell size (Figure 2.24) (Branden and Tooze, 1991).

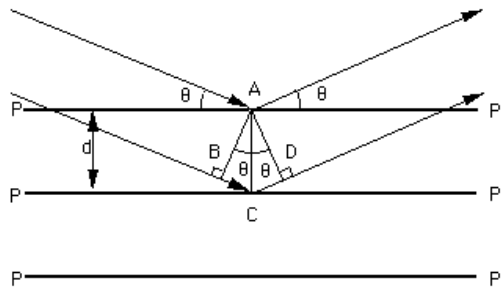


Figure 2.24. Bragg's law (Herrerros, 1996)

In diffraction experiments, parallel and narrow X-ray beams are produced by X-ray sources and directed onto the crystal. They are diffracted by the crystal and recorded either on a film, which is the classical method, or by an electronic detector as shown in Figure 2.25. An example of X-ray diffraction pattern was shown in Figure 2.26. The film is measured and digitalized by scanner, whereas electronic detectors collect the X-ray diffraction data and directly transfers them into a computer in a digitalized form. The mathematical tool used to extract information from diffracted spots is the Fourier transform (Branden and Tooze, 1991).

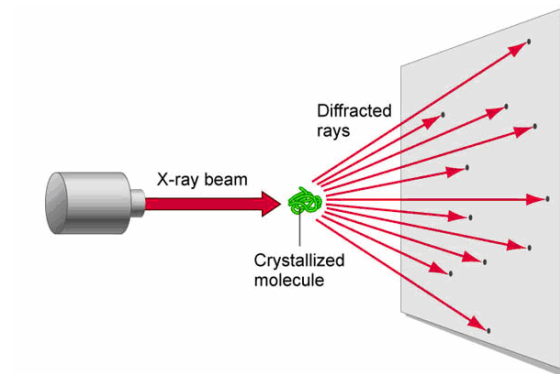


Figure 2.25. X-ray data collection (Mallery, 2007)

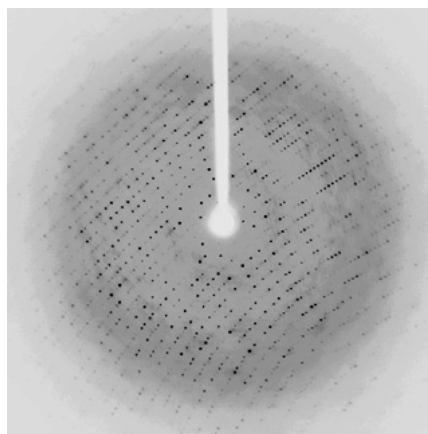


Figure 2.26. An example of X-ray diffraction pattern (a bacterial carbonic anhydrase) (Rowlett, 2005)

The diffraction data collected from the protein crystals are used to calculate the electron density maps. The most important factor affecting the map quality is the resolution of the diffraction data, which in turn depends on how well-ordered the crystals are. The resolution is measured in Å units; the smaller this value is, the higher the resolution

and therefore the greater the amount of structural detail of the protein molecule can be seen (Figure 2.27) (Branden and Tooze, 1991).

Structure solving by X-ray crystallography involves seven main steps to get the final structure model; protein production and purification, crystallization, X-ray diffraction and data collection, data processing, structure refinement, model building, model validation (Figure 2.28) (O'Reilly *et al.*,2006). First four steps were explained previously in detail. Other steps necessary to get the structure will be described in this section.

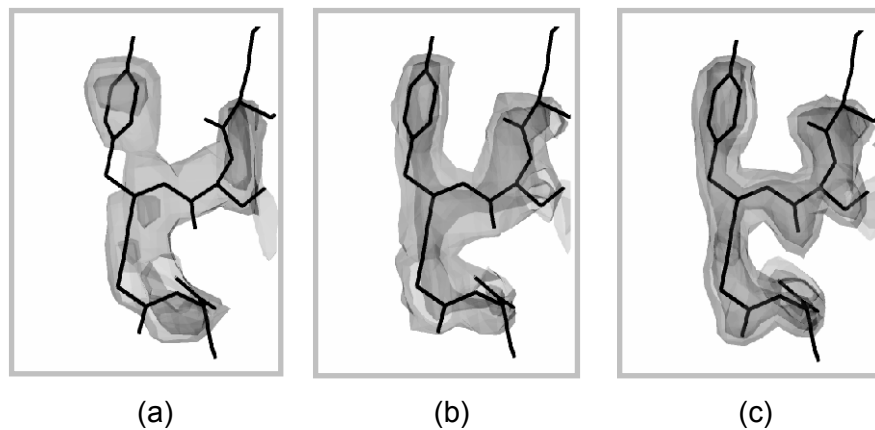


Figure 2.27. Electron density map at different resolutions (a) Low, (b) Medium and (c) High (DiMaio, 2007)

To extract the structural data encoded in the X-ray diffraction data, collected from a crystal in a synchrotron facility can be computationally processed and analyzed by structure determination packages ([Table 2.2](#)). The development of integrated structure building, optimization and validation software has enforced more automatic structure refinement,

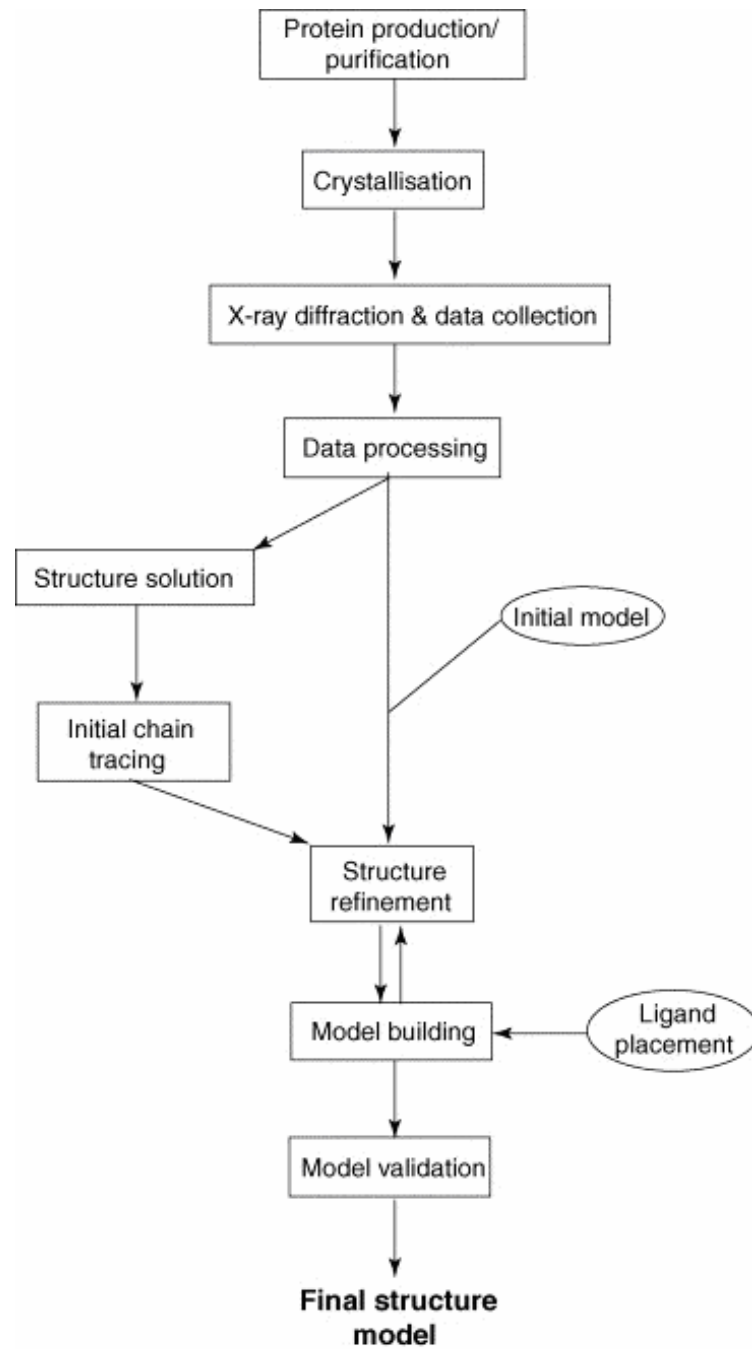


Figure 2.28. Flow diagram showing the processes necessary for progressing from gene to X-ray crystal structure (O'Reilly *et. al.*, 2006).

although some manual interference is still required. The main question in computational structure determination studies is to reduce and ideally eliminate the need for manual interference in the form of structure rebuilding (O'Reilly *et al.*, 2006).

Most X-ray structures are determined at a resolution between 1.7-3.0 Å. But, it is not possible to determine the structure from a map at this resolution, without having the amino acid sequence data. Electron density maps should be interpreted by fitting the known amino acid sequences into electron density regions, where individual atoms can not be solved (Branden and Tooze, 1991).

In the early days of protein crystallography, solving the structure was laborious and time consuming. Data collection a few years ago, which required many months of work, can now be collected in a few days using computational technology. The technical advances used today have greatly facilitated use of X-ray crystallography but one significant problem still remains; growing crystals that diffract to high resolution. Some proteins give excellent crystals after the first few trials, whereas some proteins never give crystals (Branden and Tooze, 1991). Therefore, the success and time schedule X-ray crystallography research is always unknown at the beginning of the study.

Catalase was subject of many structural studies, where the first catalase structure solved and deposited in Protein Data Bank (PDB) database was a monofunctional catalase from *Penicillium vitale*. The study covered the three-dimensional structure of catalase from *Penicillium vitale* at 2.0 Å resolution and was published by Vainshtein *et al.* in 1996. Bovine (*Bos taurus*) catalase structure was also one of the earliest researches of catalase structures. Currently, 74 structural studies about catalases from 19 different sources are in PDB database. The distribution of all catalase structures and their sources given in PDB were summarized in Table 2.3.

Table 2.2. Software packages used for protein X-ray crystallography  
(O'Reilly *et al.*, 2006)

Program/package	Function
Data processing	
Crystalclear/D*trek	Data reduction/scaling
Mosfilm/scala	Data reduction/scaling
HKL2000	Data reduction/scaling
XDS	Data reduction/scaling
Structure determination and refinement	
Shake and bake	Heavy atom location
Shelxs/shelxd	Direct methods
Solve	Heavy atom location
	Phase refinement
Sharp	ML phase refinement
CCP4	'Complete' structure solution suite
CNS/CNX	'Complete' structure solution suite
Phenix	'Complete' structure solution suite
Phaser	Molecular replacement
Molrep	Molecular replacement
Amore	Molecular replacement
Refmac	Structure refinement
CNS/CNX	Structure refinement
Buster	ML structure refinement
Arp/warp	Automatic model building
Resolve	Automatic model building
Textal	Automatic model building
AutoSolve®	Automated ligand fitting
Graphical model building	
Quanta includes X-ligand	Graphical model building semi-automatic ligand fitting
Coot	Graphical model building
O	Graphical model building
AstexViewer™	Java based structure display

Table 2.3. The distribution of all catalase structures and their sources given in PDB

	Source	PDB accession number
Monofunctional catalases	<i>Penicillium vitale</i>	4CAT, 2IUF
	<i>Bos taurus</i> (bovine)	7CAT, 8CAT, 4BLC, 1TGU, 1TH2, 1TH3, 1TH4
	<i>Proteus mirabilis</i>	2CAG, 2CAH, 1M85, 1MQF, 1E93, 1H7K, 1NM0, 1H6N
	<i>Saccharomyces cerevisiae</i>	1AE4
	<i>Homo sapiens</i> (erythrocyte)	1DGB, 1DGF, 1DGG, 1DGH, 1F4J, 1QQW
	<i>Escherichia coli</i>	1GGE, 1IPH, 1CF9, 1GG9, 1GGF, 1GGH, 1GGJ, 1GGK, 1QF7, 1P7Y, 1P7Z, 1P80, 1P81, IQWS,
	<i>Micrococcus lysodeikticus</i>	1GWE, 1HBZ, 1GWF, 1GWH, 1YE9
	<i>Pseudomonas syringae</i>	1M7S
	<i>Helicobacter pylori</i>	1QWL, 1QWM, 2A9E
	<i>Neurospora crassa</i>	1SY7
	<i>Exiguobacterium oxidotolerans</i>	2J2M
	<i>Vibrio salmonicida</i>	2ISA
Catalase-peroxidases	<i>Haloarcula marismortui</i>	1ITK
	<i>Burkholderia pseudomallei</i>	1MWV, 1X7U, 2B2O, 2B2Q, 2B2R, 2B2S, 2DV1, 2DV2, 2FX6, 2FXH, 2FXJ
	<i>Mycobacterium tuberculosis</i>	1SJ2, 2CCA, 2CCD
	<i>Escherichia coli</i>	1U2J, 1U2K, 1U2L
	<i>Synechococcus sp.</i>	1UB2
Manganase catalases	<i>Lactobacillus plantarum</i>	1JKU, 1JKV, 1O9I
	<i>Thermus thermophilus</i>	2CWL

## 2.7. Scope of the Study

The aim of this study was to produce, purify, biochemically characterize and crystallize the bifunctional catalase of a thermophilic fungus, *Scytalidium thermophilum* and determine its preliminary three dimensional structure by X-ray analysis. According to our previous studies, the enzyme was analyzed as a phenol oxidase at the initial stages of the research. During purification and amino acid sequencing studies, the enzyme was determined as a catalase, with an additional catechol oxidase activity, therefore the enzyme was named as catalase-catechol oxidase (CCO). CCO was purified by anion exchange and gel filtration chromatographies. Enzyme was characterized in terms of its native and subunit molecular weights, isoelectric point, optical spectrum, kinetic behavior at different pH and temperatures, substrate specificity and effect of inhibitors.

To determine the three dimensional structure, *S. thermophilum* CCO was crystallized and X-ray diffraction data of the crystal was collected at the Daresbury Synchrotron Radiation Source (United Kingdom). The preliminary structure was solved by molecular replacement using *Penicillium vitale* catalase which has a tetrameric structure.

## CHAPTER 3

### MATERIALS AND METHODS

#### 3.1. Materials

FPLC purification system (ÄKTAPrime, Sweden) and its columns were purchased from Amersham Biosciences (USA). Chemical reagents, markers and the apparatus used in gel electrophoresis were supplied from BioRad (Germany), Invitrogen (UK), Amersham Biosciences (USA), Fermantas (Canada) and Sigma-Aldrich (Germany). Centrifugal concentrators (Amicon, USA) were used to concentrate protein samples. Membranes (Millipore, USA) were used for buffer filtering in purification experiments. Glycosylation detection kit was purchased from Sigma-Aldrich (Germany). The spectrophotometers used were from Thermospectronic (USA) and Shimadzu (Japan). Crystallization equipments and chemicals were from Hampton Research (USA) and (Douglas Instruments, USA). All other chemical reagents were analytical grade and purchased either from Merck (Germany), Applichem (Germany) or Sigma-Aldrich (Germany). Ultrapure water was used throughout this research.

#### 3.2. Microbial Strain, Maintenance and Cultivation

*Scytalidium thermophilum* (type culture *Humicola insolens*) kindly provided by ORBA Inc., Istanbul, was cultivated on YpSs agar plates as

described in Appendix A (Cooney and Emerson, 1964). Incubation was performed at 45 °C until sporulation, followed by storage at 20 °C for maximum 2 months. Inoculation and pre-cultivation procedures were conducted as described by Arifoğlu and Ögel (2000).

The enzyme production medium was YpSS except the presence of glucose as a carbon source, instead of starch. In addition, the main culture was supplemented with copper sulphate. Pre-culture volume was 2 % of the main culture volume. After 24 h of incubation at 45 °C, the pre-culture was used to inoculate 800 ml of main culture medium (Appendix A). Cultures were incubated in a shaker incubator at 45 °C and 155 rpm shaking rate for 5 days. The growth media were filtered through Whatman No.1 filter paper and the filtrate was centrifuged at 8,000 x *g* for 5 min. The supernatant was used as the crude enzyme solution.

### **3.3. Total Protein Determination**

Total protein was determined according to the Bradford method (1976) by using bovine serum albumin (BSA) as standard (Appendix B).

### **3.4. Enzyme Assays**

*S. thermophilum* catalase and catechol oxidase activities were determined spectrophotometrically by using a temperature-controlled spectrophotometer (Thermospectronic).

Catalase activity was measured at 60 °C in 100 mM sodium phosphate buffer (pH 7) by mixing 10 µl of suitably diluted enzyme with 10 mM hydrogen peroxide (H<sub>2</sub>O<sub>2</sub>) in a total volume of 1 ml. The decrease in absorbance at 240 nm was monitored. Enzyme activity was determined

using the initial rate of the reaction and the extinction coefficient for H<sub>2</sub>O<sub>2</sub> as 39.4 M<sup>-1</sup> cm<sup>-1</sup> (Merle *et al.*, 2007). One enzyme unit was defined as the amount of enzyme that catalyzes the decomposition of 1 μmol H<sub>2</sub>O<sub>2</sub> per min. Standard catechol oxidase assay was performed by following the increase in absorbance at 420 nm of the reaction mixture, consisting of 0.5 ml 100 mM catechol solution in 100 mM phosphate buffer (pH 7) as substrate, 0.5 ml enzyme solution at specified concentrations and 1 ml 100 mM phosphate buffer at pH 7 and 60 °C was followed. The reference cuvette contained buffer instead of the enzyme. Enzyme activity was determined using the initial rate of the reaction and the extinction coefficient as 3450 M<sup>-1</sup> cm<sup>-1</sup> for catechol (Ögel *et al.*, 2006) and one enzyme unit was defined as the amount of enzyme required for the formation of one nanomole of product per min.

### **3.5. Determination of Optimum Culture Conditions of CCO Production**

Effect of glucose concentration on *S. thermophilum* CCO and biomass production and effect of nitrogen source concentrations and different inducers on CCO production were investigated. CCO activity was followed using only catechol as substrate because at the early stages of the study, bifunctional nature (catalase and catechol oxidase activities) of the enzyme was unknown.

#### **3.5.1. Effect of Glucose Concentration on CCO Production and Biomass Generation**

Effect of glucose concentration on *S. thermophilum* CCO production was performed between 0.1-4.5 % glucose concentration. The highest CCO activity was determined at 5<sup>th</sup> day of cultivation. Therefore samples at 5<sup>th</sup> day were taken from main cultures containing different amounts of

glucose and were checked for their CCO activity using standard enzyme assay. Amount of dry biomass was determined by filtering the cultures through Whatman no.1 filter paper and drying the biomass until constant dry weight was reached.

### **3.5.2. Effect of Nitrogen Source Concentration on CCO Production**

Effect of nitrogen source concentration on *S. thermophilum* CCO production was performed in a concentration interval of 0.1-0.8 % for yeast extract and urea. Enzyme activities were measured at 5<sup>th</sup> day using the standard assay procedure.

### **3.5.3. Effect of Inducers on CCO Production**

Different phenolic compounds; 4-amino-*N,N*-diethylaniline (ADA), catechol, L-ascorbic acid, *p*-coumaric acid and tannic acid were added to main culture medium on inoculation day, to improve *S. thermophilum* CCO production. The effects of ADA and catechol were studied at concentrations of 0.02 and 0.04 % where L-ascorbic acid and *p*-coumaric acid were tested at a concentration of 0.04 %. Tannic acid was studied in a wider concentration range; between 0.02-0.2 %. Enzyme activities were measured at 5<sup>th</sup> day using the standard assay procedure.

### **3.6. CCO purification**

Enzyme purification was performed with the ÄKTA Prime FPLC system, (Amersham Biosciences, Sweden) according to a two-step technique including anion exchange and gel filtration. Crude CCO solution was prepared by centrifugation of 5<sup>th</sup> day culture at 8,000 x *g* for 5 minutes. Supernatant was taken and filtered through Whatman no.1 filter paper.

The pH of the solution was adjusted to pH 8 by adding concentrate Tris-HCl buffer and it was ultrafiltered through 0.22 µm-pore-size membrane.

First step of the purification was anion exchange chromatography which was performed in a 20 ml prepacked HiPrep 16/60 Q XL column (Amersham Biosciences, USA). Column specifications were given in Appendix C. The column was operated at 50 mM pH 8.0 Tris-HCl buffer at 2 ml/min flow rate. Enzyme was eluted by collecting 3 ml fractions with a salt gradient in the range of 0-1 M sodium chloride (NaCl), prepared in the same buffer. All fractions were checked for both catalase and catechol oxidase activities. CCO-active fractions of anion exchange concentrated by a 10k centrifugal concentrator (Amicon, USA).

Gel filtration chromatography was the second step of purification which was conducted in a prepacked HiPrep 16/60 or 26/60 Sephacryl S-100 high resolution gel filtration column (Amersham Biosciences, USA). Column specifications were given in Appendix D. Column was equilibrated with 50 mM pH 8.0 Tris-HCl buffer and operated at a flow rate of 1 ml/min by collecting 3 ml fractions in 200 ml elution volume. Similar to anion exchange, each fraction was tested for both catalase and catechol oxidase activities. All liquids used for purification studies were filtered through 0.45 µm-pore-size membrane (Millipore, USA) before use. Specific activities, yields and purification folds were calculated by using Equations 3.1, 3.2 and 3.3, respectively.

$$\text{Specific activity} = \text{CCO total activity} / \text{Total protein} \quad (3.1)$$

$$\text{Yield (\%)} = \text{CCO total activity} / \text{Crude CCO total activity} \times 100 \quad (3.2)$$

$$\text{Purification fold} = \text{CCO specific activity} / \text{Crude CCO specific activity} \quad (3.3)$$

### 3.7. Comparison of CCO with Catalases from Different Sources

Since *S. thermophilum* catalase was able to catalyze catechol oxidation, it was compared with other catalases in terms of their catalase and catechol oxidase activities. For this purpose, in addition of the purified *S. thermophilum* CCO, catalases from three different sources *Aspergillus niger*, human (erythrocytes), bovine liver catalases (Sigma-Aldrich, Germany) were used. All of the enzymes, except bovine liver catalase, were prepared at the same concentration of 8 µg/ml in 50 mM Tris-HCl buffer at pH 8. The activity of bovine liver catalase was detectable at 800 µg/ml. Enzyme assays for catalase and catechol oxidase activities were performed as explained in Section 3.4. The catechol oxidase efficiency of catalases were calculated by dividing the observed catechol oxidase activity to catalase activity.

### 3.8. Analytical Gel Electrophoresis and Isoelectric Focusing of CCO

Polyacrylamide gel electrophoresis in the presence of sodium dodecylsulphate (SDS-PAGE) was performed in precast NuPage 4-12% gel (Invitrogen, UK) as described in Appendix E. Gel was run at 100 V constant voltage. The molecular weight standards were Low Molecular Weight Calibration Kit (Amersham Biosciences, USA) containing phosphorylase (97 kDa), albumin (66 kDa), ovalbumin (45 kDa), carbonic anhydrase (30 kDa), trypsin inhibitor (20.1 kDa) and α-lactalbumin (14.4 kDa).

Native-PAGE was performed on precast NativePAGE Novex 4-16% gel (Invitrogen, UK). The native molecular weight standards were Native Mark unstained protein standards (Invitrogen, UK) containing IgM hexamer (1236 kDa), IgM pentamer (1048 kDa), apoferritin band 1 (720 kDa), apoferritin band 2 (480 kDa), B-phycoerythrin (242 kDa), lactate dehydrogenase (146 kDa), BSA (66 kDa), soybean trypsin inhibitor (20 kDa).

Electrophoresis runs were performed in X-Cell Sure Lock Novex Mini-Gel System (Invitrogen) and the gels were stained by a coomassie-based staining procedure; Simply Blue Safe Stain microwave protocol (Invitrogen, UK) (Appendix F).

Analytical isoelectric focusing of the pure CCO was determined on an IEF gel containing ampholytes in a pH range of 3.5-10.0 (Sigma-Aldrich, Germany) in an IEF cell (Biorad, Germany) in METU Molecular Biology and Biotechnology R&D Centre. Isoelectric point of the visible IEF markers, were in a range of 3.5-9.3 (Amersham Biosciences, USA). Each gel was run at 100 V for 15 min, at 200 V for 15 min, and at 450 V for 4 h. Afterwards, the gels were stained by the coomassie blue staining method.

### **3.9. Activity Staining of CCO**

To determine the catalase activity on polyacrylamide gel electropherogram, CCO was electrophoresed under native conditions as described in Section 3.5 and stained according to procedure of Clare *et al.* (1984). The gel was soaked first in 50 µg/ml horseradish peroxidase in 100 mM phosphate buffer for 45 minutes. Then hydrogen peroxide was added to a concentration of 5 mM and soaked for 10 minutes. The gel was then rapidly rinsed twice with distilled water and further soaked in 0.5 mg/ml diaminobenzidine until staining was completed. The bands corresponding to catalase were expected to remain unstained whereas the gel was expected to become dark in color.

CCO was also stained to determine for an additional peroxidase activity according to procedure explained by Conyers and Kidwell (1991). A substrate system of 60 mM of *N,N*-dimethylphenylenediamine (DMPDA) and 110 mM 4-chloro-1-naphtol (4-CN) was prepared in acetonitrile. Hydrogen peroxide solution of 2.9 mM was made in 100 mM sodium citrate buffer at pH 6. The acetonitrile solution of dye precursors (DMPDA

and 4-CN) was mixed with the buffer-hydrogen peroxide solution at a ratio of 1:50 and the blot was developed with the CCO on native gel. The bands corresponding to peroxidase were expected to become blue whereas the gel was expected to remain unstained.

### **3.10. Glycosylation of CCO**

Glycoprotein detection kit (Sigma-Aldrich, Germany) was used to detect possible sugar moieties of CCO. Electrophoresis of pure CCO was performed under denaturing conditions (SDS-PAGE) and the gel was stained according to procedure given in Appendix G to predict the carbohydrate contents as purple bands. Peroxidase with 18% carbohydrate content and BSA were used as positive and negative controls, respectively. Marker proteins were from Fermentas (Canada) containing  $\beta$ -galactosidase (116.2 kDa), BSA (66.2 kDa), ovalbumin (45 kDa), lactate dehydrogenase (35 kDa), restriction endonuclease *Bsp981* (25 kDa),  $\beta$ -lactoglobulin (18.4 kDa) and lysozyme (14.4 kDa).

### **3.11. Aminoacid Sequencing of CCO**

Purified CCO was digested using sequencing grade trypsin (Promega) for different time periods: 2, 5, 10, 20, 30, 45, 60, 90 and 120 minutes. To predict the digestion, samples were checked by SDS-PAGE standard procedure (Appendix E). Undigested protein was also loaded into the gel. Two gels with the same protein sample load were prepared: one for blotting, one for staining and locating the protein bands. After performing the electrophoresis, one gel was stained using Simply Blue Safe Stain microwave protocol (Invitrogen) (Appendix F) and the proteins in the second gel were blotted onto the polyvinylidene difluorobenzene (PVDF) membrane (Biorad) using XCell II Blot Module (Invitrogen). The procedure was described in Appendix H. PVDF membrane was also stained using Simply Blue Safe Stain microwave protocol (Invitrogen) after blotting (Appendix F).

The digested protein was sequenced in LIGHT Laboratory Facility, School of Biochemistry and Molecular Biology of University of Leeds by Procise 494 high-throughput gas-phase/liquid-pulse protein sequencer.

### **3.12. UV-Vis Spectroscopy of CCO**

Absorption spectrum of purified CCO (3mg/ml) was recorded using a Shimadzu UV-2401 PC scanning spectrophotometer in 1 cm quartz cuvette between 200-800 nm at room temperature.

### **3.13. Characterization of CCO Catalase and Catechol Oxidase Activities**

CCO was characterized in terms of catalase and catechol oxidase activities.

#### **3.13.1. Effect of pH on CCO Activity and Stability**

To determine the effect of pH on CCO catalase and catechol oxidase activities, the enzyme assays were performed at various pH values in a range of 5.0-9.0 using 100 mM of the following buffers: citrate-sodium phosphate (pH 5.0-5.5), sodium phosphate (pH 6.0-8.0) and Tris-HCl (pH 8.5-9.0). Enzyme concentration and temperature were kept constant as stated in standard assay conditions. The residual activities were calculated by taking the ratio of the enzyme activities at different pH values to the maximum enzyme activity.

To determine the effect of pH on CCO catalase and catechol oxidase stabilities, enzyme samples were incubated in a pH range of 5.0-9.0 for 1, 6 and 24 h. After incubations, the residual activities were determined by

the standard activity assay methods and reported as the ratio of the enzyme activity after pH treatment to the initial maximum activity at pH 7.

### **3.13.2. Effect of Temperature on CCO Activity and Stability**

Effect of temperature on CCO catalase and catechol oxidase activities were determined in a range of 35-80 °C with 5 °C intervals by assaying the enzyme activities at specified temperatures. Enzyme concentration and pH were kept constant as stated in standard assay conditions. The residual activities were calculated by the ratios of enzyme activities at different temperatures to the maximum enzyme activity.

To determine the effect of temperature on CCO catalase and catechol oxidase stabilities, CCO was incubated at 40-80 °C up to 2 h and samples were taken with 30 min time intervals. Remaining enzyme activities were measured by the standard assay procedures and reported after dividing to the enzyme activity prior to heat treatment. The reaction activation energy ( $E_a$ ) was calculated from the Arrhenius equation (Arrhenius, 1889).

### **3.14. Crystallization of CCO**

The most important part of any protein crystallography study is the crystallization step because it is not possible to perform a crystallographic structural study without having a perfect crystal. Protein crystallization was consisted of two steps including screening for crystallization conditions and setting crystallization experiments.

### 3.14.1. Screening for Crystallization Conditions

Crystallization plates with 96 wells (Greiner) were used for screening. Eight different ready-to-use screening kits were used. Each screening kit contained either 48 or 96 types of solutions, including different buffers, precipitants, salts and additives.

To setup crystallization screening trays, crystal screen solution of 60  $\mu$ l was pipetted into the each well manually. Purified enzyme of 0.5  $\mu$ l in a concentration range of 1-20 mg/ml was mixed with 0.5  $\mu$ l of the well solution by a liquid handling robot Oryx4 (Douglas Instruments, USA). Sitting drop vapor diffusion technique was used for preliminary screening trials. Plates were covered with the adhesive sealing film (Hampton Research, USA) and incubated at 4, 18 and 30 °C to optimize the temperature.

To evaluate the results of screening experiments, drops were observed under a microscope everyday for any crystal formation. Generally in the first screening, crystals are predicted at more than one crystallization condition. Before stating this particular condition as the “best” condition and study further, it must be proved that the crystal is a protein crystal. Commonly, salts remain in the protein sample during purification steps and they crystallize easily in screening experiments. This situation often happens and belies crystallographers. To predict the nature of the crystal observed, c. 1  $\mu$ l of coomassie dye solution can be added to the drop. After an hour of incubation, if the color of the crystal did not change, it is a salt crystal. If a protein crystal is grown, it would become dark blue after coomassie staining.

### 3.14.2. Setting Crystallization Experiments

After predicting the initial crystallization conditions in screening experiments, 24-well crystallization plates were used for large scale protein crystallization at that condition and around. Since the physical conditions were different in screening and large scale crystallization experiments, the condition at which first crystal was observed, was optimized by changing the protein concentration, pH, buffer type, temperature, salt type and concentration, additive type and concentration and temperature.

The hanging drop vapor diffusion technique was used in this step. The mother liquor (well solution) was not a commercial screen kit, it was prepared in the laboratory. One ml of mother liquor was pipetted into the well and 1  $\mu$ l purified CCO were mixed with the well solution at a ratio of 1:1 on the cover slip. Inverted siliconized coverslip was placed over the reservoir (Figure 3.1) and incubated at different temperatures; 4, 18 and 30 °C. To evaluate the results of crystallization, drops were observed everyday under a microscope for any crystal formation. Observations were recorded on a crystallization score sheet (Appendix I).

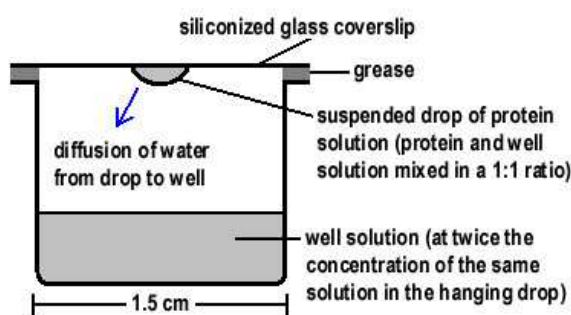


Figure 3.1. Hanging drop vapor diffusion plate setting technique (Kurtz, 1999)

### **3.14.3. Seeding**

If it is not possible to simultaneously optimize the conditions for nucleation and growth of the crystal, perfect crystals might not be grown for structural analysis. In this case, seeding could be an alternative technique to alter the size and quality of the crystals. The seeding method used in this research was a the streak seeding method. The probe used for streak seeding was a cat whisker mounted to a capillary. It was used to touch an existing crystal and dislodge seeds from it. Seeds were introduced into a pre-equilibrated drop by rapidly running the probe in a straight line across the middle of the protein-precipitant drop as shown in Figure 3.2.

### **3.14.4. Storing Protein Crystal at Cryo-Conditions**

Cryo-crystallography generally helps to increase the the lifetime of the protein crystal and reduces the radiation damage. The main problem is the stability of the crystal in cryo-protective solvent. Different cryo-protective solvents such as ethylene glycol, PEG, MPD, glycerol, xylitol, oil (paratone-*n*) and combinations of these were tried in this study in a range of 30-50 % (v/v). Cryo-protectants were added to the drop either directly at the final concentration or in small steps by increasing the concentration slowly.

Stable crystals were immediately transferred into the liquid nitrogen by using a sample loop (Hampton Research, USA). The key point in cryo-crystallography was to replace the water in the void volume of the crystal by cryo-protectant. The reason for that was to prevent the ice formation in and around the crystal which causes problems in data collection process.

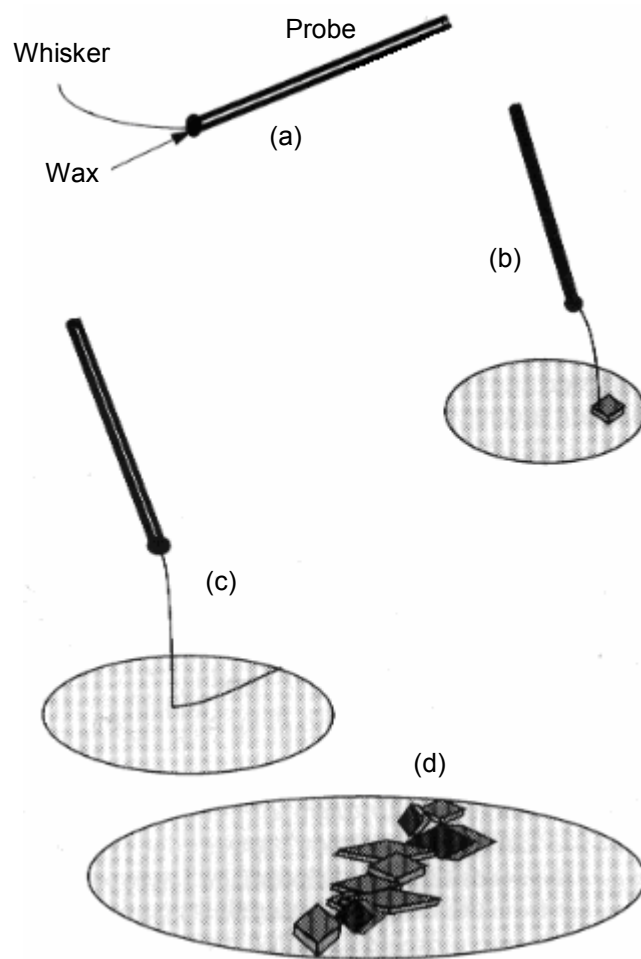


Figure 3.2. Streak seeding technique (a) Probe consisting of a animal whisker attached to a capillary using wax (b) Probe was touched an existing crystal and seeds were dislodged from it, (c) Seeds were introduced into a pre-equilibrated drop, (d) Crystals were grown along the streak line (Hampton Research, 2005)

### 3.14.5. X-Ray Data Collection and Solving Protein Structure

The best *S. thermophilum* CCO crystals were grown at 18 °C. Crystals appeared after 3 days and were grown for about two weeks. Crystals were orthorhombic with a brownish green color. A crystal (0.2 mm x 0.12 mm x 0.07 mm) was soaked in paratone-*n* oil and flash-cooled in liquid nitrogen. X-ray diffraction data were collected at Beamline-10.1 of the Daresbury Synchrotron Radiation Source (SRS) under nitrogen stream at 100 K.

Reflection data of 360 frames were recorded between angles 0-180 ° with an interval of 0.5 °. To solve the structure, collected data were processed using HKL2000 and CCP4 computer programs. The structure of a suitable homologue (*Penicillium vitale* catalase), available in the Protein Data Bank database, was used as a template to solve the structure of CCO by molecular replacement using the program MOLREP. By using the sequence given in the free United States Patent (No. 5646025), structural model was built. For computer graphics, model building program COOT was used.

## CHAPTER 4

### RESULTS AND DISCUSSIONS

The enzyme of *S. thermophilum* studied in this research was reported as an extracellular phenol oxidase (STEP) in our first article (Ögel *et al.*, 2006) where the enzyme activity was determined by measuring the rate of catechol oxidation reaction. Therefore, in the early stages in this current study, in medium optimization experiments, catechol was used as the substrate. After purifying the enzyme, it was sequenced and its catalase nature with an additional catechol oxidase activity was determined. The enzyme was named as CCO (catalase-catechol oxidase). Due to this bifunctional nature of the enzyme, studies after medium optimization were performed by using both catechol and hydrogen peroxide as substrates to determine catechol oxidase and catalase activities, respectively.

#### 4.1. Medium Optimization Results

Medium optimization studies include the effects of glucose, nitrogen sources and inducers on *S. thermophilum* CCO production. Optimization of cell growth in liquid medium has been studied in our laboratory by Mete (2003) and Kaptan (2004). According to the results of these studies, medium optimization experiments were performed at 5<sup>th</sup> day of cultivation in this research.

#### **4.1.1. Effect of Glucose Concentration on CCO Production and Biomass Generation**

Effect of glucose concentration on *S. thermophilum* CCO production was performed in a concentration interval of 1-45 g/L. As shown in Figure 4.1, the highest CCO activity was observed at 30-40 g/L glucose concentrations.

Low glucose concentrations caused a decrease in biomass generation (Figure 4.1). Only 0.25 g dried biomass was produced by using 1 g/L glucose, whereas 1.4 and 1.5 g dried biomass values were observed by using 35 and 40 g/L glucose, respectively.

Although the highest biomass generation and enzyme activity was obtained at 40 g/L glucose concentration, 30 g/L glucose can also be used, considering the slight decrease in enzyme activity. Despite having highest activity at 40 g/L glucose concentration, the highest specific enzyme production (U/mg biomass) was observed at 20 g/L glucose concentration. The second best specific enzyme production was determined at 30 g/L glucose.

#### **4.1.2. Effect of Nitrogen Source Concentration on CCO Production**

Effect of nitrogen source and concentration on *S. thermophilum* CCO production was performed using two different nitrogen sources, one organic and one inorganic, in a concentration interval of 1-8 g/L. The highest CCO activity was observed at 4 g/L yeast extract concentration (Figure 4.2). Using higher amounts of yeast extract up to 8 g/L did not induce CCO production. Therefore, 4 g/L yeast extract was used in further experiments.

Urea was also effective as a nitrogen source at 4 g/L and 8 g/L concentrations. Urea can be preferred to use where it is more economical than yeast extract but the lower enzyme activity should be considered. Use of urea can be also more advantageous for purification studies.

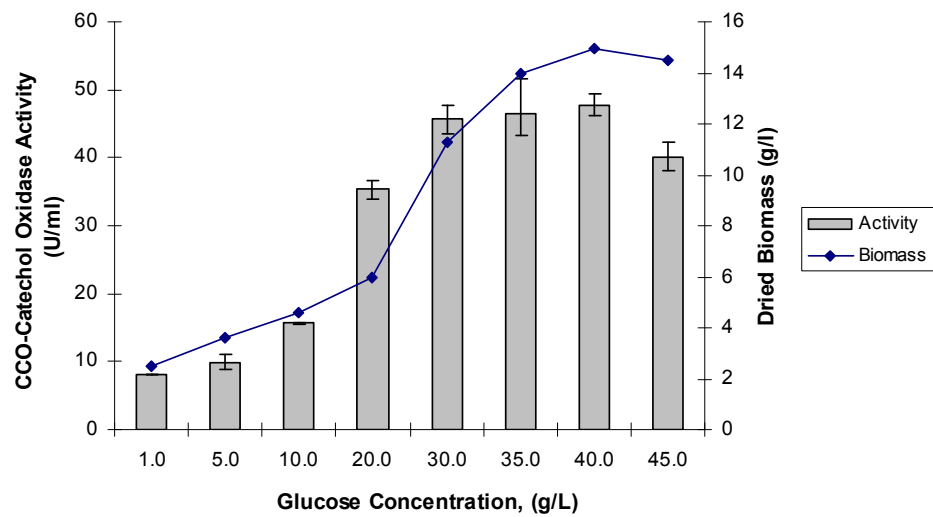


Figure 4.1. Effect of glucose concentration on *S. thermophilum* CCO production and biomass generation (Medium composition: 4 g/L yeast extract, 1 g/L  $K_2HPO_4$ , 0.5 g/L  $MgSO_4$ , 0.1 g/L  $CuSO_4$ , 0.17 g/L gallic acid and glucose at different concentrations at 45 °C and 155 rpm, 5<sup>th</sup> day of cultivation)

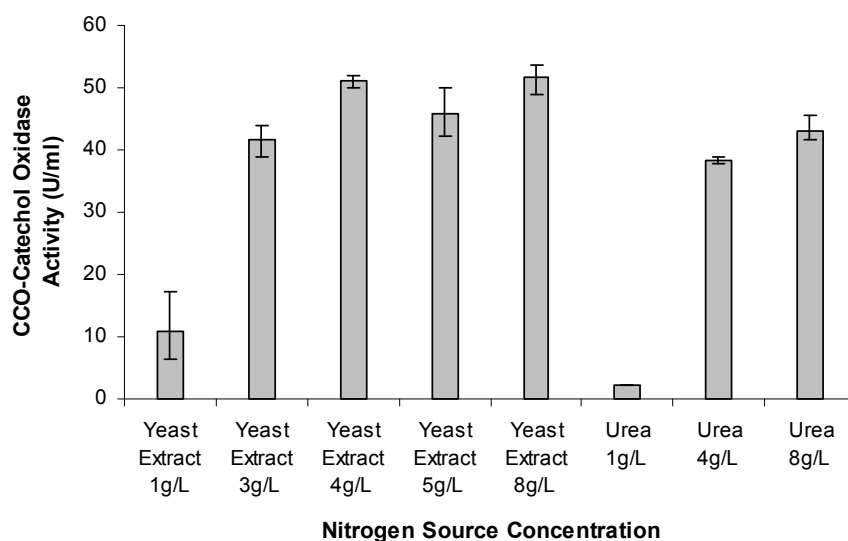


Figure 4.2. Effect of nitrogen source concentration on *S. thermophilum* CCO production (Medium composition: 4 g/L glucose, 1 g/L  $K_2HPO_4$ , 0.5 g/L  $MgSO_4$ , 0.1 g/L  $CuSO_4$ , 0.17 g/L gallic acid and nitrogen sources at different concentrations at 45 °C and 155 rpm, 5<sup>th</sup> day of cultivation)

#### 4.1.3. Effect of Inducers on CCO Production

To improve *S. thermophilum* CCO production, five different phenolic compounds; 4-amino-*N,N*-diethylaniline (ADA), catechol, L-ascorbic acid, *p*-coumaric acid and tannic acid were added to the culture medium at various concentrations. When ADA, L-ascorbic acid and *p*-coumaric acid were used, nearly same amount of biomass (about 1.5 g/100 ml culture medium) was produced but CCO production decreased as shown in Figure 4.3. Addition of catechol at concentrations of 0.2 and 0.4 g/L totally inhibited cell growth. As a result, none of these phenolics, including catechol, can be used as inducer for *S. thermophilum* CCO production.

Effect of tannic acid as an inducer was not easy to determine. At the beginning of the experiments, addition of tannic acid increased CCO

production approximately 3-fold. Later, it was realized that tannic acid left in the culture medium reacted with catechol during enzyme assay studies and caused an artificial absorbance increase. Therefore, without addition of enzyme, catechol and tannic acid reaction was followed spectrophotometrically at 420 nm, and CCO assay absorbance data was corrected accordingly.

After the spectrophotometric correction, enzyme activities were calculated and shown in Figure 4.3. When 0.6 g/L tannic acid was added to the medium, about 2-fold increase in CCO activity was achieved. Similar spectrophotometric interference of gallic acid was also detected in the presence of catechol. Adding 0.2 g/L gallic acid to the medium was reported to increase CCO activity 100 % (Mete, 2003) but after spectrophotometric correction, actual increase in CCO activity was calculated as about 15-20 %.

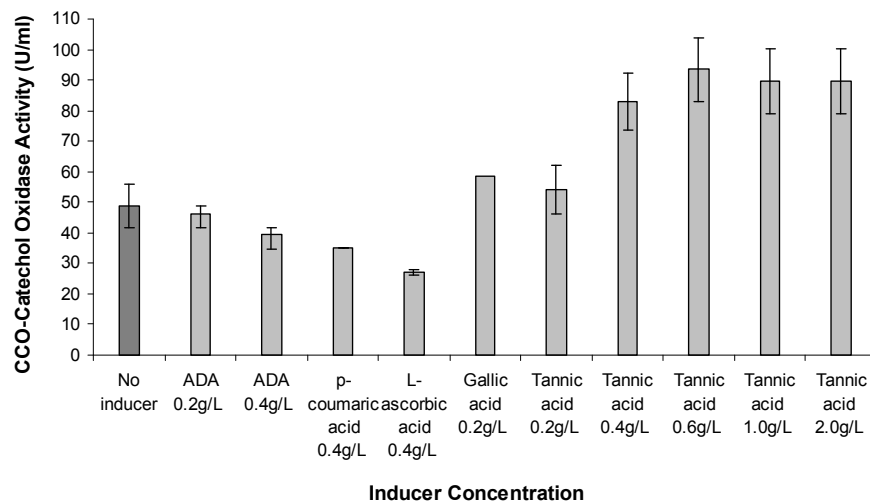


Figure 4.3. Effect of inducers on *S. thermophilum* CCO production (Medium composition: 4 g/L yeast extract, 40 g/L glucose, 1.0 g/L  $K_2HPO_4$ , 0.5 g/L  $MgSO_4$ , 0.1 g/L  $CuSO_4$ , inducers at different concentrations at 45 °C and 155 rpm, 5<sup>th</sup> day of cultivation)

In overall, medium optimization experiments showed that 30-40 g/L glucose and 4 g/L yeast extract concentration, showing highest biomass generation and enzyme activity, are optimum carbon and nitrogen sources and concentrations. None of ADA, L-ascorbic acid, *p*-coumaric acid and catechol can be used as inducer for *S. thermophilum* CCO production. Only gallic acid and tannic acid resulting in 15-20 % and 2-fold increase in CCO activity were determined as suitable inducers, respectively.

#### **4.2. Purification of CCO**

CCO purification was performed using a two-step column chromatography technique including anion exchange and gel filtration. Both catalase and catechol oxidase activities were followed in the eluted fractions and the yield and purification fold values were calculated using both catalase and catechol oxidase data.

As the first step of purification, anion exchange was performed in 20 ml prepacked HiPrep 16/60 Q XL column (Amersham Biosciences) at a flow rate of 2 ml/min by collecting 3 ml fractions in 400 ml elution volume. Column was equilibrated at pH 8.0 with 50 mM Tris-HCl buffer and elution was carried out with the same buffer containing 1 M NaCl. As expected depending on the previous work done using crude enzyme (Ögel *et al.*, 2006), CCO was bound to the column at pH 8.0, so, the enzyme was separated from many other proteins having negative charge at this pH. CCO was eluted at c. 0.3 M NaCl concentration of 0-0.4 M NaCl gradient. CCO activity was detected in fractions between 120-144 ml elution volume (Figure 4.4).

To predict CCO activity, each fraction was tested for catalase and catechol oxidase activities separately as shown in Figures 4.5 and 4.6, respectively. Enzyme activities were proportional to the protein content in

the fractions, showed by the absorbance curve at 280 nm. The distribution profile of catalase and catechol oxidase activities were similar in the same fractions (120-145 ml).

Anion exchange was resulted in 75 % activity recovery and 2.7 fold purification for CCO-catalase (Table 4.1) and 83 % activity recovery and 3.0 fold purification for CCO-catechol oxidase (Table 4.2), respectively. The difference in the recovery and purification fold values between two activities of the enzyme can be due the higher sensitivity of the catalase activity at higher salt concentrations. Without performing dialysis after anion exchange, activity assays were performed in fractions containing c. 0.3 M NaCl, which might affect the observed enzyme activity.

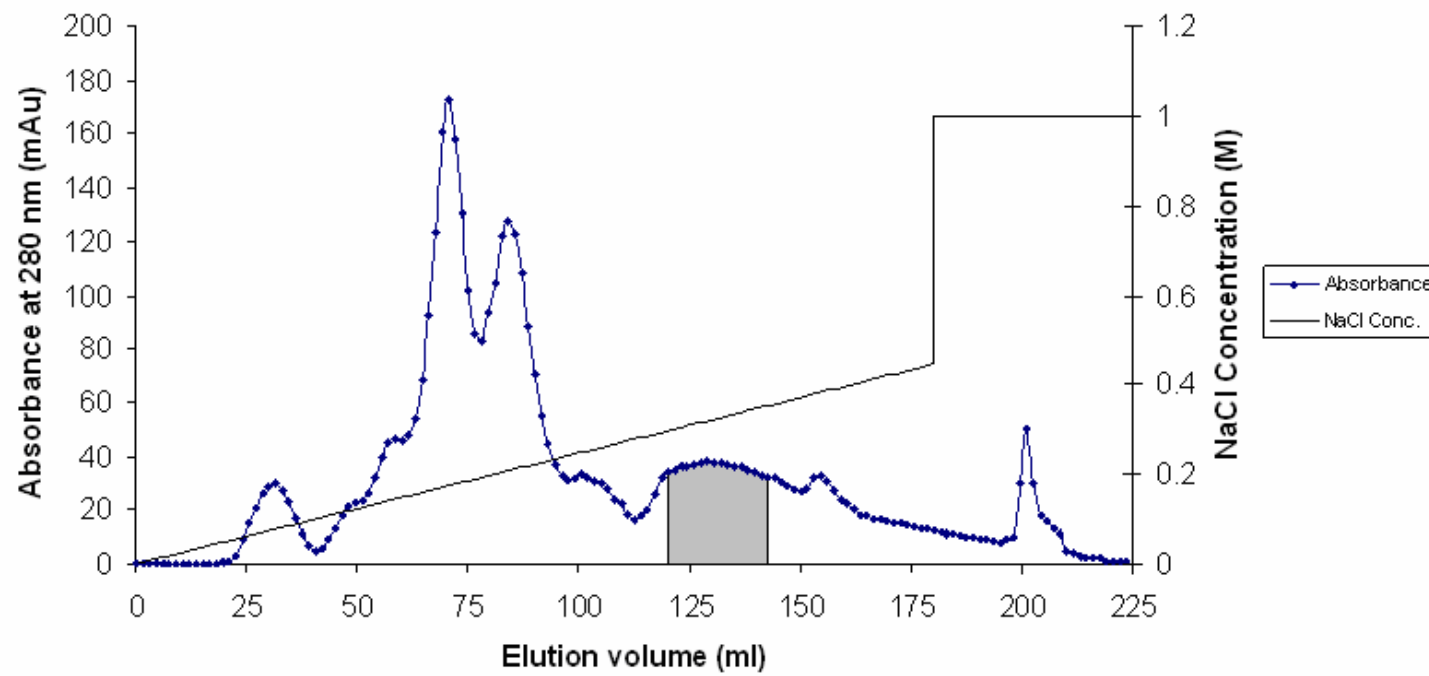


Figure 4.4. *S. thermophilum* CCO purification by anion exchange chromatography (2 ml/min flow rate, at pH 8.0 with 50 mM Tris-HCl buffer, elution with the same buffer containing 1 M NaCl)

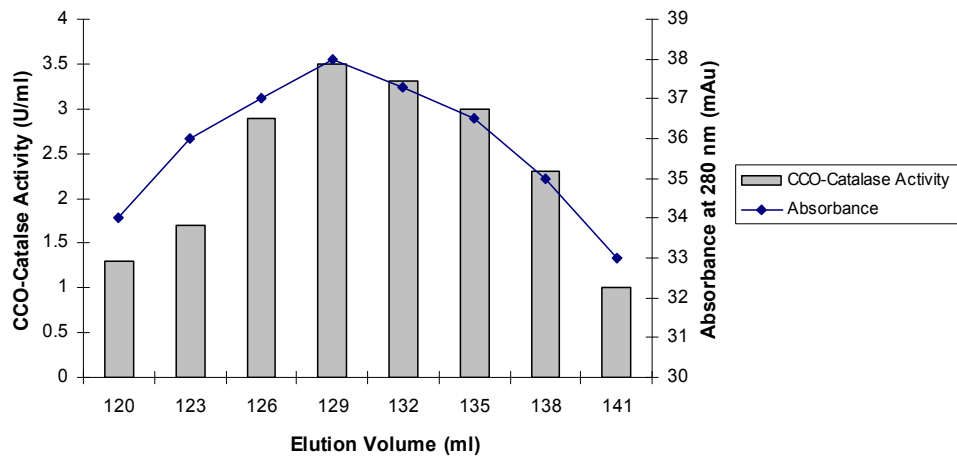


Figure 4.5. CCO-Catalase activity distribution in anion exchange fractions

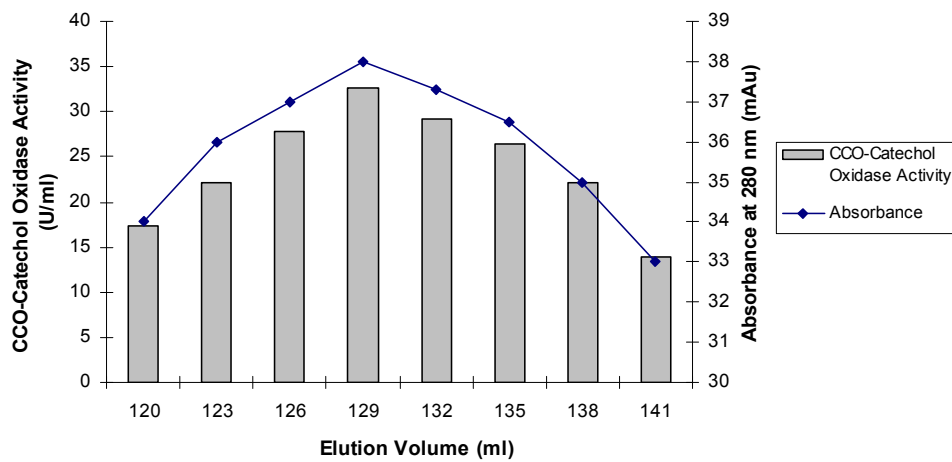


Figure 4.6. CCO-Catechol oxidase activity distribution in anion exchange fractions

Gel filtration chromatography was the second step of CCO purification.

CCO-active fractions of anion exchange chromatographies were mixed and concentrated by a centrifugal concentrator (Amicon, USA). Gel filtration was performed in 120 ml prepacked HiPrep 16/60 or 26/60 Sephacryl S-100 high resolution gel filtration column (Amersham Biosciences, USA) at a flow rate of 1 ml/min by collecting 3 ml fractions in 200 ml elution volume. Column was equilibrated at pH 8.0 with 50 mM Tris-HCl buffer. CCO was eluted in 3 fractions (3 ml each) between 39-48 ml as shown in Figure 4.7.

Similar to anion exchange, each fraction eluted from gel filtration column was tested for catalase and catechol oxidase activities, separately. Both activities were predicted in the same fractions (39-48 ml) as shown in Figures 4.8 and 4.9. The change in catalase activity in eluted fractions was proportional to the protein concentration but the change in catechol oxidase was not. This might be due to the primarily catalase nature of the enzyme with an additional catechol oxidase activity.

At the end of gel filtration, CCO was purified with 45 % activity recovery and 10 fold purification for CCO-catalase (Table 4.1); and 46 % activity recovery and 10 fold purification for CCO-catechol oxidase (Table 4.2), respectively.

As a result of the two-step purification procedure, CCO was purified with *c.* 45% yield and 10 fold purification. Purity and molecular weight of CCO was checked by SDS-PAGE and Native-PAGE.

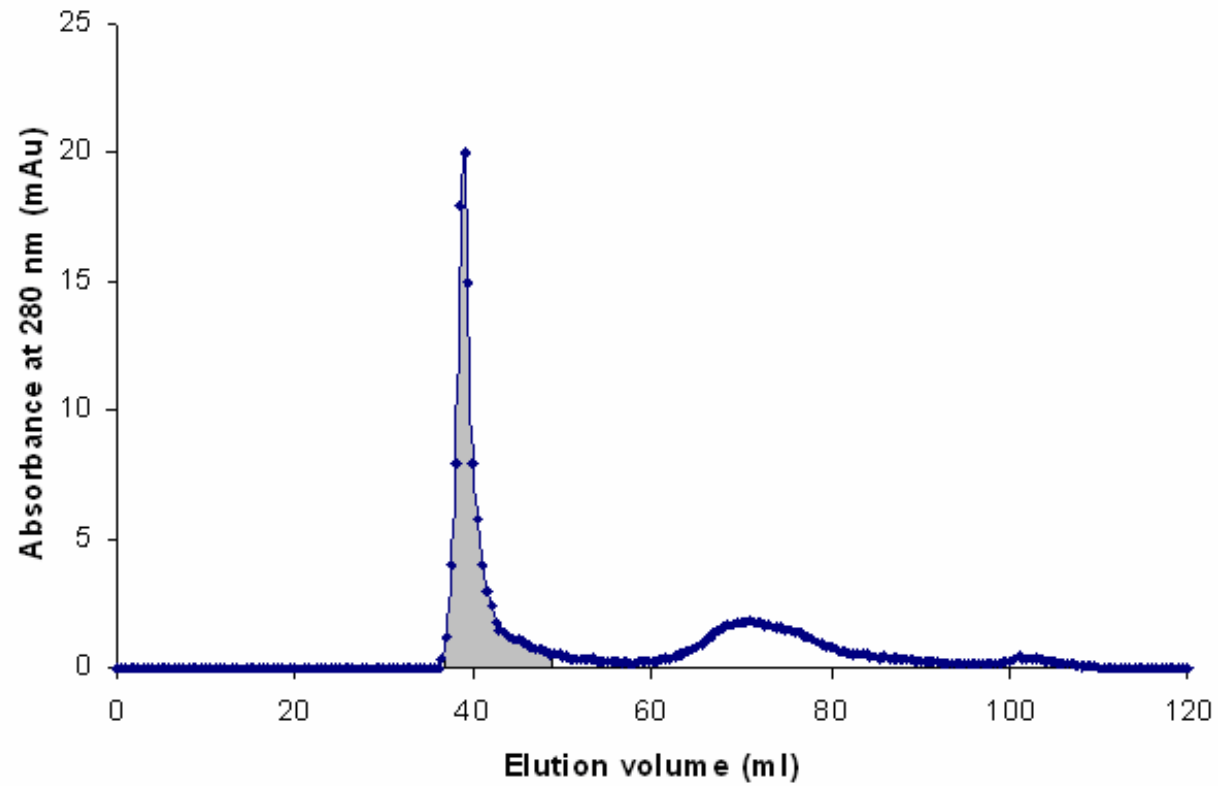


Figure 4.7. *S. thermophilum* CCO purification by gel filtration chromatography (1 ml/min flow rate, at pH 8.0 with 50 mM Tris-HCl buffer)

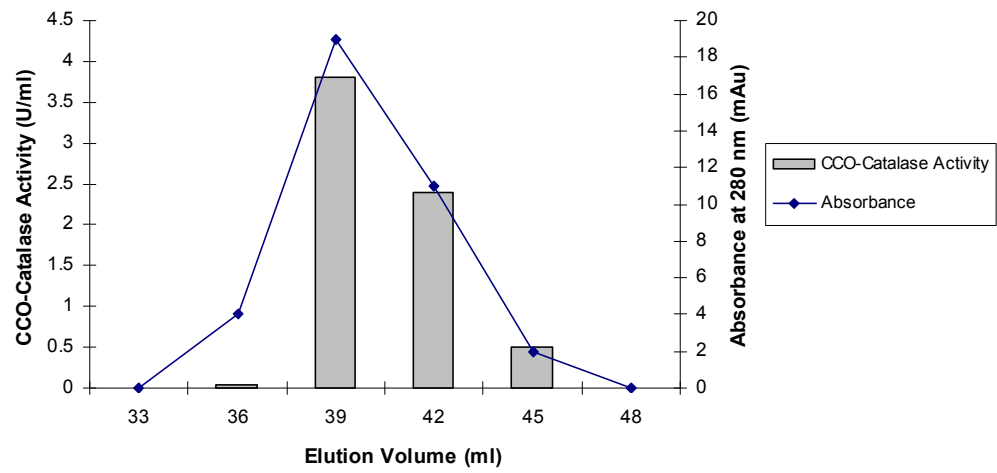


Figure 4.8. CCO-Catalase activity distribution in gel filtration fractions

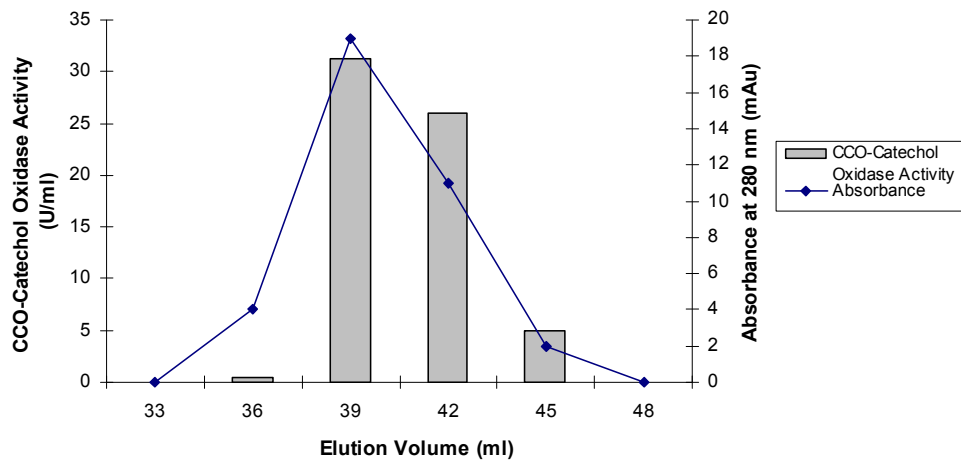


Figure 4.9. CCO-Catechol Oxidase activity distribution in gel filtration fractions

Table 4.1. Two-step purification results of *S. thermophilum* CCO based on catalase activity

Step	Volume (ml)	Catalase Activity (U/ml)	Total Activity (U)	Protein Conc. (mg/ml)	Total Protein (mg)	Specific Activity (U/mg)	Yield (%)	Purification Fold
Crude extract	20	4.0	80	0.090	1.800	44.4	100	1.0
Anion exchange chromatography	24	2.5	60	0.021	0.504	119.0	75	2.7
Gel filtration chromatography	9	4.0	36	0.009	0.081	444.4	45	10.0

Table 4.2. Two-step purification results of *S. thermophilum* CCO based on catechol oxidase activity

Step	Volume (ml)	Catechol Oxidase Activity (U/ml)	Total Activity (U)	Protein Conc. (mg/ml)	Total Protein (mg)	Specific Activity (U/mg)	Yield (%)	Purification Fold
Crude extract	20	35.0	700	0.090	1.800	389	100	1.0
Anion exchange chromatography	24	24.3	583	0.021	0.504	1157	83	3.0
Gel filtration chromatography	9	36.0	324	0.009	0.081	4000	46	10.0

#### 4.3. Comparison of *S. thermophilum* CCO with Catalases from Different Sources

*S. thermophilum* CCO was detected to have both catalase and catechol oxidase activities. To compare this bifunctional nature of *S. thermophilum* CCO with other catalases, catalases from three other sources, namely *Aspergillus niger*, human (erythrocytes) and bovine liver were used. All of the enzymes, except bovine liver catalase, were prepared at a concentration of 8 µg/ml whereas the activity of bovine liver catalase was detectable at 800 µg/ml. The catechol oxidase efficiency of catalases were calculated by dividing the observed catechol oxidase activity to catalase activity and the results are given in Table 4.3.

At the same concentration (w/v) of the enzymes tested, human catalase showed the highest activity towards hydrogen peroxide. *S. thermophilum* CCO was the second most active catalase. *A. niger* and bovine liver catalases showed lower activities (Table 4.3).

The highest catechol oxidase activity was observed with *S. thermophilum* CCO. Despite having three-fold higher catalase activity, human catalase showed nearly same level of catechol oxidase activity as *S. thermophilum* CCO. The catechol oxidase efficiency of human and *S. thermophilum* catalases were found as c. 8 and 23, respectively. *A. niger* catalase had higher catechol oxidation efficiency than human catalase, c. 14. The least active catalase tested was bovine liver catalase which had comparable catechol oxidation efficiency to human catalase (Table 4.3). As a result, *S. thermophilum* catalase had the highest catechol oxidation efficiency over the enzymes tested.

Catechol oxidation feature of catalases are not widely studied, except the study of Vetrano *et al.* (2006) involving the characterization of the oxidase activity in mammalian catalases; mouse and bovine liver, mouse and human keratinocytes and hamster fibroblasts. They used 10-acetyl-3,7-dihydroxyphenoxazine as substrate to characterize the oxidase

activity of catalase and found that mammalian catalases exhibit a previously unrecognized oxidase activity independent of hydrogen peroxide. They also predicted that mammalian catalases were able to oxidize catechol and other functionally important phenolic compounds.

The results of our research showed that in addition to *S. thermophilum* CCO, other catalases from *Aspergillus niger*, human, bovine liver also have catechol oxidase activity. This result can be regarded as an improvement of the study of Vetrano *et al.* (2006) and might be generalized to include all the catalases, which could be a new research area.

The catechol oxidase activity of *S. thermophilum* CCO was *c.* 4-fold higher than mammalian catalase. The reason for that might be the high assay temperature (60 °C) of standard enzyme assay procedure used for all assays due to the thermophilic nature of *S. thermophilum* CCO. Experiments, in the future, can be repeated after optimizing the temperature for each of the tested enzymes. In spite of expected change in catalase and catechol oxidase activities at different temperatures, the ratio of them probably will not change. In combination with the results of Vetrano *et al.* (2006), the findings of our research might be a guide for studies about screening and characterization of catechol oxidase activities of other catalases, including plant catalases.

Table 4.3. Comparison of *S. thermophilum* CCO with other catalases

Catalase Source	Catalase Activity (U ml <sup>-1</sup> mg <sup>-1</sup> )	Catechol Oxidase Activity (U ml <sup>-1</sup> mg <sup>-1</sup> )	Catechol Oxidase Efficiency of Catalase (Catechol oxidase act./ Catalase act.)
<i>S. thermophilum</i>	190±18	4350±130	23±3
<i>A. niger</i>	58±5	788±23	14±2
Human	505±60	4175±84	8±1
Bovine liver	9±0.6	70±6	8±1

#### 4.4. Molecular Weight and Isoelectric Point of CCO

Molecular weight of CCO was detected in University of Leeds under denaturing and native conditions by SDS-PAGE and Native-PAGE, respectively. CCO was observed as a single band on the SDS-PAGE with a size of 80 kDa (Figure 4.10) and on native gel with a size of 320 kDa (Figure 4.11-a). This result indicated the presence of the tetrameric enzyme with four identical subunits.

This result was not surprising since catalase of *S. thermophilum* expressed in *Aspergillus oryzae* was reported to have a tetrameric structure with four identical subunits, having 74.9-86 kDa size each (Kulys *et al.*, 2003). Catalase from another thermophilic fungus, *Thermoascus aurantiacus*, is also a homotetrameric enzyme with a similar molecular weight of 330 kDa (Wang *et al.*, 1998). Catalases from other fungi have also generally tetrameric structures with a subunit size in the range of 61-97 kDa.

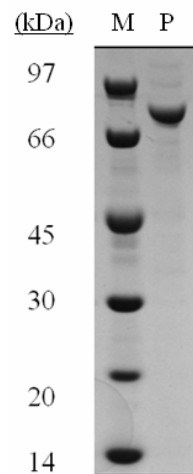


Figure 4.10. SDS-PAGE of *S.thermophilum* CCO. Lanes; M: Markers and P: Purified CCO.

To determine the catalase activity on polyacrylamide gel by activity staining, CCO was electrophoresed under native conditions and stained according to procedure of Clare *et. al.* (1984) in University of Leeds. Enzyme was also stained to determine whether it has an additional peroxidase activity according to procedure explained by Conyers and Kidwell (1991).

In catalase staining, the band corresponding to catalase activity was expected to remain unstained whereas the gel background was expected to become dark in color. As shown in Figure 4.11-b, the band corresponding to CCO with a native molecular weight of 320 kDa was remained unstained whereas the gel was brownish in color. This result visualized the catalase activity of CCO.

In peroxidase activity staining, the gel was expected to remain unstained whereas peroxidase band becomes dark in color. After staining of CCO, the gel became light-blue (due to the bromophenol blue dye added to follow up the electrophoresis) and no additional band was observed corresponding to peroxidase activity (Figure 4.11-c). This result showed that peroxidase activity of CCO was not present.

In our previous publication (Ögel *et. al.*, 2006) activity staining was performed according to the method described by Rescigno *et al.* (1997) for differentiation of laccase, tyrosinase and peroxidase activities. According to the results of the experiments, the enzyme was named as *S. thermophilum* extracellular phenoloxidase (STEP).

The method used for phenol oxidase staining previously (Ögel *et. al.*, 2006) was also based on the use of the different chromogenic substrates, 4-amino-*N,N*-diethylaniline (ADA) (or *N,N*-diethyl-*p*-phenylenediamine), hydrogen peroxide and 4-*tert*-butyl-catechol. Analysis resulted in a single distinct pink colored band after treatment with ADA, indicating oxidation in the absence of hydrogen peroxide. Hydrogen peroxide and 4-*tert*-butyl-catechol did not generate additional visible bands, but 4-*tert*-butyl-

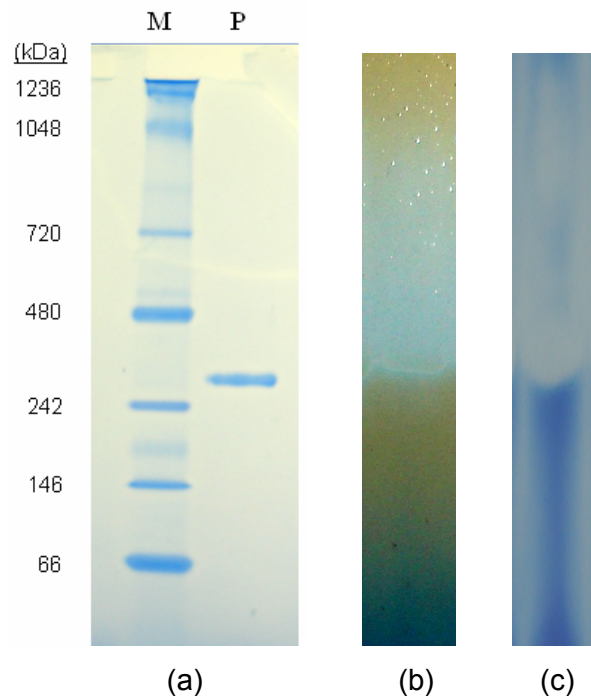


Figure 4.11. Native PAGE and activity staining of CCO on 4-16 % native-PAGE (a) Coomassie stained native-PAGE of *S.thermophilum* CCO. Lanes; M: Markers and P: Purified CCO. (b) Catalase activity staining (c) Peroxidase activity staining

catechol caused the pink color to turn into a deep blue color, indicating oxidation of the compound. These results suggested that there is a single major oxidative enzyme in the culture supernatant of *S. thermophilum*. STEP was acting as an oxidative enzyme in the absence of hydrogen peroxide.

The results of our previous study (Ögel *et. al.*, 2006) using culture supernatants were similar to the findings of this research performed with pure enzyme. In both studies, the enzyme was able to oxidize the substrate in the absence of hydrogen peroxide, verifying the lack of peroxidase activity. Thus, the presence of catechol oxidation ability of the enzyme was verified in both studies.

In addition, the catalase activity of the enzyme was determined both by spectrophotometric assay and colorimetric detection in this research. This result supported our suggestion of the bifunctional (catalase-catechol oxidase) nature of the enzyme.

The isoelectric point (pI) of CCO was determined as c. 5.0 on IEF gel (Figure 4.12). This result is similar to the pI value found as 5.4 in our previous study (Ögel *et al.*, 2006) of the partially purified enzyme and the calculated pI value of *S. thermophilum* catalase as 5.1 and 4.0 by Kulys *et al.* (2003).

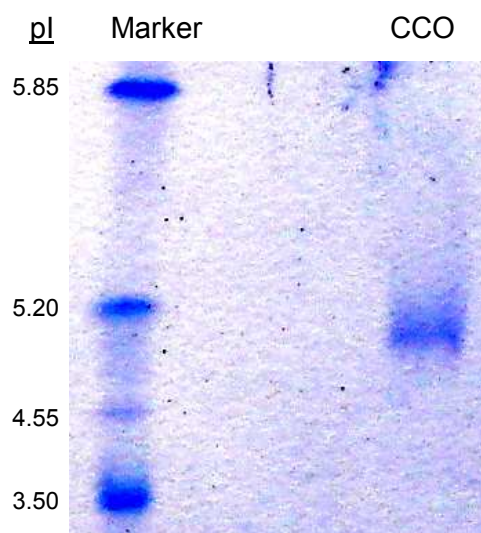


Figure 4.12. IEF of *S.thermophilum* CCO. Lanes; M: IEF markers and purified CCO.

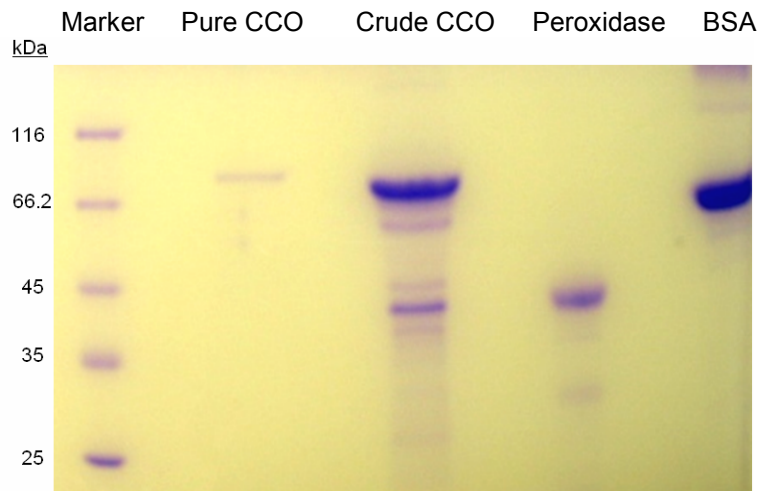
#### 4.5. Glycosylation of CCO

Glycoprotein detection kit (Sigma) was used to detect possible sugar moieties of CCO. In Figure 4.13-a, coomassie stained SDS-PAGE profiles of tested proteins; pure and crude CCO, peroxidase (positive control, 18% carbohydrate) and BSA (negative control), were shown. Gel after glycoprotein detection test was given in Figure 4.13-b.

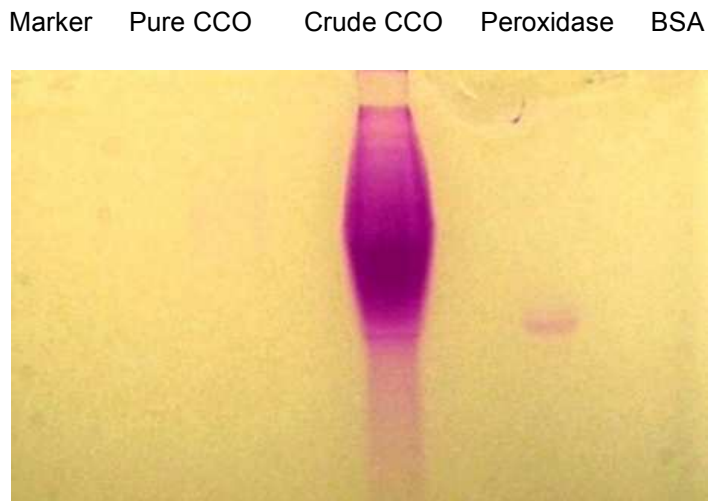
Crude CCO supernatant and peroxidase showed purple bands as a result of their carbohydrate content. No purple band was detected in marker proteins and BSA lanes but a very slightly visible band was observed in pure CCO lane. This information did not give a quantitative information about the glycosylation of the enzyme but obviously, CCO appeared as an enzyme with a small amount of carbohydrate.

This result was also confirmed by the deglycosylation study of CCO. Purified CCO was incubated with N-glycosidase enzyme (BioLabs, UK) to remove possible sugar moieties and no decrease in molecular weight was observed on gel electrophoresis (data not shown).

Wassermann and Hultin (1981) isolated the catalase from *Aspergillus niger* from a commercial preparation. They reported the enzyme to be a glycoprotein containing 9 % neutral sugar and 3 % hexosamine but there are not many studies reporting glycosylation level of catalases in the literature.



(a)



(b)

Figure 4.13. Glycosylation test of *S. thermophilum* CCO on 4-12 % SDS-PAGE gel (a) Coomassie stained (b) Glycosylation stained

#### 4.6. Amino Acid Sequencing of CCO

In our previous study (Ögel *et al.*, 2006) the enzyme was determined as a novel phenol oxidase since it showed unique properties to catechol oxidase and no fungus was reported as catechol oxidase producer before. Therefore, our attempt was directed to find the sequence of this novel enzyme. Therefore, enzyme was digested using sequencing grade trypsin (Promega). Different time periods between 2-120 minutes were used. Undigested protein was also loaded into the gel and samples were checked by SDS-PAGE to predict the level of digestion as shown in Figure 4.14. At t=0, the undigested CCO was shown. At t=2, CCO was digested to five main bands, mainly around 60-80 kDa, and the trypsin band was also visible around 23 kDa. As digestion time increased, digestion level also increased and enzyme was digested to smaller polypeptides. After 120 minutes of operation, polypeptides having sizes between 60-80 kDa disappeared and smaller bands around 30 kDa became more visible.

The polypeptides in the second identical and unstained SDS-PAGE gel were blotted onto the polyvinylidene difluoride (PVDF) membrane and stained using coomassie-based staining procedure as given in Appendix F. The undigested CCO and the lower digested protein band shown in black box in t=120 min. lane (Figure 4.14) were sequenced in LIGHT Laboratory Facility, School of Biochemistry and Molecular Biology of University of Leeds by Procise 494 high-throughput gas-phase/liquid-pulse protein sequencer.

First amino acid sequence result was obtained using the undigested CCO. Ten amino acids were determined from the N-terminus of CCO as:

Ser-Gly-Gln-Ser-Pro-Leu-Ala-Ala-Tyr-Glu

This sequence was screened to match other sequences deposited to the National Center for Biotechnology Information (NCBI) database. Having no homology to other phenol oxidases made us to consider this enzyme as indeed a novel form of oxidase.

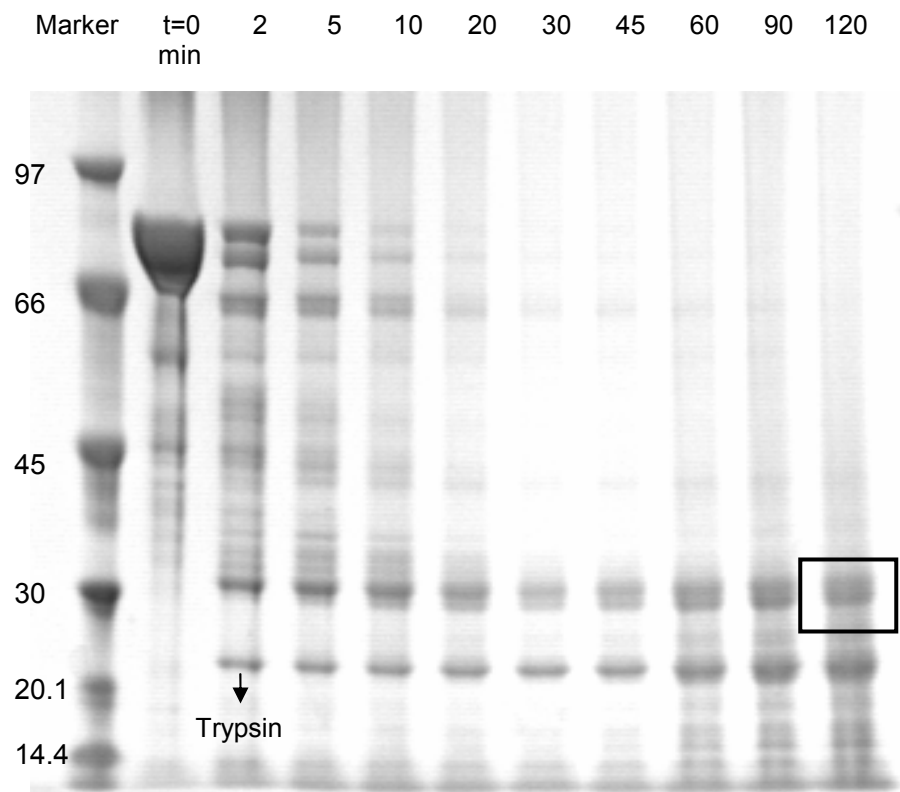


Figure 4.14. Determination of CCO digestion by trypsin on 2-12 % SDS-PAGE gel with coomassie staining

The second amino acid sequence data was obtained from the lower digested protein band obtained after 120 min digestion as:

Leu-Phe-Phe-Asn-Ser-Leu-Thr-Pro-Val-Glu-Gln-Gln

The result of the search for homologous proteins in BLAST (Basic Local Alignment Search Tool) programme revealed that this internal amino acid sequence was surprisingly 100 % identical to the catalase-3 of *Neurospora crassa* (NCBI number: AAK15807). High similarities were also obtained with other catalases from different sources. This information was the starting point of our studies on the catalase nature of the enzyme of *S. thermophilum*.

The next step was to search for literature information on the catalase gene of *S. thermophilum*. Although the gene was absent in the NCBI database, *Scytalidium thermophilum* catalase gene was found to be patented (United States Patent, No. 5646025) (Inventor: Donna Moyer from Davis, CA, USA), (Appendix J).

At this point, the enzyme was determined as a catalase having catechol oxidase activity. To be sure, catalase activity was also revealed by spectroscopic techniques. After these findings, sequencing studies were stopped and the sequence given in the free patent was used for further studies.

This bifunctional enzyme was named as catalase-catechol oxidase (CCO). All further purification and characterization studies were conducted by following both catalase and catechol oxidase activities of CCO.

To predict the similarity of CCO with other catalases, sequence alignment studies were performed. The sequence of CCO, given in free United States Patent (No. 5646025), had 717 amino acids. Similar sequences were investigated by BLAST (Basic Local Alignment Search Tool) search on NCBI (National Center for Biotechnology Information) using non-redundant database, which includes all translations of coding sequences of GenBank nucleotide sequences as well as amino acid sequences from Protein Data Bank (PDB), SwissProt, Protein Information Resource and

Protein Resource Foundation. PDB was also searched separately because of the structural studies. Taxonomic trees found after sequence and structure alignments were shown in Figures 4.15 and 4.16, respectively.

Results of BLAST search can be evaluated by two numbers; score and expect (E) value. Score is a value calculated from the number of gaps and substitutions associated with each aligned sequence. The higher the score, the more significant the alignment. E value describes the likelihood that a sequence with a similar score will occur in the database by chance. The smaller the E value, the more significant the alignment. Other factors are identities, positives and gaps. The identities mean the same amino acids which are identical in both sequences and positives mean where the amino acids are different but their physico-chemical properties are conserved. Gaps represent the non-aligned pairs of residues. The scores, identities, positives and gaps were given in Table 4.4. The organisms with highest scores (>1000) with zero E values were chosen for multiple alignment and shown in Figure 4.17.

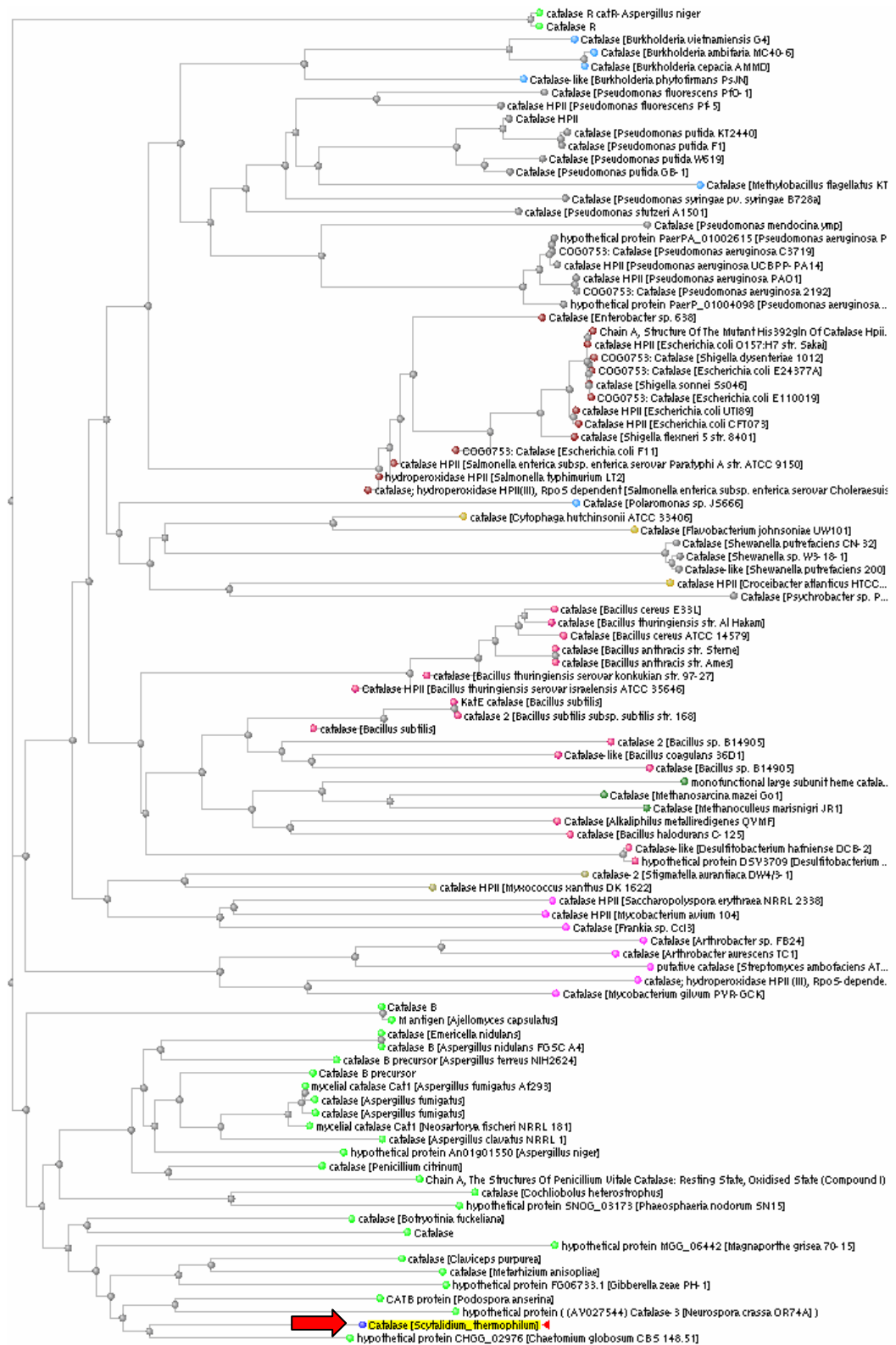


Figure 4.15. Taxonomic tree of sequence alignment of *S. thermophilum* CCO

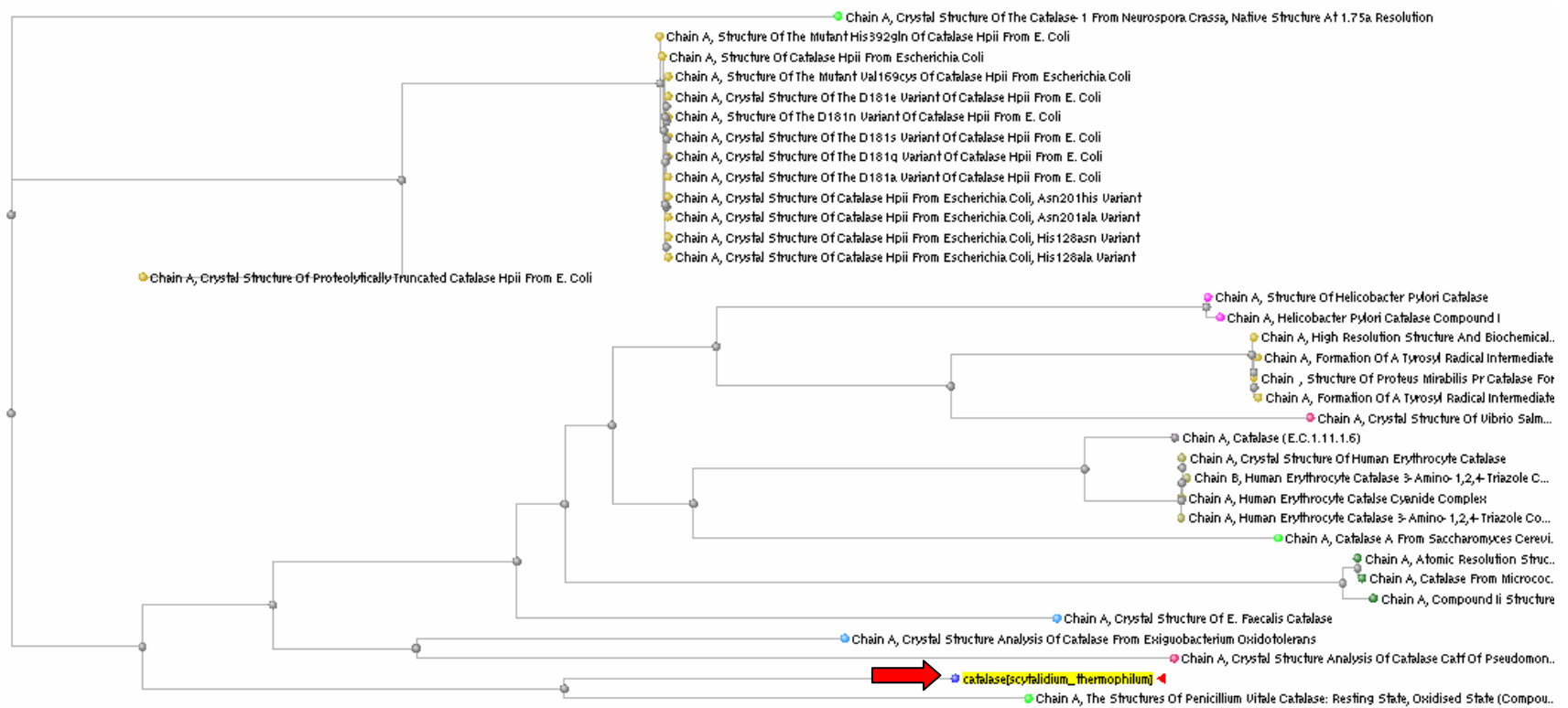


Figure 4.16. Taxonomic tree of structural alignment of *S. thermophilum* CCO

The microorganisms having the highest similarities were; *Chatemium globosum*, *Podospora anserine*, *Claviceps purpurea*, *Neurospora crassa*, *Gibberella zeae* and *Metarhizium anisopliae*. The highest structural similarity was predicted with *Penicillium vitale* catalase. All of these microorganisms, including *S. thermophilum*, belonging to fungal kingdom and *Pezizomycotina* subphylum. Moreover, except *C. purpurea* and *P. vitale*, all were in the same class of *Sordariomycetes*. Therefore, the taxonomic classification and degree of similarity showed that catalase is almost completely conserved among the order and the phylum.

Table 4.4. Sequence alignment statistics of *S. thermophilum* CCO

	Length	Score	Identities (%)	Positivies (%)	Gaps (%)
<i>C.globosum</i>	705	1105	75	84	2
<i>P.anserina</i>	726	1049	72	82	1
<i>C.purpurea</i>	716	1026	72	82	1
<i>N.crassa</i>	719	1014	69	80	0
<i>P.vitale</i>	688	875	63	77	1
<i>G.zeae</i>	716	994	68	79	1
<i>M.anisopliae</i>	715	991	69	81	0



Figure 4.17. Sequence alignment of *S. thermophilum* CCO

#### 4.7. UV-Vis Spectra of CCO

The UV-Vis spectra of purified CCO (3 mg/ml) determined in a range of 200-800 nm was shown in Figure 4.18. The absorption maxima were determined at 280 nm, 406 nm, 584 nm and 691 nm. The highest peak was observed at 280 nm which is the indicator of the protein content of the sample. The second highest peak was predicted at 406 nm. This result is similar to that of catalase from a thermophilic fungus, *Thermoascus aurantiacus*, where absorption maxima were recorded at 405 nm and 588 nm (Wang *et al.*, 1998) and from a bacterium, *Klebsiella pneumoniae*, with absorption maxima at 405, 590 and 630 nm (Goldberg and Hochman, 1989).

All of these enzymes have strong absorption in the Soret band around 406 nm, showing their heme-content. Catalases from other sources such as *Saccharomyces cerevisiae* (Zámocký and Koller, 1999), *Penicillium simplicissimum* (Fraaije *et al.*, 1996) also show strong absorbance in Soret Band at 406 nm and 407 nm, respectively. The spectra of *S. thermophilum* CCO was recorded at different enzyme concentrations and the average value of R ( $A_{406}/A_{280}$ ) was calculated as c. 0.5, which is quite different from *Thermoascus aurantiacus* (Wang *et al.*, 1998) and *Saccharomyces cerevisiae* (Zámocký and Koller, 1999) catalase R values of c. 1. This might be an indication of a lower concentration of heme in CCO molecule.

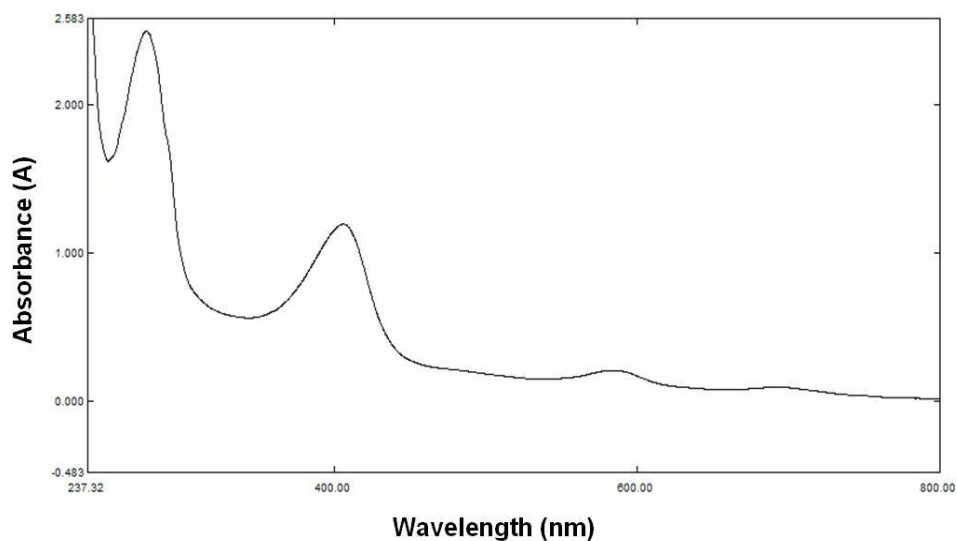


Figure 4.18. UV-Vis spectra of CCO

#### 4.8. Characterization of CCO Activities

The enzyme was found to have a bifunctional nature and therefore it was characterized in terms of its both activities; catalase and catechol oxidase.

##### 4.8.1. Effect of pH on CCO activity and stability

The effect of pH on CCO catalase and catechol oxidase activities and stabilities were determined in a pH range of 5.0-9.0 under standard assay conditions. The highest activity was observed at pH 7 for both catalase and catechol oxidase as shown in Figure 4.19 and Figure 4.20, respectively. CCO-catechol oxidase was most active between pH 7-8, retaining c. 80 % of its activity at pH 8. CCO-catalase was also most active around pH 7. Catalase retained c. 80% of its activity in the pH range of 6-7, where catechol oxidase preserved only c. 25%. Catalase

was active in the broad pH range of 5-9 retaining more than 60 % of its activity but this percentage is c. 15 % for catechol oxidase.

Accordingly, catalase and catechol oxidase were most stable at pH 7.0 as shown in Figure 4.21 and 4.22, respectively. More than 90 % of their initial activity was observed after 24 h incubation at pH 7. Except catechol oxidase at pH 9, both catalase and catechol oxidase retained c. 80 % of their initial activities even after 24 hours incubation.

A wide pH stability was reported as a common feature of catalases (Kulys *et al.*, 2003). They generally exhibit stability in a broad pH range from 5 to 10. Wang *et al.* (1998) found that the catalase of *Thermoascus aurantiacus* was stable in the pH range of 5-13. Similarly, catalase activity of CCO was stable in the pH range of 5-9 in this study.

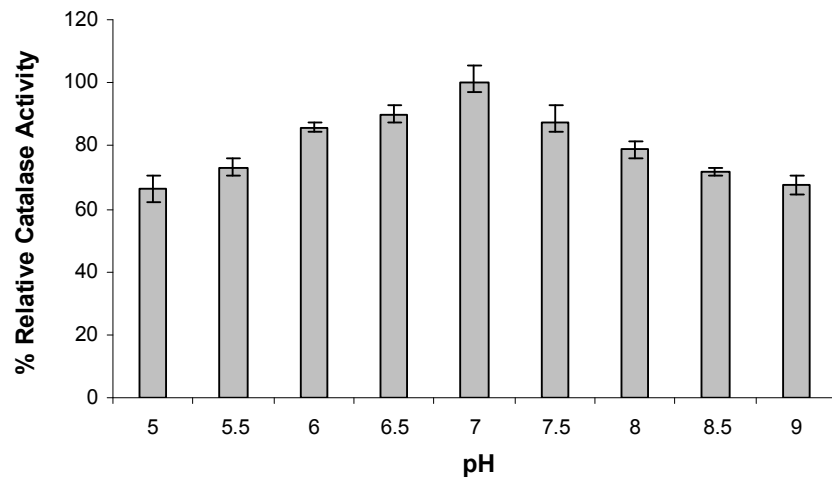


Figure 4.19. pH-dependence of CCO-catalase activity (under standard assay conditions at 60 °C and different pH values)

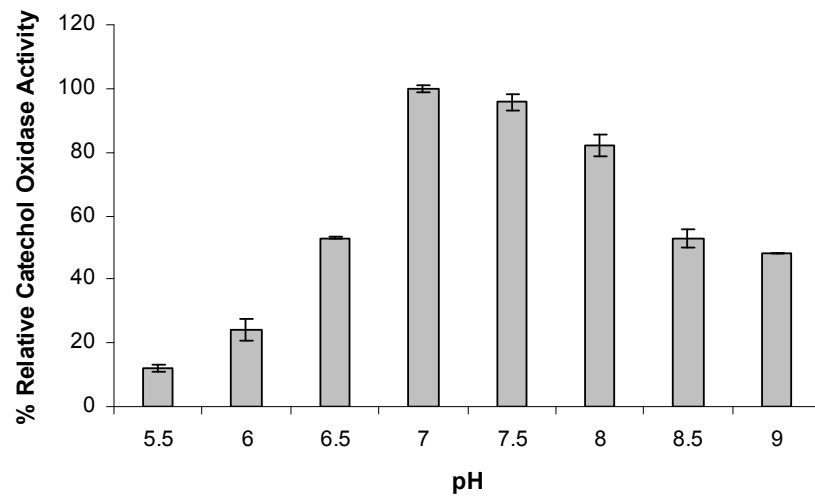


Figure 4.20. pH-dependence of CCO catechol oxidase activity (under standard assay conditions at 60 °C and different pH values)

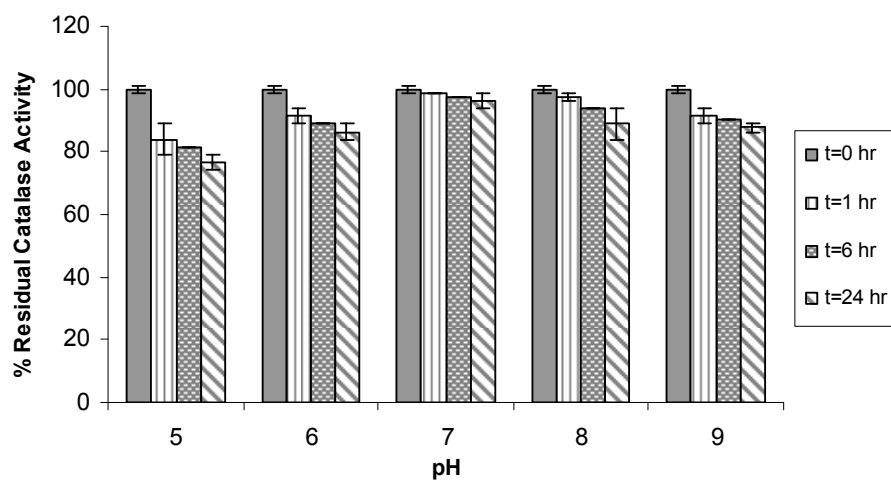


Figure 4.21. pH-dependence of CCO catalase stability (under standard assay conditions at 60 °C, at different pH values and incubation times)

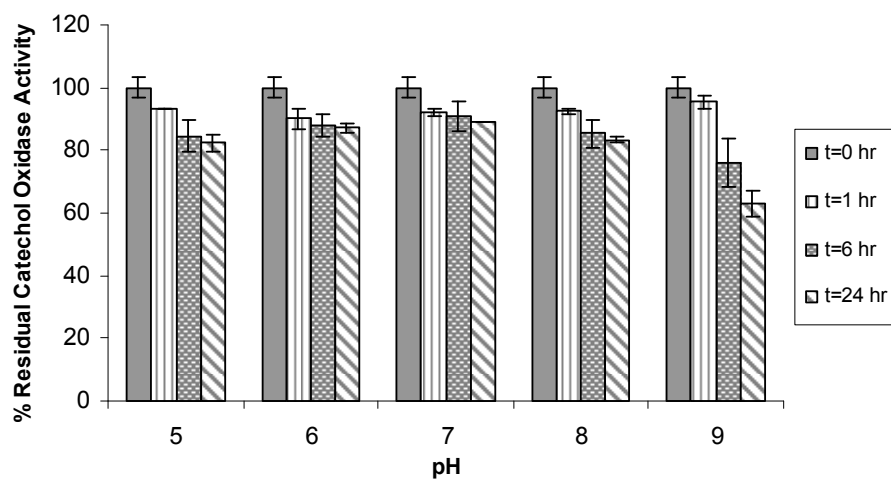


Figure 4.22. pH-dependence of CCO catechol oxidase stability (under standard assay conditions at 60 °C, at different pH values and incubation times)

#### 4.8.2. Effect of Temperature on CCO Activity and Stability

A temperature range of 30-80 °C was searched for the temperature at which the highest CCO catalase and catechol oxidase activities were present. Relative activities were over 70 % between 30-75 °C for catalase (Figure 4.23) and between 55-75 °C for catechol oxidase (Figure 4.24), having the maximum activity at 60 °C for both activities. Catechol oxidase activity was more sensitive to temperature below 60 °C than catalase. If the temperature would be decreased from 60 °C to 30 °C, catechol oxidase would show only 20 % of its highest activity but this value would be more than 70 % for catalase. At temperatures above 60 °C upto 80 °C, behavior of catalase and catechol oxidase activities of CCO was similar, showing c. 60 % of the maximum activity. The positive effect of increase in temperature up to 60 °C was more apparent in catechol oxidase activity. In overall, catalase activity of CCO was higher than catechol oxidase activity in the temperature range tested.

Thermostability of CCO catalase and catechol oxidase activities were tested over the temperature range of 50-80 °C and shown in Figure 4.25 and 4.26, respectively. After treatment of enzyme samples at various temperatures for 2 h, no decrease in activity was observed at 50 °C for both activities. Enzyme retained 80 % and 45 % of its original catalase activity and 90 % and 60 % of its original catechol oxidase activity at 60 and 70 °C, respectively. Catalase and catechol oxidase activities were almost totally lost at 80 °C after 2 h incubation. Catechol oxidase activity of CCO was more thermostable than catalase activity in the tested range. Especially at 80 °C, catalase activity was rapidly lost in 30 min. This can be because of the nature of the enzyme or the unstability of hydrogen peroxide at high temperatures.

Similarly, in the study of Wang *et al.* (1998), thermostability of a catalase from *Thermoascus aurantiacus* was investigated. It was reported as stable up to 80 °C and the optimum temperature was predicted as 70 °C.

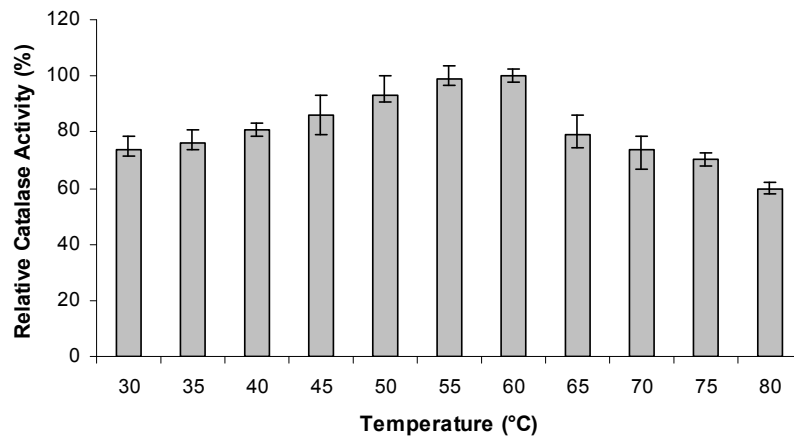


Figure 4.23. Temperature dependence of CCO catalase activity (under standard assay conditions at pH 7.0 and different temperatures)

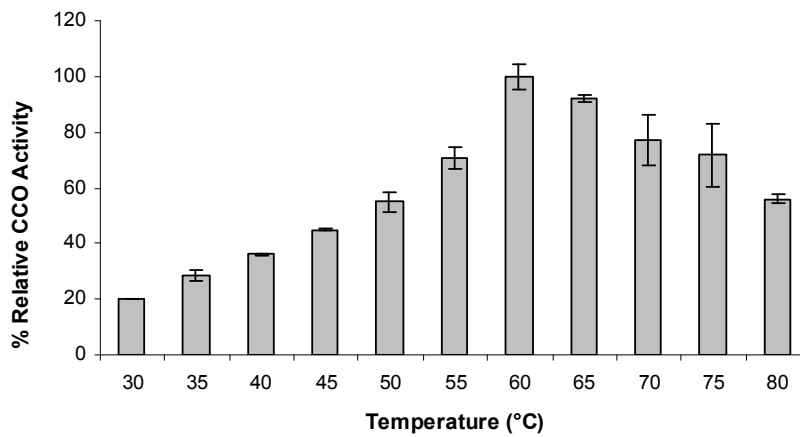


Figure 4.24. Temperature dependence of CCO catechol oxidase activity (under standard assay conditions at pH 7.0 and different temperatures)

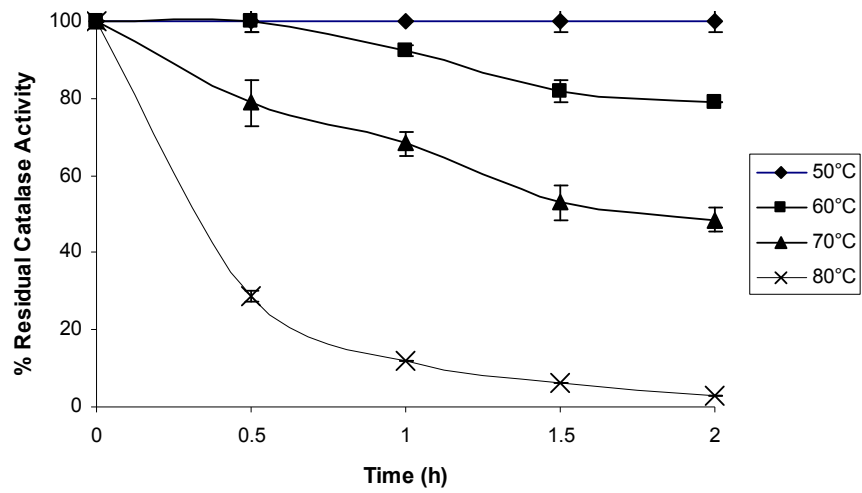


Figure 4.25. Temperature dependence of CCO catalase stability (under standard assay conditions at pH 7.0, at different temperatures and incubation times)

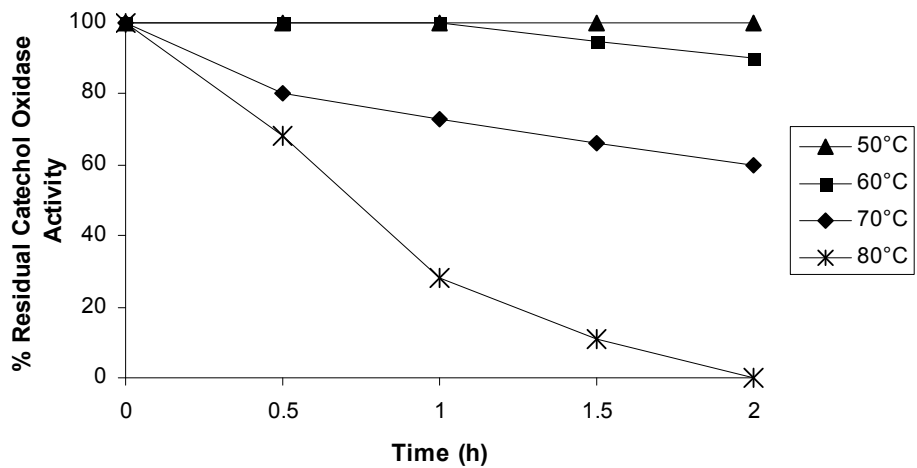


Figure 4.26. Temperature dependence of CCO catechol oxidase stability (under standard assay conditions at pH 7.0, at different temperatures and incubation times)

Activation energies for both activities of CCO were calculated using the Arrhenius equation as shown in Figure 4.27 and Figure 4.28, respectively. Activation energies of catalase and catechol oxidase were determined as  $2.7 \pm 0.2$  and  $10.1 \pm 0.4$  kcal/mol, respectively.

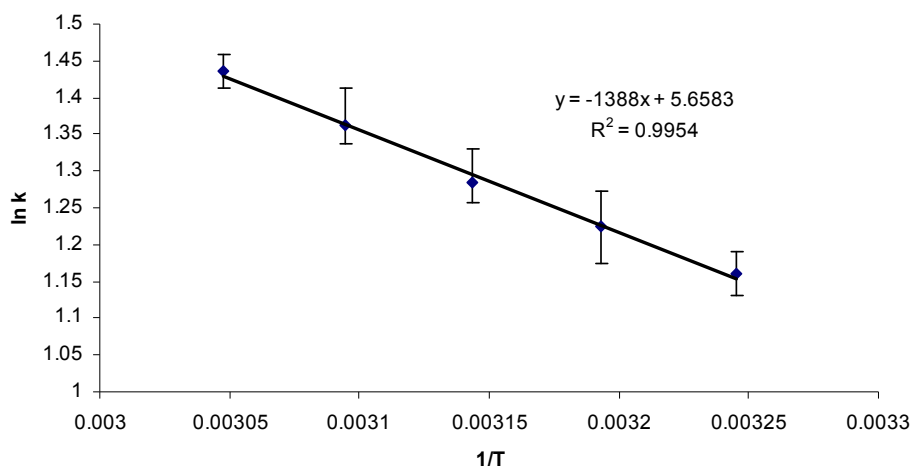


Figure 4.27. Activation energy of CCO catalase activity (under standard assay conditions at pH 7.0 at different temperatures)

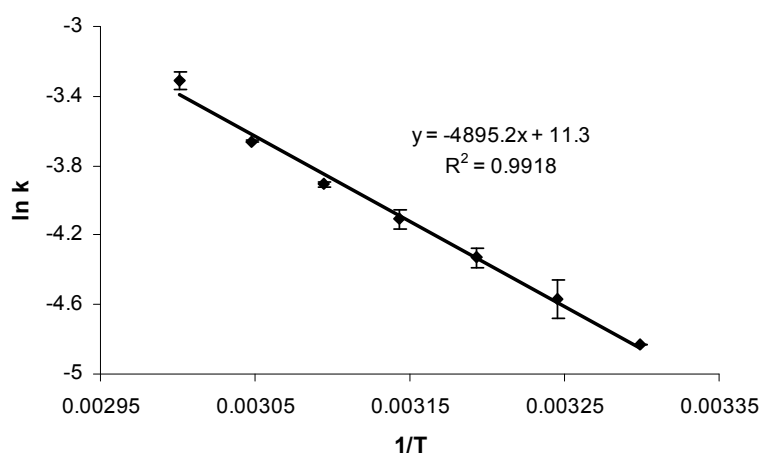


Figure 4.28. Activation energy of CCO catechol oxidase activity (under standard assay conditions at pH 7.0 at different temperatures)

#### 4.8.3. Substrate Specificity and Effect of Inhibitors on CCO Catechol Oxidase Activity

Different phenolic substrates; ABTS, caffeic acid, L-dopa, tyrosine, *p*-hydroquinone and syringaldazine were used to determine the substrate specificity of CCO phenol oxidase activity. Relative activities were given in Table 4.5 with respect to catechol, the substrate used in standard assay procedure. CCO showed catechol oxidase activity but no laccase-like activity since the pure enzyme oxidizes neither syringaldazine nor ABTS which are accepted as unique substrates for true laccase activity (Burke and Cairney, 2002). A very low activity was observed towards *p*-hydroquinone which is a *p*-diphenol. Tyrosine is not hydroxylated by CCO, showing absence of the cresolase activity. However oxidation of L-DOPA is another indication of the enzyme having catechol oxidase activity.

Table 4.5. Phenolic substrate specificity of CCO

Substrate	% Relative Activity
100 mM catechol	100
100 mM caffeic acid	49
50 mM L-DOPA	30
100 mM <i>p</i> -hydroquinone	2
5 mM ABTS	No activity
5 mM tyrosine	No activity
5 mM syringaldazine	No activity

Table 4.6. Effect of inhibitors on CCO catechol oxidase activity

Inhibitor	% Relative Activity
100 mM catechol + no inhibitor	100
0.25 mM salicylhydroxamic acid	59
0.5 mM salicylhydroxamic acid	36
10 mM <i>p</i> -coumaric acid	54
20 mM <i>p</i> -coumaric acid	28
30 mM <i>p</i> -coumaric acid	14

Along with the substrate selection, catechol oxidase inhibitors, namely salicylhydroxamic (SHAM) and *p*-coumaric acids, inhibited catechol oxidase activity of CCO as presented in Table 4.6. Moreover, the inhibitory effect of *p*-coumaric acid is higher toward the pure enzyme than the crude enzyme (Ögel *et al.*, 2006). This could be due to the difference in three dimensional structure of the crude enzyme in culture supernatant and pure enzyme in the buffer solution.

The inhibitory effect of SHAM can be explained by its ability to bind to the iron and copper in the enzymes and its effect has been reported before on catechol oxidase copper (Allan and Walker, 1988) and peroxidase heme (Ikeda-Saito *et al.*, 1991). The inhibitory effect of SHAM on CCO catechol oxidase activity can be due to its binding to the heme since we are sure about the presence of the heme in CCO according to the strong absorption in the Soret band. But the R value was lower than the typical catalases, which might be an indication of presence of other metals. Combination of these data may suggest that the CCO contains copper in addition to the heme in different subunits of the enzyme. Preliminary ICP-MS analysis (data not shown) supports this suggestion.

#### 4.9. CCO Kinetics

Kinetic parameters of CCO were investigated for both catalase and catechol oxidase activities. For CCO-catalase activity, the concentration range of hydrogen peroxide was 0-50 mM. Results for catalase obeyed Michaelis-Menten kinetics upto 15 mM hydrogen peroxide concentration. At higher substrate concentrations, activity measurements could not be done properly because of very high absorbance values. Therefore, results with 0-15 mM hydrogen peroxide were used and given in Figure 4.29. Substrate inhibition was not observed up to 15 mM hydrogen peroxide concentration. Lineweaver-Burk plot was shown in Figure 4.30.  $K_m$  and  $V_{max}$  values for catalase were calculated as 11.4 mM and 6.1 U/ml, respectively.

Chelikani *et al.* (2004) reported that most of the small subunit catalases begin to suffer inactivation by hydrogen peroxide at concentrations above 300–500 mM. These catalases never reach the Michaelis-Menten  $V_{max}$  determined from rates at low substrate concentrations. Large subunit catalases start to suffer inhibition only above 3 M hydrogen peroxide concentration. The presentation of observed data in terms of the typical constants  $K_m$  and  $V_{max}$  is not possible because true Michaelis-Menten kinetics are not valid. The  $K_m$  value calculated from the hydrogen peroxide concentration at  $V_{max}/2$  ranged from 38 to 599 mM.

To determine CCO-catechol oxidase activity kinetic constants, the concentration range of 0-300 mM catechol was used. Catechol oxidase activities vs. substrate concentrations are illustrated in Figure 4.31. Results for catechol oxidase activity did not perfectly obey Michaelis-Menten kinetics. Substrate inhibition was observed above 250 mM concentration. Lineweaver-Burk plot was given in Figure 4.32.  $K_m$  and  $V_{max}$  values for catechol oxidase were calculated as 155 mM and 294 U/ml, respectively.

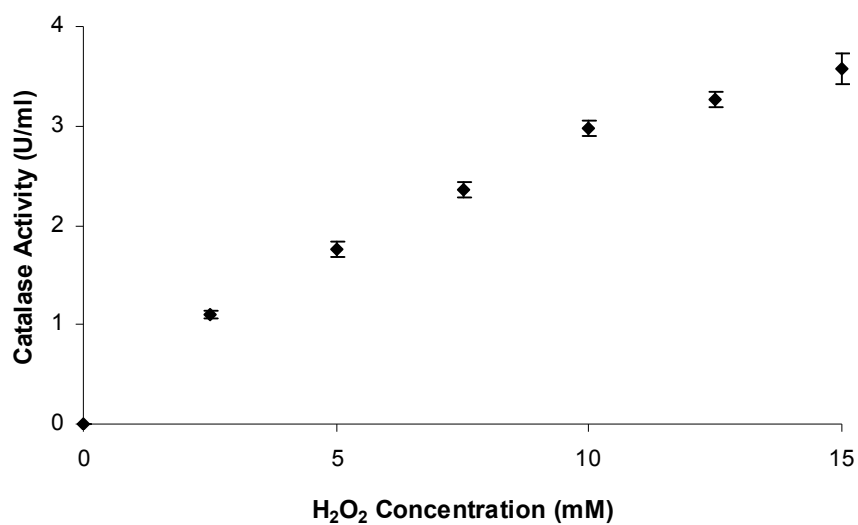


Figure 4.29. Michaelis Menten curve of CCO catalase activity (under standard assay conditions at 60 °C and pH 7.0)

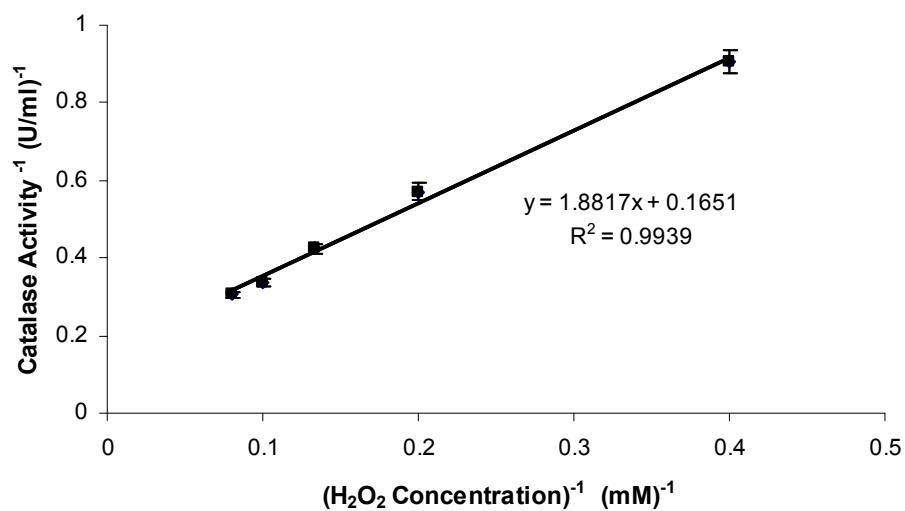


Figure 4.30. Lineweaver Burk plot of CCO catalase activity (under standard assay conditions at 60 °C and pH 7.0)

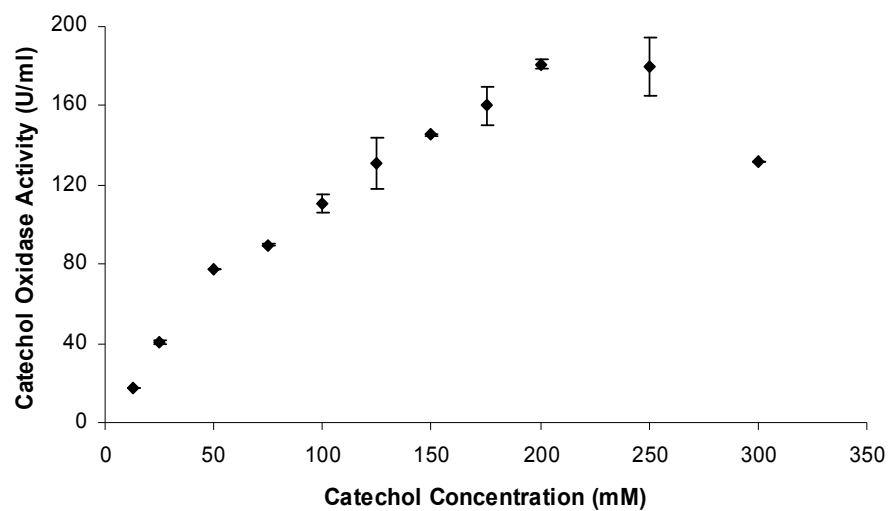


Figure 4.31. Michaelis Menten curve of CCO catechol oxidase activity (under standard assay conditions at 60 °C and pH 7.0)

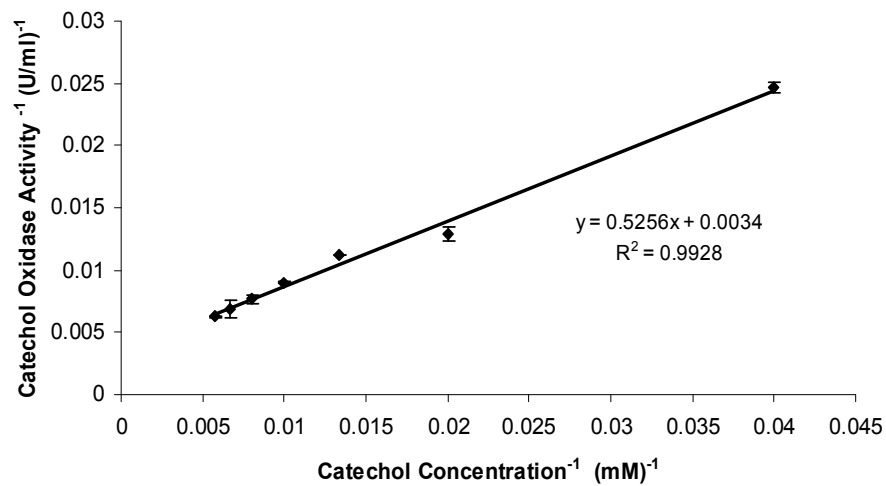


Figure 4.32. Lineweaver Burk plot of CCO catechol oxidase activity (under standard assay conditions at 60 °C and pH 7.0)

#### **4.10. Determination of Crystal Structure of CCO**

Three dimensional structure of CCO was determined by crystallization of the protein using hanging drop vapor diffusion technique and collecting data by X-ray analysis. This part of the studies was performed in Astbury Center Protein Crystallization Department of Leeds University, in Prof. Simon E.V. Phillips's laboratory.

##### **4.10.1. Crystallization of CCO**

The aim of the first step in crystallization experiments was to determine the initial crystallization conditions from screening experiments. Eight different screening kits namely Crystal Screen 1 (50 reagents), Crystal Screen 2 (48 reagents), Index (96 reagents), Membfac (48 reagents), SaltRx (96 reagents) and Natrix (48 reagents) from Hampton Research (USA) and Wizard 1 and Wizard 2, 48 reagents each, from Emerald Biosystems (USA) were tested. The parameters changed and used at different concentrations in the kits were given in Table 4.7. First crystal was observed in 28 % PEG-1500, at 100 mM -6.5 Bis-Tris buffer pH 5.0 at 18 °C. Using these initial conditions, large scale crystal trays were prepared. The first crystals were observed as shown in Figure 4.33. These brownish-green butterfly-shaped crystals contained multi-layers and were not ordered crystals, therefore were not suitable for X-ray data collection.

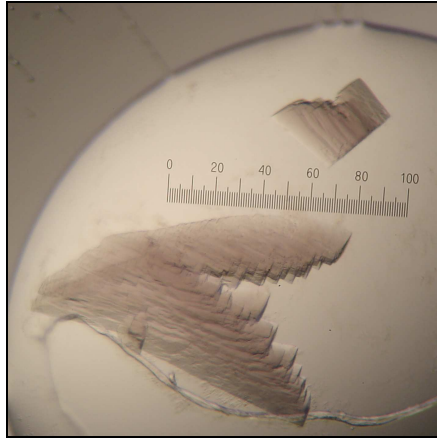


Figure 4.33. Initial large scale CCO crystal in 28 % PEG-1500 at pH 6.0 and 18 °C

In addition to initial screening conditions, different conditions were tested by changing the temperature, protein concentration, PEG type and concentration, buffer type and pH. Another crystallization condition, 24 % PEG-3500 at pH 5.0-6.5 with 100 mM Bis-Tris buffer resulted with rod-shaped and better ordered crystals (Figure 4.34). However, their quality was also not good enough for X-ray analysis.

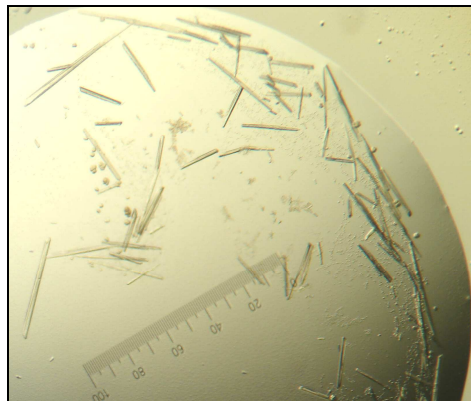


Figure 4.34. CCO crystal in 24 % PEG-3500 at pH 6.0 and 18 °C

Table 4.7. Screening kit parameters

Precipitants	Buffers	Salts
(+,-)-2-Methyl-2,4-pentanediol	Bis-Tris	Ammonium acetate
1,4-butanediol	CAPS	Ammonium nitrate
1,6-hexanediol	CHES	Ammonium sulphate
2-propanol	Citric acid	Ammonium hydrogen-phosphate
Ammonium sulphate	HEPES	Calcium chloride
Ethanol	Imidazole	Lithium sulphate
Jeffamine	MES	Magnesium acetate
Magnesium formate-dehydrate	n-(2-Acetamino)iminodiacetic acid	Magnesium chloride
PEG 10000	Sodium acetate	Magnesium formate
PEG 1500	Sodium cacodylate	Potassium bromide
PEG 2000	Sodium citrate	Potassium chloride
PEG 3350	Tris	Potassium chloride
PEG 4000		Potassium thiocyanate
PEG 5000		Sodium chloride
PEG 8000		Sodium formate
Polypropylene glycol		Sodium malonate
Potassium-sodium tartarate		Sodium nitrate
Sodium chloride		Sodium succinate
Sodium citrate		Succinic acid
Sodium phosphate		Taccimate
Succinic acid		
Taccimate		

It was known from previous studies that salt addition generally improves the crystal quality. Changing the PEG type generally results with a better crystal. Therefore, different salts and PEG were tested in crystallization solution and the results were shown in Figure 4.35. Addition of salt and using 24 % PEG-2000 increased the crystal quality significantly. Addition of calcium chloride ( $\text{CaCl}_2$ ) was beneficial (Figure 4.35-a) but sodium

chloride (NaCl) resulted in better crystals (Figure 4.35-b and c). In spite of these improvements, crystals were still not suitable for data collection.

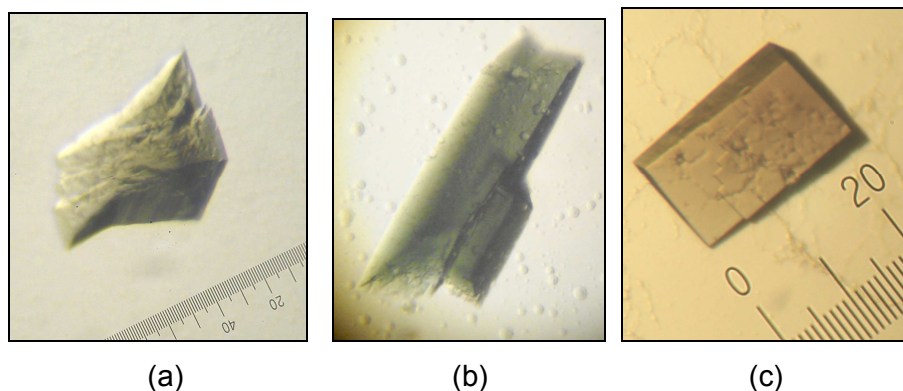


Figure 4.35. CCO crystal in 24 % PEG-2000 at 18 °C and (a) pH 6.0 and 10 mM CaCl<sub>2</sub>, (b) pH 6.0 and 10 mM NaCl, (c) pH 6.5 and 10 mM NaCl

Since it is sometimes difficult to simultaneously optimize the conditions for nucleation and growth of the crystal, a new strategy involving the separate optimization of these processes should be developed. This can be accomplished by seeding, in which crystals are transferred from nucleation conditions to those that will support only growth. Therefore, in the next step of the study, seeding was applied. Disordered crystals were grown and crashed to get a very small piece of a CCO crystal. This crystal particle was used a “seed” and transferred into a new drop. This time, better crystals were observed as shown in Figure 4.36. As expected, crystals were better in quality basis but sizes of the new crystals were small and they were grown as a cluster.

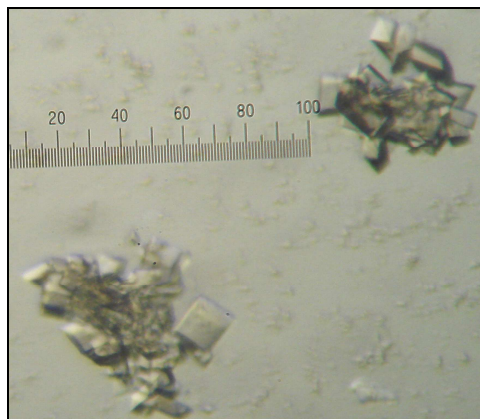


Figure 4.36. CCO crystals after seeding in 24 % PEG-2000, 10 mM NaCl at pH 6.5 100 mM Bis-Tris buffer

Because using some additives generally improves the crystal quality, Additive Screen (Hampton Research, USA) with 96 reagents such as 6-aminocaproic acid, phenol, sodium fluoride, urea, sarcosine, EDTA, acetone, acetonitrile, ethyl acetate, methanol, xylitol etc. was used. Among the additives tested, 3% (w/v) 6-amino-caproic acid was determined to be the best additive. Adding  $\text{CaCl}_2$  was found beneficial in previous experiments, therefore it was tested at different concentrations in a range of 5-50 mM.

As a result, the best crystal was obtained as shown in Figure 4.37 at the condition of 24 % PEG-2000 at pH 6.5 100 mM Bis-Tris buffer with 10 mM NaCl, 10 mM  $\text{CaCl}_2$  and 3% 6-amino-caproic acid at 18 °C. Under these conditions, several crystal trays were set and many single good-quality ordered crystals were grown in one week. These crystals were cryo-cooled in liquid nitrogen using paratone-n oil as cryoprotectant and used for X-ray data collection in Daresbury-SRS facility.

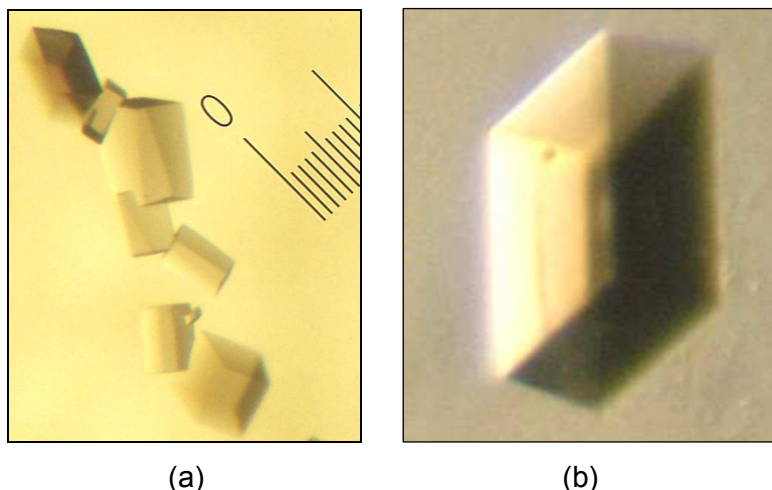


Figure 4.37. The best CCO crystal in 24 % PEG-2000 at pH 6.5 100 mM Bis-Tris buffer with 10 mM NaCl, 10 mM CaCl<sub>2</sub> and 3 % 6-amino-caproic acid at 18 °C (a) Streak seeding line (b) Single CCO crystal

In the structural sequence analysis, it was predicted that the structure *P. vitale* had the highest similarity to *S. thermophilum* CCO. In the study of Alfonso-Prieto *et al.* (2007), *P. vitale* catalase (PVC) was purified and crystallized by the hanging-drop vapor diffusion method, as similar to our study. A precipitant solution of 38 % MPD and 50 mM sodium acetate buffer pH 5.2 was used. These conditions were not similar to the conditions used in our study.

Proteins are very sensitive molecules and each of them has its own specific properties. Crystallization conditions are also one of these characteristic properties of the proteins. Therefore, having differences in crystallization conditions of even very similar proteins is a common case.

#### 4.11. Solving Crystal Structure of CCO

CCO crystals obtained after seeding in 24 % PEG-2000 at pH 6.5 100 mM Bis-Tris buffer with 10 mM NaCl, 10 mM CaCl<sub>2</sub> and 3% 6-amino-caproic acid at 18 °C were cryo-cooled and used for X-ray analysis. Diffraction data were collected at Beamline-10.1 in Daresbury Synchrotron Radiation Source (SRS). Crystals diffracted upto 2.7 Å resolution. In total, 360 images were taken at 100K under liquid nitrogen conditions. X-ray diffraction patterns of *S. thermophilum* CCO at angles 10 °, 30 °, 45 °, 90 °, 135 ° and 180 ° were shown in Figure 4.38-a, b, c, d, e and f, respectively.

To solve the structure, collected data were processed using HKL2000. After achieving suitable completeness, the structure of a suitable homologue was searched for molecular replacement. After getting N-terminus (10 aa) and internal (12 aa) amino acid sequences from LIGHT Laboratory, the enzyme of *S. thermophilum* was determined as catalase. Therefore, *Penicillium vitale* catalase, which was found to be the closest structural homolog, was used to solve the structure by molecular replacement using the program MOLREP. The sequence of the enzyme given by free United States Patent (No. 5646025) was used to build the structure model. For computer graphics, model building program COOT, and for crystallographic refinement REFMAC were used. The resolution was improved from 2.7 Å to 2.6 Å by the first refinement analysis. The solvent ratio in the crystal was found to be 43.57 %. The preliminary structure was shown in Figure 4.39. Refinement studies are still in progress.

As shown in Figure 4.39, CCO was composed of two homodimers. The structure was very similar to *P. vitale* catalase structure. The electron density map shown in Figure 4.40 showed an apparent metal center. The electron density corresponding to amino acids includes also the back bone (shown in yellow), but in Figure 4.41, there is the electron density map containing no amino acid back bone. This region corresponds to a

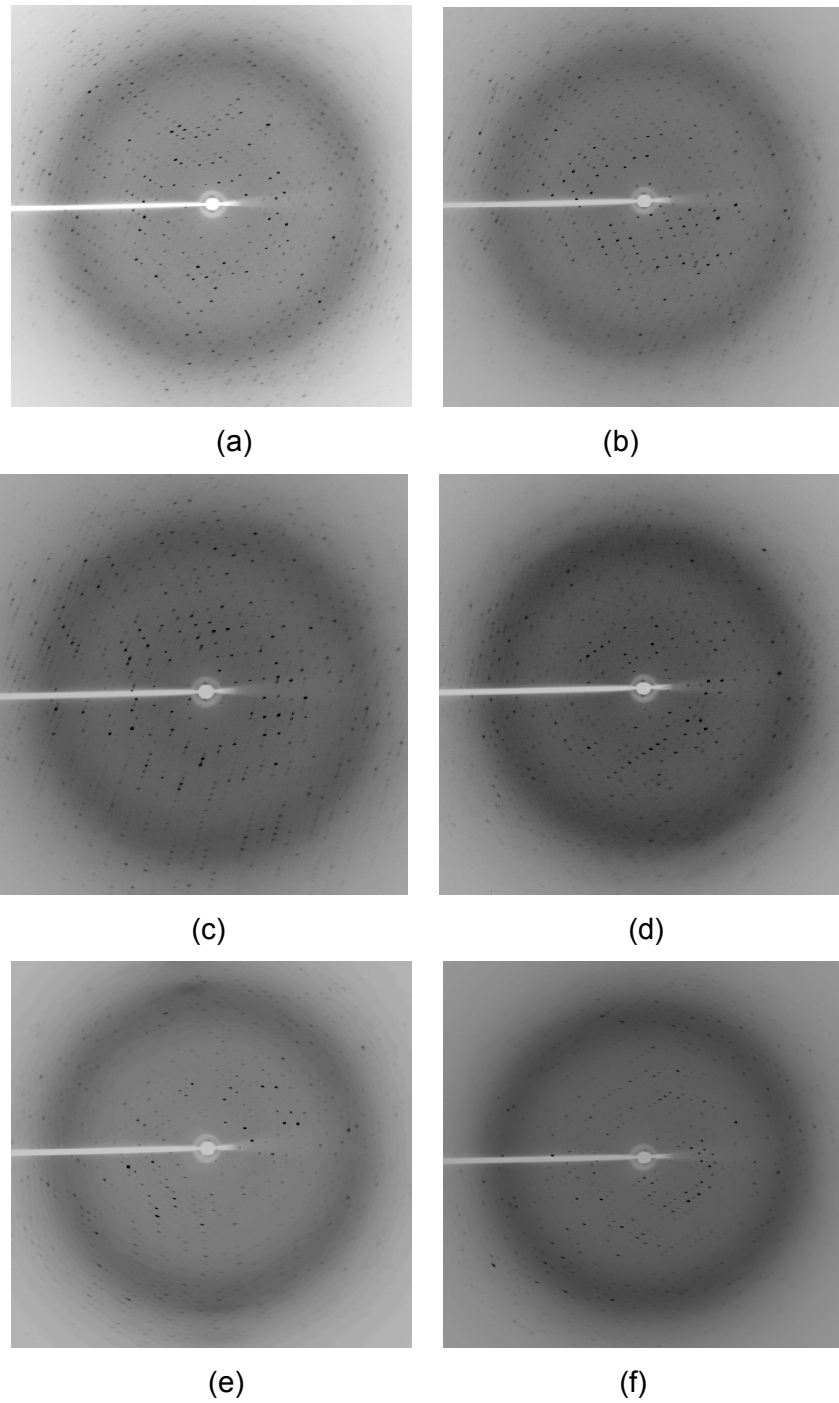


Figure 4.38. X-ray diffraction patterns of *S. thermophilum* CCO at angles (a) 10°, (b) 30°, (c) 45°, (d) 90°, (e) 135° and (f) 180°.

metal center. It was possible to conclude on a metal center, but not easy to determine, which metal it is, by using only the electron density map data. In the article about *P. vitale* catalase structure published by Alfonso-Prieto *et al.* (2007), very similar heme center was demonstrated. Therefore, the metal center in *S. thermophilum* CCO polypeptide chain was determined as heme. The OH group on the end of the side chain of tyrosine (A chain, amino acid no. 352) is in direct contact with the heme as shown in Figure 4.41. As declared previously, presence of the heme in CCO was also determined according to the strong absorption in the Soret band. Since the R value was lower than the typical catalases, it might be an indication of presence of other metals. It was concluded that, combination of these data might mean that the CCO may contain copper in addition to the heme in different subunits of the enzyme. In fact, presence of copper and iron has been determined by preliminary ICP-MS analysis (data not shown). This question will be accurately answered after finishing structural refinement studies.

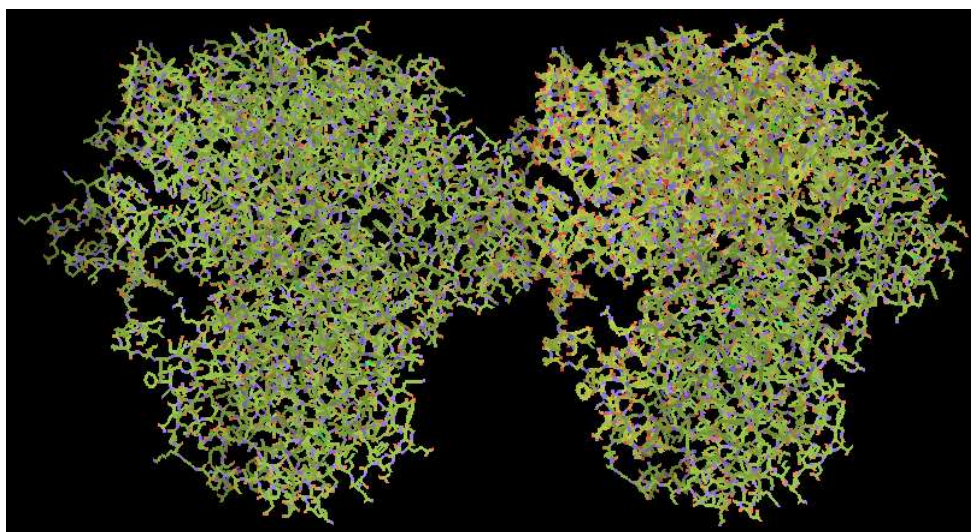


Figure 4.39. Three dimensional CCO structure

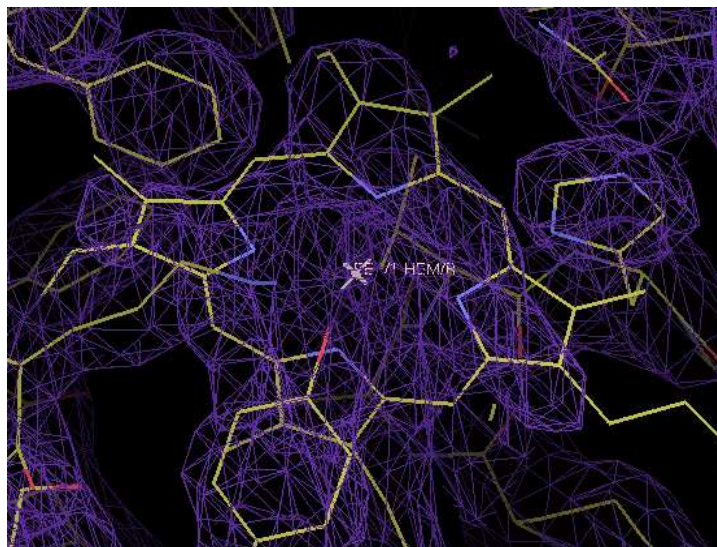


Figure 4.40. Heme center in CCO structure with electron density map

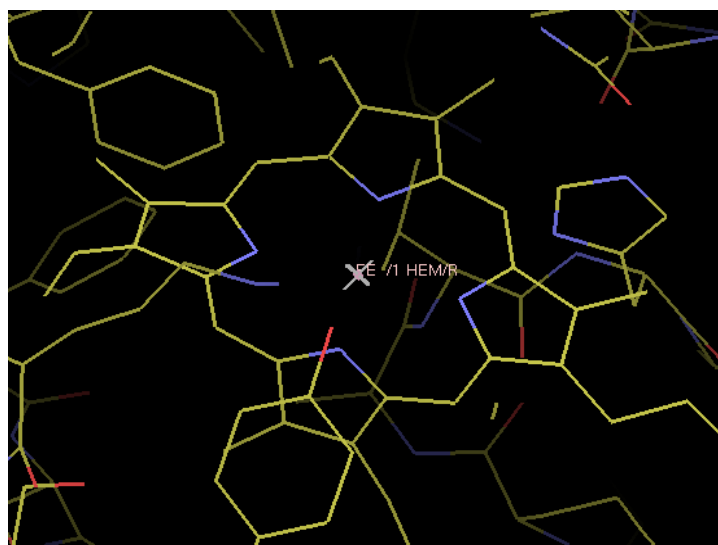


Figure 4.41. Heme center in CCO structure without electron density map

## CHAPTER 5

### CONCLUSIONS

In this study, the aim was to produce, purify, biochemically characterize and crystallize the bifunctional catalase of a thermophilic fungus, *Scytalidium thermophilum*, and then determine its preliminary three dimensional structure by X-ray analysis. The enzyme was named as catalase-catechol oxidase (CCO) because it was able to decompose the hydrogen peroxide (catalase activity) and oxidize catechol (catechol oxidase activity).

Main conclusions can be summarized as given below:

- At the beginning of the research, this enzyme was considered as a phenol oxidase. However, in further studies, it was found to be a “catalase”, with an additional catechol oxidase activity.
- The enzyme was a novel bifunctional catalase-catechol oxidase (CCO). It is novel since detailed information about such a fungal catalase-catechol oxidase is not apparent in the literature.
- Enzyme was unable to oxidize laccase and tyrosinase-specific substrates. It was also not capable to act as peroxidase. The only phenol oxidase activity was determined as catechol oxidase.
- Having both catalase and catechol oxidase activities in the same enzyme can be advantageous for industrial applications, especially in phenol oxidase enzyme electrode preparation for phenolic concentration determinations.

- CCO was observed as a suitable enzyme for various industrial applications since the enzyme has high thermal and pH stability in terms of catalase and catechol oxidase activities. Thermophilic nature of *S. thermophilum* makes the use of CCO beneficial in industrial processes, where higher operating temperatures are used.
- In addition to *S. thermophilum* CCO, catechol oxidase activities of other catalases from *Aspergillus niger*, human and bovine liver were also determined. The bifunctionality of *S. thermophilum* CCO was a new feature, with a possibility of including mostl other catalases, which could be a new research area.

## CHAPTER 6

### RECOMMENDATIONS

On the basis of this present research;

- Further screening and characterization studies can be performed for detailed analysis of phenol oxidase activities of other catalases
- The microorganism used in this research, *S. thermophilum*, was wild-type, therefore over-expression of CCO and modification of the enzyme can be done using genetic engineering tools .
- Attempts to optimizing the conditions for kinetic constants determination of CCO activities could be the next step of the characterization experiments.
- To determine the CCO three dimensional structure more accurately to find out the metal content and structure-function relationships, refinement studies are still in progress, but efforts towards growing better crystals to get structural data at higher than 2.7 Å resolution should also be considered in the future.

## REFERENCES

Aguirre, J., Momberg, M.R., Hewitt, D., Hansberg, W., 2005. "Reactive oxygen species and development in microbial eukaryotes", *Trends in Microbiology*, 13(3), 111-118.

Akagawa, M., Shigemitsu, T., Suyama, K., 2003. "Production of hydrogen peroxide by polyphenols and polyphenol-rich beverages under quasi-physiological conditions", *Bioscience, Biotechnology and Biochemistry*, 67(12), 2632-2640.

Alfonso-Prieto, M., Borovik, A., Carpena, X., Murshudov, G., Melik-Adamyanyan, W., Fita, I., Rovira, C., Loewen, P.C., 2007. "The structures and electronic configuration of compound I intermediates of *Helicobacter pylori* and *Penicillium vitale* catalases determined by X-ray crystallography and QM/MM density functional theory calculations", *Journal of American Chemical Society*, 129, 4193-4205.

Allan, A.C., Walker, J.R.L., 1988. "The selective inhibition of catechol oxidases by salicylhydroxamic acid", *Phytochemistry*, 27, 3075-3076.

Amitai, G., Adani, R., Sod-Moriah, G., Rabinovitz, I., Vincze, A., Leader, H., Chefetz, B., Leibovitz-Persky, L., Friesem, D., Hadar, Y., 1998. "Oxidative biodegradation of phosphorothiolates by fungal laccase", *FEBS Letters*, 438(3), 195-200.

Amorim, A.M., Gasques, M.D.G., Andreaus, J., Scharf, M., 2002. "The application of catalase for the elimination of hydrogen peroxide residues after bleaching of cotton fabrics", *Annals of the Brazilian Academy of Sciences*, 74(3), 433-436.

Aoshima, H., Ayabe, S., 2007. "Prevention of the deterioration of polyphenol-rich beverages", *Food Chemistry*, 100, 350-355.

Arifoğlu, N., Z.B. Ögel., 2000. "Avicel-adsorbable endoglucanase production by the thermophilic fungus *Scytalidium thermophilum* type culture *Torula thermophila*", *Enzyme and Microbial Technology*, 27, 560-569.

Arrhenius, S., 1889. "Reaktionsgeschwindigkeit bei der Inversion von Rohrzucker durch Säuren", *Zeitschrift für Physical Chemistry*, 4, 226-248.

Bauer, G.C., Kühn A., GAjovic N., Skorobogatko O., Holt P.J., Bruce C.N., Makover A., Lowe R.C., Scheller W.F., 1999. "New enzyme sensors for morphine and codeine based on morphine dehydrogenase and laccase", *Journal of Analytical Chemistry*, 364, 179-183.

Bemmann, W., Voigt, A., Tröger, R., 1981. "Enzymatic studies of the thermophilic hydrocarbon utilizing fungi strains *Aspergillus fumigatus* and *Mucor lusitanicus*". *Zentralblatt für Bakteriologie, Parasitenkunde, Infektionskrankheiten und Hygiene Zweite Naturwissenschaftliche Abteilung: Mikrobiologie der Landwirtschaft der Technologie und des Umweltschutzes*, 136(8), 661-681.

Berg, J.M., Tymoczko, J.L., Stryer, L., *Biochemistry, 5th Ed.*, W.H. Freeman and Company, New York, USA, 2002.

Blundell, T.L., Johnson, L.N., *Protein Crystallography, 1st Ed.*, Academic Press Inc., London, Great Britain, 1976.

Bonomo, R., Boudet, A.M., Cozzolino, R., Rizzarelli, E., Santoro, A.M., Sterjiades, R., Zappala, R., 1998. "A comparative study of two isoforms of laccase secreted by the white-rot fungus *Rigidoporus lignosus*, exhibiting significant structural and functional differences", *Journal of Inorganic Biochemistry*, 71(3-4), 205-211.

Bradford, M.M., 1976. "A rapid and sensitive method for the quantitation of microgram quantities of protein utilizing the principle of protein-dye binding", *Analytical Biochemistry*, 72, 248–254.

Branden, C., Tooze, J., *Introduction to Protein Structure, 1st Ed.*, Garland Publishing Inc., New York, USA, 1991.

Brock, T.D., Madigan, M.T., *Biology of Microorganisms, 5th Ed.*, Prentice-Hall Inc., New Jersey, USA, 1988.

Burke, R.M., J.W.G. Cairney., 2002. "Laccases and other polyphenol oxidases in ecto- and ericoid mycorrhizal fungi", *Mycorrhiza*, 12, 105-116.

Cadimaliev, D.A., Revin, V.V., Atykyan, N.A., Samuilov, V., 2005. "Extracellular oxidases of the lignin-degrading fungus *Panus tigrinus*", 70(6), 703-707.

Calera, J.A., Sánchez-Weatherby, J., López-Medrano, R., Leal, F., 2000. "Distinctive properties of the catalase B of *Aspergillus nidulans*", *FEBS Letters*, 475, 117-120.

Cambria, M.T., Cambria, A., Ragusa, S., Rizzarelli, E., 2000. "Production, purification, and properties of an extracellular laccase from *Rigidoporus lignosus*", *Protein Expression and Purification*, 18(2), 141-147.

Caridis, K.A., Christakopoulos, P., Macris, B.J. 1991, "Simultaneous production of glucose oxidase and catalase by *Alternaria alternata*", *Applied Microbiology and Biotechnology*, 34(6), 794-797.

Chefetz, Benny., Chen, Y., Hadar, Y., 1998. "Purification and characterization of laccase from *Chaetomium thermophilium* and its role in humification", *Applied and Environmental Microbiology*, 64(9), 3175-3179.

Chelikani, P. Fita, I., Loewen, P.C., 2004. "Diversity of structures and properties among catalases", *Cellular and Molecular Life Sciences*, 61, 192-208.

Chen, J., Wang, Q., Hua, Z., Du, G., 2007. "Research and application of biotechnology in textile industries in China", *Enzyme and Microbial Technology*, 40(7), 1651-1655.

Chirgadze, D., 07 April 2004. *University of Cambridge*.  
<http://mordred.bioc.cam.ac.uk/~dima/whitepapers/xtal-in-action/node3.html> (Last accessed: April, 2007)

Chu, H., Leeder, J., Gilbert, S., 1975. "Immobilized catalase reactor for use in peroxide sterilization of dairy products", *Journal of Food Science*, 40, 641-643.

Clare, D.A., Duong, M.N., Darr, D., Archibald, F., Fridovich, I., 1984. "Effects of molecular oxygen on detection of superoxide radical with nitroblue tetrazolium and on activity stains for catalase". *Analytical Biochemistry*, 140, 532-537.

Conyers, S.M., Kidwell, D.A., 1991. "Chromogenic substrates for horseradish peroxidase". *Analytical Biochemistry*, 192, 207-211.

Cooney, D.G., Emerson, R., *Thermophilic Fungi: An Account of Their Biology, Activities and Classification.*, W.H. Freeman Publishers, San Francisco, USA, 1964.

Cortina, J., 2004. [http://www.revistaecosistemas.net/admin/Archivos/Imagenes/editor/XIV\\_2/lafig6.jpg](http://www.revistaecosistemas.net/admin/Archivos/Imagenes/editor/XIV_2/lafig6.jpg) (Last accessed: April, 2007).

DiMaio, F., 2007. *The University of Wisconsin Madison* [www.cs.wisc.edu/~dimaio/files/dimaio.ismb3dsig06.ppt](http://www.cs.wisc.edu/~dimaio/files/dimaio.ismb3dsig06.ppt) (Last visited: April, 2007).

Dittmer, J.K., Patel, N.J., Dhawale, S.W., Dhawale, S.S., 1997. "Production of multiple laccase isoforms by *Phanerochaete chrysosporium* grown under nutrient sufficiency". *FEMS Microbiology Letters*, 149(1), 65-70.

Drenth, J., *Principles of Protein X-Ray Crystallography, 2nd Ed.*, Springer, New York, USA, 1999.

Ducruix, A., Giegé, R., *Crystallization of Nucleic Acids and Proteins, 1st Ed.*, Oxford University Press, New York, USA, 1992.

Durán, N., Esposito, E., 2000. "Potential applications of oxidative enzymes and phenoloxidase-like compounds in wastewater and soil treatment: a review", *Applied Catalysis B: Environmental*, 28, 83-99.

Durante, D., Casadio, R., Martelli, L., Tasco, G., Portaccio, M., De Luca, P., Bencivenga, U., Rossi, S., Di Martino, S., Grano, V., Diano, N., Mita, D.G., 2004. "Isothermal and non-isothermal bioreactors in the detoxification of waste waters polluted by aromatic compounds by means of immobilised laccase from *Rhus vernicifera*", *Journal of Molecular Catalysis B: Enzymatic*, 27(4-6), 191-206.

Eisenthal, R., Danson, M.J., *Enzyme Assays, 1st Ed.*, Oxford University Press, New York, USA, 1992.

Fraaije, M.W., Roubroeks, H.P., Hagen, W.R., Van Berkel, W.J.H., 1996. "Purification and characterization of an intracellular catalase-peroxidase from *Penicillium simplicissimum*", *European Journal of Biochemistry*, 235, 192-198.

Garcia-Molina, F., Hiner, A.N.P., Fenoll, L.G., Rodriguez-Lopez, J.N., Garcia-Ruiz, P.A., Garcia-Canovas, F., Tudela, J., 2005. "Mushroom tyrosinase: Catalase activity, inhibition and suicide inactivation". *Journal of Agricultural and Food Chemistry*, 53, 3702-3709.

Gerdemann, C., Eicken, C., Magrini, A., Meyer, H.E., Rompel, A., Spener, F., Krebs, B., 2001. "Isoenzymes of Ipomoea batatas catechol oxidase differ in catalase-like activity", *Biochemica et Biophysica Acta*, 1548, 94-105.

Gessler, N.N., Sokolov, A.V., Bykhovsky, V.Y., Belozerskaya, T.A., 2002. "Superoxide dismutase and catalase activities in carotenoid-synthesizing fungi *Blakeslea trispora* and *Neurospora crassa* fungi in oxidative stress", *Applied Biochemistry and Microbiology*, 38(3), 205-209.

Goldberg, I., Hochman, A., 1989. "Purification and characterization of a novel type of catalase from the bacterium *Klebsiella pneumoniae*", *Biochemica et Biophysica Acta*, 991, 330-336.

Hampton Research, 2005. <http://www.hamptonresearch.com> (Last accessed: May, 2007)

Herreros, B., 1996. <http://chemmac1.usc.edu/Bruno/zeodat/XRD.html> (Last accessed: May, 2007)

Hisada, H., Hata, Y., Kawato, A., Abe, Y., Akita, O., 2005. "Cloning and expression analysis of two catalase genes from *Aspergillus oryzae*". *Journal of Bioscience and Bioengineering*, 99(6), 562-568.

Horton, H.R., Moran, L.A., Ochs, R.S., Rawn, J.D., Scrimgeour, K.G., *Principles of Biochemistry, 2nd Ed.*, Prentice-Hall Inc., New Jersey, USA, 1996.

Howard, G.C., Brown, W.E, *Modern Protein Chemistry, 1st Ed.*, CRC Press LLC, USA, 2002.

Hudkova, L.V., Dehtiar, R.H., Chumachenko, I.V., Hulyi, M.F., 1975. "Comparative characteristics of catalase from the fungus *Penicillium vitale*, which is synthesized under different nutritional conditions". *Ukrainskyi Biokhimichnyi Zhurnal*, 47(3), 342-346.

International Biopharmaceutical Association, 2004.

<http://www.ibpassociation.org/encyclopedia/Chemistry/Enzyme.php> (Last accessed: April, 2007)

Isobe, K., Inoue, N., Takamatsu, Y., Kamada, K., Wakao, N. 2006. Production of catalase by fungi growing at low pH and high temperature. *Journal of Bioscience and Bioengineering*, 101(1): 73-76.

Johjima, T., Ohkuma, M., Kudo, T., 2003. "Isolation and cDNA cloning of novel hydrogen peroxide-dependent phenol oxidase from the basidiomycete *Termitomyces albuminosus*", *Applied Microbiology and Biotechnology*, 61(3), 220-225.

Jolley, R. L., J.R., Evans, L.H., Mason, H.S., 1972. "Reversible oxygenation of tyrosinase", *Biochemical and Biophysical Research Communications*, 46, 878-884.

Jones, C., Mulloy, G., Sanderson, M. *Methods in Molecular Biology, Crystallography Methods and Protocols Vol 56*, Humana Press Inc., Totowa, NJ, 1996.

Kaptan, Y., 2004, "Utilization of *Scytalidium thermophilum* phenol oxidase in bioorganic synthesis", M.Sc. Thesis, METU, Ankara, Turkey.

Katayama, Y, Nishida, T., Morohoshi, N., Kuroda, K., 1989. "The metabolism of biphenyl structures in lignin by the wood-rotting fungus *Coriolus versicolor*", *FEMS Microbiology Letters*, 61(3), 307–313.

Kikuchi-Torii, K, Hayashi, S., Nakamoto, H., Nakamura, S., 1982. "Properties of *Aspergillus niger* catalase", *Journal of Biochemistry*, 92(5), 1449-1456.

Knight, W., 2006. *University of Montana*. <http://dbs.umt.edu/courses/fall2006/bioc380/lectures/013/lecture.html> (Last accessed: May, 2007)

Kulys, J., Kriauciunas, K., Vidziunaite, R., 2003. "Biphasic character of fungal catalases inhibition with hydroxylamine in presence of hydrogen peroxide", *Journal of Molecular Catalysis B: Enzymatic*, 26, 79-85.

Kwon, S.I., Anderson, A.J., 2001. "Catalase activities of *Phanerochaete chrysosporium* are not coordinately produced with ligninolytic metabolism: Catalases form a white-rot fungus", *Current Microbiology*, 42(1), 8-11.

Laboratory of Synchrotron Light, 2007. [www.lsls.cells.es/AboutUs/WhatIs](http://www.lsls.cells.es/AboutUs/WhatIs) (Last accessed: May, 2007)

Levy, E., Eyal, Z., Hochman, A., 1992. "Purification and characterization of a catalase-peroxidase from the fungus *Septoria tritici*", *Archives of Biochemistry and Biophysics*, 296(1), 321-327.

Luft, J.R., DeTitta, G.T., 1999. "A Method to Produce Microseed Stock for Use in the Crystallization of Biological Macromolecules", *Acta Crystallographica D*, 55, 988-993.

Luke, A.K., Burton, S.G., 2001. "A novel application for *Neurospora crassa*: Progress from batch culture to a membrane bioreactor for the bioremediation of phenols", *Enzyme and Microbial Technology*, 29, 348-356.

Mäkelä, M.R., Hildén, K.S., Hakala, T.K., Hatakka, A., Lundell, T.K., 2006. "Expression and molecular properties of a new laccase of the white rot fungus *Phlebia radiata* grown on wood". *Current Genetics*, 50(5), 323-333.

Mallery, C., 2007. *University of Miami*. <http://fig.cox.miami.edu/~cmallery/150/gene/sf13x1box.jpg> (Last accessed: April, 2007)

Marusek, M.C., Trobaugh, N.M., Flurkey, W.H., Inlow, J.K., 2006. "Comparative analysis of polyphenol oxidase from plant and fungal species", *Journal of Inorganic Biochemistry*, 100(1), 108-123.

Mayer, M.A., R.C. Staples., 2002. "Phenol oxidase: New functions for an old enzyme", *Phytochemistry*, 60, 551-565.

McPherson, A., 2004. "Introduction to protein crystallization", *Methods*, 34, 254-265.

Mete, S., 2003. "Scytalidium thermophilum polyphenol oxidase: production and partial characterization", M.Sc. Thesis, METU, Ankara, Turkey.

Millard, J., 2006. Madison Area Technical Collage, The Biotechnology Project. [http://matcmadison.edu/biotech/resources/proteins/labManual/chapter\\_2.htm](http://matcmadison.edu/biotech/resources/proteins/labManual/chapter_2.htm) (Last accessed: April, 2007)

Min, K.L., Kim, Y.H., Kim, Y.W., Jung, H.S., Hah, Y.C., 2001. "Characterization of a novel laccase produced by the wood-rotting fungus *Phellinus ribis*", *Archives of Biochemistry and Biophysics*, 392(2), 279-286.

Montavon, P., Kukic, K.R., Bortlik, K., 2007. "A simple method to measure effective catalase activities: Optimization, validation, and application in green coffee", *Analytical Biochemistry*, 306, 207-215.

Mosavi-Movahedi, A.A., Wilkinson, A.E., Jones, M.N., 1987. "Characterization of *Aspergillus niger* catalase", *International Journal of Biological Macromolecules*, 9(6), 327-332.

Mosbach, R., 1963. "Purification and some properties of laccase from *Polyporus versicolor*", *Biochimica et Biophysica Acta (BBA) - Specialized Section on Enzymological Subjects*, 73(2), 204-212.

O'Reilly, M., Vinkovic, M., Sharff, A., Jhoti, H., 2006. "High throughput protein crystallography: Developments in crystallisation, data collection and data processing", *Drug Discovery Today: Technologies*, 3(4), 451-456.

Opie, S.C., Clifford, M.N., Robertson A., 1995. "The formation of thearubigin-like substances by in-vitro polyphenol oxidase mediated fermentation of individual flavon-3-ols". *Journal of the Science of Food and Agriculture*, 67, 501-505

Ögel, Z.B., Yüzügüllü, Y., Mete, S., Bakır, U., Kaptan, Y., Sutay, D., Demir, AS., 2006. "Production, properties and application in biocatalysis of a novel extracellular alkaline phenol oxidase from the thermophilic fungus *Scytalidium thermophilum*", *Applied Microbiology and Biotechnology*. 71(6), 853-862.

Packer, L. *Methods in Enzymology Vol 105, 1<sup>st</sup> Ed.*, Academic press Inc., Orlando, USA, 1984.

Palmieri, G., Cennamo, G., Faraco, V., Amoresano, A., Sannia, G., Giardina, P., 2003. "Atypical laccase isoenzymes from copper supplemented *Pleurotus ostreatus* cultures", *Enzyme and Microbial Technology*, 33(2-3), 220-230.

Pan, Y., 28 November 2005. *New Mexico State University*.  
<http://darwin.nmsu.edu/~molb470/fall2005/projects/pan/> (Last accessed: May, 2007)

Paris, S., Wysong, D., Debeaupuis, J.P., Shibuya, K., Philippe, B., Diamond, R.D., Latgé, J.P., 2003. "Catalases of *Aspergillus fumigatus*", *Infection and immunity*, 71(6), 3551-3562.

Pazarlıoğlu, N.K., Sarıışık, M., Telefoncu, A., 2005. "Laccase: production by *Trametes versicolor* and application to denim washing", *Process Biochemistry*, 40(5), 1673-1678.

Pereza, L., Hansberg, W., 2002. "Neurospora crassa catalases, singlet oxygen and cell differentiation", *Biological Chemistry*, 383(3-4), 569-575.

Pongpom, P., Cooper Jr., C.R., Vanittanakom, N., 2005. "Isolation and characterization of a catalase-peroxidase gene from the pathogenic fungus, *Penicillium marneffe*", *Medical Mycology*, 43(5), 403-411.

Powell, D., 2007. *University of Oklahoma*. <http://xrayweb.chem.ou.edu/notes/crystallography.html> (Last accessed: April, 2007)

Rescigno, A., Sanjust, E., Montanari, L., Sollai, F., Soddu, G., Rinaldi, A.C., Oliva, S., Rinaldi, A., 1997. "Detection of laccase, peroxidase and polyphenol oxidase on a single polyacrylamide gel electrophoresis". *Analytical Letters*, 30, 2211-2220.

Rhodes, G. *Made Crystal Clear*, 2<sup>nd</sup> Ed., Academic Press, USA, 2000.

Rowlett, R.S., 2005. *University of Colgate*. [http://departments.colgate.edu/chemistry/rowlett\\_research.html](http://departments.colgate.edu/chemistry/rowlett_research.html) (Last accessed: April, 2007)

Russell, I.M., Burton, S.G., 1999. "Development and demonstration of an immobilised-polyphenol oxidase bioprobe for the detection of phenolic pollutants in water", *Analytica Chimica Acta*, 389, 161-170.

Rupp, B., 2006. *X-Ray Tutorial*. <http://www.ruppweb.org/xray/tutorial/lattice.gif> (Last accessed: April, 2007)

Russell, L. Jolley, JR., Evans, L.H., Makino, N., Mason, H.S., 1973. The Journal of Biological Chemistry, 249(2), 335-345.

Sanchez-Amat, A., Solano, F., 1997. "A pluripotent polyphenol oxidase from the melanogenic marine *Alteromonas sp* shares catalytic capabilities of tyrosinases and laccases", *Biochemical and Biophysical Research Communications*, 240, 787-792.

Schliephake, K., Jones, I.K. and Lonergan, G.T., 1997. "*Pycnoporus cinnabarinus* laccase catalyses the decolourisation of a disazo dye", *International Biotechnology Conference*. Jakarta, Indonesia.

Schrader, M., Fahimi, H.D., 2006. "Peroxisomes and oxidative stress", *Biochemica et Biophysica Acta*, 1763, 1755-1766.

Score, A.J., Palfreyman, J.W., White, N.A., 1997. "Extracellular phenoloxidase and peroxidase enzyme production during interspecific fungal interactions", *International Biodeterioration and Biodegradation*, 39, 225-233.

Shi, X., Feng, M., Shi, J., Shi, Z., Zhong, J., Pei, Z., 2007. "High-level expression and purification of recombinant human catalase in *Pichia pastoris*", *Protein Expression and Purification*, 54(1), 24-29.

Shibuya, K., Paris, S., Ando, T., Nakayama, H., Hatori, T., Latgé, J.P., 2006. "Catalases of *Aspergillus fumigatus* and inflammation in aspergillosis", *Japanese Journal of Medical Mycology*, 47(4), 249-255.

Tomás-Barberán, A.F., Espin, J.C., 2001. "Phenolic compounds and related enzymes as determinants of quality in fruits and vegetables", *Journal of the Science of Food and Agriculture*, 81, 853-876.

Tuomela, M., Vikman, M., Hatakka, A., Itavaara, M., 2000. "Biodegradation of lignin in a compost environment: a review", *Bioresource Technology*, 72(2), 169-183.

Universtiy of California, 2006. [http://www.physics.ucla.edu/demoweb/demomanual/matter\\_and\\_thermodynamics/matter/bravais.jpg](http://www.physics.ucla.edu/demoweb/demomanual/matter_and_thermodynamics/matter/bravais.jpg) (Last accessed: April, 2007)

University of Oxford, 2006. [http://www.ncl.ox.ac.uk/icl/heyese/structure\\_of\\_solids/Lecture1/Bravais.gif](http://www.ncl.ox.ac.uk/icl/heyese/structure_of_solids/Lecture1/Bravais.gif) (Last accessed: May, 2007)

Vainshtein, B.K., Melik-Adamyanyan, W.R., Barynin, V.V., Vagin, A.A., Grebenko, A.I., Borisov, V.V., Bartels, K.S., Fita, I., Rossmann, M.G., 1986. "Three-dimensional structure of catalase from *Penicillium vitale* at 2.0 Å resolution", *Journal of Molecular Biology*, 188, 49-61.

Vetrano, A.M., Heck, D.E., Mariano, T.M., Mishin, V., Laskin, D.L., Laskin, J.D., 2005. "Characterization of the oxidase activity in mammalian catalase", *The Journal of Biological Chemistry*, 280(42), 35372-35381.

Vlasits, J., Jakopitsch, C., Schwanninger, M., Holubar, P., Obinger, C., 2007. "Hydrogen peroxide oxidation by catalase-peroxidase follows a non-scrambling mechanism", *FEBS Letters*, 581, 320-324.

Wang, H., Tokusige, Y., Shinoyama, H., Fujii, T., Urakami, T., 1998. "Purification and characterization of a thermostable catalase from culture broth of *Thermoascus aurantiacus*", *Journal of Fermentation and Bioengineering*, 85(2), 169-173.

Wassermann, B.P., Hultin, H.O., 1981. "Effect of deglycosylation on the stability of *Aspergillus niger* catalase", *Archives of Biochemistry and Biophysics*, 212(2), 385-392.

Weber, P., *Methods in Enzymology: Overview of Protein Crystallization Methods*, Vol. 276, Academic Press Inc., 1997.

Whitford, D., *Proteins: Structure and Function, 1st Ed.*, John Wiley & Sons Ltd., West Sussex, England, 2005.

Wiegant, W.M., 1992. "Growth characteristics of the thermophilic fungus *Scytalidium thermophilum* in relation to production of mushroom compost", *Applied and environmental Microbiology*, 58(4), 1301-1307.

Wiestreich, G.A., Lechtman, M.D., *Microbiology, 3rd Ed.*, Macmillan Publishing Co., USA, 1980.

Willmot, C., 2005. *University of Leicester Department of Biochemistry*.  
<http://www.le.ac.uk/by/teach/biochemweb/tutorials/michment2print.html>  
(Last accessed: April, 2007)

Xu, F., Shin, W., Brown, Wahleithner, J.A., Sundaram, U.M., Solomon, E.L., 1996. "A study of a series of recombinant fungal laccases and bilirubin oxidase that exhibit significant differences in redox potential, substrate specificity, and stability", *Biochimica et Biophysica Acta (BBA) - Protein Structure and Molecular Enzymology*, 1292(2), 303-311.

Yamada, K., T.H. Chen, G. Kumar, O. Vesnovsky, L.D.T. Topoleski, G.F. Payne., 2000. "Chitosan based water-resistant adhesive. Analogy to mussel glue", *Biomacromolecules*, 1(2), 252-258.

Yamazaki, S., Morioka, C., Itoh, S., 2004. "Kinetic evaluation of catalase and peroxygenase activities of tyrosinase", *Biochemistry*, 43, 11546-11553.

Zámocký, M., Koller, F., 1999. "Understanding the structure and function of catalases: clues from molecular evolution and in vitro mutagenesis", *Progress in Biophysics and Molecular Biology*, 72, 19-66.

## APPENDIX A

### MEDIUM COMPOSITIONS

#### **YpSs Agar Medium**

4.0 g/L Yeast extract  
1.0 g/L  $K_2HPO_4$   
0.5 g/L  $MgSO_4 \cdot 7H_2O$   
15.0 g/L Soluble starch  
20.0 g/L Agar

#### **Preculture Medium**

4.0 g/L Yeast extract  
1.0 g/L  $K_2HPO_4$   
0.5 g/L  $MgSO_4 \cdot 7H_2O$   
10.0 g/L Glucose

#### **Mainculture Medium**

4.0 g/L Yeast extract  
1.0 g/L  $K_2HPO_4$   
0.5 g/L  $MgSO_4 \cdot 7H_2O$   
0.1 g/L  $CuSO_4 \cdot 5H_2O$   
40 g/L Glucose  
(0.17 g/L Gallic acid)

## APPENDIX B

### PROTEIN MEASUREMENT BY BRADFORD METHOD

Bovine serum albumin (BSA) was used as the protein standard according to Bradford (1976). To prepare 1 mg/ml stock BSA solution, 25 mg BSA was dissolved in 25 ml of 100 mM pH 7 sodium phosphate buffer.

To measure the protein content, 0.5 ml BSA solution and 5 ml of Bradford reagent (Sigma) were mixed in a glass test tube. Ten minutes later absorbances at 595 nm were measured by using a spectrophotometer and BSA standard curve was achieved (Figure B.1). Protein concentrations of other samples were analysed by the same method and protein concentrations were calculated using the BSA standard curve.

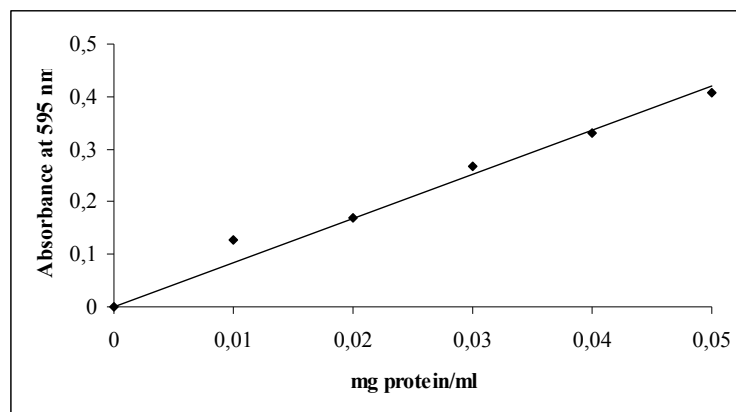


Figure B.1. BSA standard curve for Bradford Method

## APPENDIX C

### ANION EXCHANGE CHROMATOGRAPHY

Prepacked, ready to use HiPrep™ 16/10 SP XL and HiPrep 16/10 Q XL columns were tested for *S. thermophilum* CCO purification. Column data was given below.

Table C.1 Anion exchange column data

Matrix	6% highly cross-linked spherical agarose
Type of exchanger	-N <sup>+</sup> (CH <sub>3</sub> ) <sub>3</sub>
Mean particle size	90 μm
Bed height	100 mm
Bed volume	20 ml
i.d.	16 mm
Recommended flow rate	2–10 ml/min (60–300 cm/h)
Maximum flow rate	1 ml/min (30 cm/h)
Maximum pressure over the packed bed during operation	0.15 MPa, 1.5 bar, 22 psi
Hardware pressure limit	0.5 MPa, 5 bar, 73 psi
Ph stability	
Short term	2-14
Working	2-12
Long term	2-12

## APPENDIX D

### GEL FILTRATION CHROMATOGRAPHY

Prepacked, ready to use HiPrep 16/60 Sephacryl S-100 High Resolution (MW:1000-100000 Da) column was used for *S. thermophilum* CCO purification. Column data was given below.

Table D.1. Gel filtration column data

Matrix	Cross-linked copolymer of allyl dextran and N,N-methylenebisacrylamide
Mean particle size	47 $\mu\text{m}$ (25-75 $\mu\text{m}$ )
Separation range ( $M_r$ )	1000-100000 for globular proteins
Column volume	120 ml
Sample volume	Up to 5 ml
Recommended flow rate	0.5 ml/min (15 cm/h)
Maximum flow rate	1 ml/min (30 cm/h)
Maximum pressure over the packed bed during operation	0.15 MPa, 1.5 bar, 22 psi
Hardware pressure limit	0.5 MPa, 5 bar, 73 psi
pH stability	
Short term	2-13
Working	3-11
Long term	3-11

## APPENDIX E

### SODIUMDODECYLSULPHATE POLYACRYLAMIDE GEL ELECTROPHORESIS (SDS-PAGE) PROTOCOL

Instructions were provided below for electrophoresis of ready-to-use NuPAGE Novex Bis-Tris Gels (Invitrogen) using the XCell SureLock Mini-Cell (Invitrogen).

#### NuPAGE Novex Bis-Tris Gels

##### Prepare Samples

<u>Reagent</u>	<u>Reduced Sample</u>	<u>Non-reduced</u>
Sample	x $\mu$ l	x $\mu$ l
NuPAGE LDS Sample Buffer (4X)	2.5 $\mu$ l	2.5 $\mu$ l
NuPAGE Reducing Agent (10X)	1 $\mu$ l	--
Deionized Water	to 6.5 $\mu$ l	to 7.5 $\mu$ l
Total Volume	10 $\mu$ l	10 $\mu$ l

Heat samples at 70°C for 10 minutes.

##### Prepare 1x Running Buffer

Prepare 1x SDS Running Buffer by adding 50 ml 20x NuPAGE MES or MOPS SDS Running Buffer to 950 ml of deionized water.

##### Load Sample

Load the appropriate concentration of the protein sample on the gel.

**Load Buffer**

Fill the Upper Buffer Chamber with 200 ml 1x NuPAGE SDS Running Buffer.

**Reduced samples**

Use 200 ml 1x NuPAGE SDS Running Buffer containing 500  $\mu$ l NuPAGE Antioxidant. Fill the Lower Buffer Chamber with 600 ml 1x NuPAGE SDS Running Buffer.

**Run Conditions**

Run Time: 35 minutes (MES Buffer), 50 minutes (MOPS Buffer)

Expected Current: 100-125 mA/gel (start); 60-80 mA/gel (end)

## APPENDIX F

### COOMASSIE-BASED GEL STAINING PROTOCOL

Simply Blue Safe Stain Microwave Protocol (Invitrogen) for staining 1.0 and 1.5 mm mini NuPAGE Gels (Invitrogen) was described below.

Table F.1. Simply Blue Safe Stain Microwave Protocol

<b>Step</b>	<b>Protocol</b>	<b>Time</b>
1	Place the gel in 100 ml ultrapure water and microwave on high (950-1100 watts)	1 min
2	Shake the gel on an orbital shaker. Discard wash	1 min
3	Repeat Steps 1 and 2 twice.	1 min each
4	Add 20-30 ml SimplyBlue SafeStain and microwave	45 sec to 1 min
5	Shake the gel on an orbital shaker. Discard stain.	5-10 min
6	Wash the gel in 100 ml ultrapure water on an orbital shaker.	10 min
7	Add 20 ml 20% NaCl and shake the gel on an orbital shaker	5-10 min
8	Optional: Repeat Step 6 for a clear background	1 h

## APPENDIX G

### GLYCOPROTEIN DETECTION PROTOCOL

The Glycoprotein Detection Kit (Sigma) provides a system to easily detect the sugar moieties of glycoproteins on SDS-PAGE gels or on Western blotting membranes. This detection system is a modification of Periodic Acid-Schiff (PAS) methods and yields magenta bands with a light pink or colorless background. The detection limit has been found to be in the range of 25-100 ng for carbohydrates depending on the nature and the degree of glycosylation of the protein.

#### Reagents

**Oxidation Solution** - Add 950 ml of ultrapure water to the bottle labeled Oxidation Component. Stir for approximately 15 minutes or until the material is completely dissolved. Bring the final volume to 1 L. Store the Oxidation Solution at room temperature.

**Reduction Solution** - Add 950 ml of ultrapure water to the bottle labeled Reduction Component. Stir for approximately 15 minutes or until the material is completely dissolved. Bring the final volume to 1 L. Store the Reduction Solution at room temperature.

**Schiff's Reagent (Fuchsin-Sulfite Reagent)** - The reagent is supplied ready-to-use and no adjustment or dilution is necessary. Store the reagent at 2–8 °C.

**Fixing Solution** - Prepare the Fixing Solution by combining 200 ml of water with 200 ml of methanol. Store the Fixing Solution at room temperature.

**Storage Solution** - Combine 380 ml of ultrapure water with 20 ml of glacial acetic acid. Store the Storage Solution at room temperature.

**Peroxidase Positive Control** - Reconstitute the contents of the vial with 0.5 ml of ultrapure water to produce a 2 mg/ml solution. Dilute this solution to 1 mg/ml with the sample buffer appropriate for the system being used. For a large gel (15 x 18 cm), load 10  $\mu$ l of the reconstituted positive control per lane and 5  $\mu$ l per lane for mini gels (8 x 10 cm). After reconstitution of the Peroxidase Positive Control, aliquot and store at  $-20^{\circ}\text{C}$ .

### **Procedure**

Use Table 1 to determine the time required for each step based on gel or membrane size and gel thickness. Perform this staining procedure in a well-ventilated area or hood to remove aldehyde vapor generated during the oxidation step. For membrane staining, start at step 3 and proceed through step 7.

**1. Fixing:** After electrophoresis, fix the gel(s) by completely immersing in the Fixing Solution. Gently agitate.

**2. Washing:** Replace the Fixing Solution with ultrapure water and agitate gently. Repeat this step once.

**3. Oxidation:** Transfer the gel(s) or membrane(s) to the prepared Oxidation Solution and agitate gently.

**4. Washing:** Replace the Oxidation Solution with ultrapure water and agitate gently. Repeat this step once.

**5. Staining:** Replace the water with Schiff's Reagent and agitate gently.

**6. Reduction:** Replace the Schiff's Reagent with the Reduction Solution and agitate gently.

**7. Washing:** Replace the Reduction Solution with ultrapure water. Repeat 2-3 times. The magenta band(s) will intensify during this step.

**8. Storage:** Transfer the gel(s) into the Storage Solution (5% acetic acid solution).

Table G.1. Recommended gel or membrane staining conditions

Steps	Volumes		Time for gel thickness 0.5-0.75 mm or for membrane	Time for gel thickness 1.0-1.5 mm
	Size 16 x 18 cm	Size 8 x 10 cm		
1. Fixing	400 ml	200 ml	30 min	60 min
2. Washing	400 ml	200 ml	2 x 10 min	2 x 20 min
3. Oxidation	200 ml	100 ml	30 min	60 min
4. Washing	400 ml	200 ml	2 x 10 min	2 x 20 min
5. Staining	200 ml	100 ml	1-2 h or until bands turn magenta	1-2 h or until bands turn magenta
6. Reduction	200 ml	100 ml	60 min	120 min
7. Washing	400 ml	200 ml	Band color will intensify with changes of fresh water	Band color will intensify with changes of fresh water
8. Storage	400 ml	400 ml	Overnight	Overnight

## APPENDIX H

### PROTEIN BLOTTING PROCEDURE

This procedure is described by Invitrogen Company (UK) for Western Transfer Using the XCell II Blot Module.

#### Procedure

1. After opening the SDS-PAGE gel cassette, remove wells with the gel knife.
2. Place a piece of pre-soaked filter paper on top of the gel, and lay just above the slot in the bottom of the cassette, leaving the “foot” of the gel uncovered.
3. Keep the filter paper saturated with the transfer buffer and remove all trapped air bubbles by gently rolling over the surface using a glass pipette as a roller.
4. Turn the plate over so the gel and filter paper are facing downwards over a gloved hand or clean flat surface.
5. Use the Gel Knife to push the foot out of the slot in the plate and the gel will fall off.
6. When the gel is on a flat surface, cut the “foot” off the gel with the gel knife.
7. Wet the surface of the gel with transfer buffer and position the pre-soaked transfer membrane (PVDF) on the gel, ensuring all air bubbles have been removed.
8. Place another pre-soaked anode filter paper on top of the membrane. Remove any trapped air bubbles.
9. Place two soaked blotting pads into the cathode (-) core of the blot module. Carefully pick up the gel membrane assembly and place on blotting pad in the same sequence, such that the gel is closest to the cathode core.

10. Add enough pre-soaked blotting pads to rise to 0.5 cm over rim of cathode core. Place the anode (+) core on top of the pads.
11. Position the gel/membrane assembly and blotting pads in the cathode core of the XCell II™ Blot Module to fit horizontally across the bottom of the unit.
12. Hold the blot module together firmly and slide it into the guide rails on the lower buffer chamber. The blot module will only fit into the unit one way, so the (+) sign can be seen in the upper left hand corner of the blot module. Properly placed, the inverted gold post on the right hand side of the blot module will fit into the hole next to the upright gold post on the right side of the lower buffer chamber.
13. Place the Gel Tension Wedge so that its vertical face is against the blot module. Lock the Gel Tension Wedge by pulling the lever forward.
14. Fill the blot module with 1X Transfer Buffer until the gel/membrane assembly is covered in this buffer.
15. Fill the Outer Buffer Chamber with deionized water by pouring approximately 650 ml in the gap between the front of the blot module and the front of the lower buffer chamber.
16. Place the lid on top of the unit.
17. With the power turned off, plug the red and black leads into the power supply.
18. Perform transfer at 30 V constant voltage for 1 hour for PVDF membranes.

Wear gloves while performing the blotting procedure to prevent contamination of gels and membranes, and exposure to irritants commonly used in electrotransfer.

## APPENDIX I

### CRYSTALLIZATION SCORE SHEET

Protein: \_\_\_\_\_ In Buffer: \_\_\_\_\_

Tray #: \_\_\_\_\_ Date: \_\_\_/\_\_\_/\_\_\_

Protein conc: \_\_\_\_\_ mg/ml Size of drops: \_\_\_  $\mu$ l of protein + \_\_\_  $\mu$ l of well soln

Stock solns: \_\_\_\_\_

	1	2	3	4	5	6
A						
B						
C						
D						

Comments: \_\_\_\_\_  
 \_\_\_\_\_  
 \_\_\_\_\_  
 \_\_\_\_\_  
 \_\_\_\_\_

	1	2	3	4	5	6
A						
B						
C						
D						

Tray last checked on,  
 1: \_\_\_\_\_  
 2: \_\_\_\_\_  
 3: \_\_\_\_\_  
 4: \_\_\_\_\_  
 5: \_\_\_\_\_  
 6: \_\_\_\_\_  
 7: \_\_\_\_\_  
 8: \_\_\_\_\_  
 9: \_\_\_\_\_  
 10: \_\_\_\_\_

## APPENDIX J

### *S. thermophilum* CCO Amino Acid Sequence

As given in free United States Patent (No. 5646025) (Inventor: Donna Moyer from Davis, CA, USA):

MNRVTNLLAWAGAIGLAQATCPFADPAALYSRQDTTSG  
QSPLAAYEVDDSTGYLTSDVGGPIQDQTSKAGIRGPT  
LLEDFMFRQKIQHFDHERVPERAVHARGAGAHGTFTSY  
ADWSNITAASFLNATGKQTPVFRFSTVAGSRGSADTA  
RDVHGFATRFYTDEGNFDIVGNNIPVFFIQDAIQFPDLIH  
SVKPRPDNEIPQAATAHDSA WDFFSQQPSTMHTLFWA  
MSGHGIPRSYRHMDGFGVHTFRFVKDDGSSKLIKWHF  
KSRQGGKASLVWEEAQVLSGKNADFHRQDLWDAIESGN  
GPEWDVCVQIVDESQAQAFGFDLLDPTKIIPEEYAPLTK  
LGLLKLDRNPTNYFAETE QVMFQPGHIVRGIDFTEDPLL  
QGRLFSYLDTQLNRNGGPNFEQLPINMPRVPIHNNNRD  
GAGQMFIHRNKYPYTPNTLNSGYPRQANQNAGRGFFT  
APGRTASGALVREVSPTFNDHWSQPRLFFNSLTPVEQ  
QFLVNAMRFEISLVKSEEVKKNVLTQLNRVSHDVAVRV  
AAAIGLGAPDADDTYYHNNKTAGVSIVGSGPLPTIKTLR  
VGILATTSESSALDQAAQLRTRLEKDGLVVTVVAETLRE  
GVDQTYSTADATGFDG VVVVDGAAALFASTASSPLFPT  
GRPLQIFVDAYRWGKPVGVC GGSSEVLDAADVPEDG  
DGVYSEESVDMFVEEF EKGLATFRFTDRFALDS

## CURRICULUM VITAE

### PERSONAL INFORMATION

Surname, Name: Sutay, Didem

Nationality: Turkish (TC)

Date and Place of Birth: 27 April 1979, Ankara

Marital Status: Single

Phone: +90 312 213 43 48

email: [didemsutay@gmail.com](mailto:didemsutay@gmail.com)

### EDUCATION

Degree	Institution	Year of Graduation
MS	METU Chemical Engineering	2003
BS	Gazi University Chemical Engineering	2001
High School	Çankaya Anadolu High School, Ankara	1997

### WORK EXPERIENCE

Year	Place	Enrollment
2007- Present	Arçelik A.Ş.	Chemical Engineer
2001-2007	METU-Chemical Engineering	Research Assistant

### FOREIGN LANGUAGES

Advanced English, Fluent German

### PUBLICATION

- Ögel, Z.B., Yüzügüllü, Y., Mete, S., Bakır, U., Kaptan, Y., Sutay, D., Demir, AS, 2006. "Production, properties and application in biocatalysis of a novel extracellular alkaline phenol oxidase from the thermophilic fungus *Scytalidium thermophilum*", *Applied Microbiology and Biotechnology*, 71(6), 853-862.

## CONGRESSES

- XII. European Congress on Biotechnology (2005), Copenhagen-Denmark, Poster Presentation: “Production, purification and characterization of *Scytalidium thermophilum* phenol oxidases”
- XIV. National Biotechnology Congress (2005), Eskisehir-Turkey, Poster Presentation: “Production, purification and characterization of *Scytalidium thermophilum* phenol oxidases” (2. Best Poster Award)
- VI. National Chemical Engineering Congress (2004), İzmir, Turkey, Poster Presentation: “Screening, electrophoretic characterization and immobilization of polyphenol oxidases isolated from unused plant sources for use in industrial phenolic bioconversion processes”
- V. European Symposium on Biochemical Engineering Science (ESBES) (2004), Stuttgart-Germany, Poster Presentation: “Screening, isolation and characterization of plant based polyphenol oxidases”
- XIII. National Biotechnology Congress (2003), Çanakkale-Turkey, Poster Presentation: “Screening of industrially unused plant sources for polyphenol oxidase production and characterization of the enzyme”